

Observations and Modelling of Winds and Waves During the Surface Wave Dynamics Experiment

Report 4
ROWS Wind and Wave Observations
12 February - 7 March 1991

by Frederick C. Jackson

| Martin | M

Approved For Public Release; Distribution Is Unlimited

DTIC QUALITY INSPECTED 3

19961008 093

The contents of this report are not to be used for advertising, publication, or promotional purposes. Citation of trade names does not constitute an official endorsement or approval of the use of such commercial products.



DISCLAIMER NOTICE



THIS DOCUMENT IS BEST QUALITY AVAILABLE. THE COPY FURNISHED TO DTIC CONTAINED A SIGNIFICANT NUMBER OF PAGES WHICH DO NOT REPRODUCE LEGIBLY.

Observations and Modelling of Winds and Waves During the Surface Wave Dynamics Experiment

Report 4
ROWS Wind and Wave Observations
12 February - 7 March 1991

by Frederick C. Jackson 218 North Pitt Street Alexandria, VA 22314

Report 4 of a series

Approved for public release; distribution is unlimited

Prepared for U.S. Army Corps of Engineers

Washington, DC 20314-1000

and National Aeronautics and Space Administration,

Goddard Space Flight Center

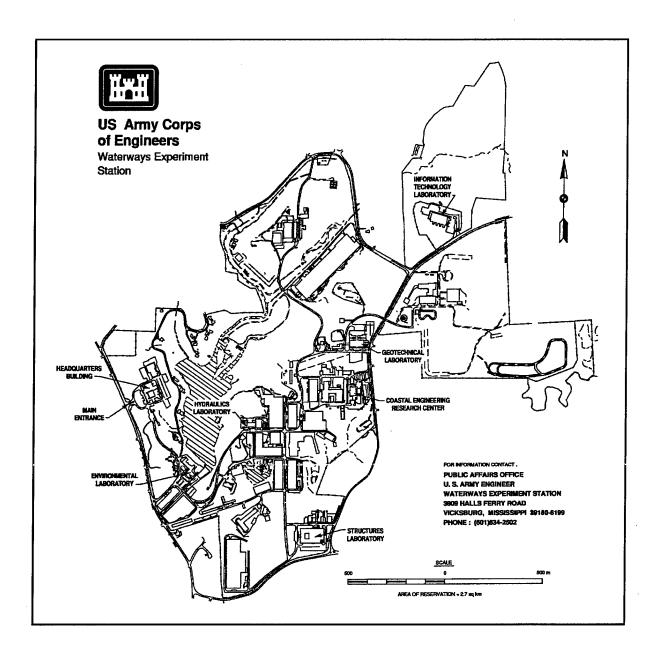
Laboratory for Hydrospheric Processes

Greenbelt, MD 20771

Monitored by U.S. Army Engineer Waterways Experiment Station

3909 Halls Ferry Road, Vicksburg, MS 39180-6199

Under Contract No. DACW-39-M-4560



Waterways Experiment Station Cataloging-in-Publication Data

Jackson, Frederick C.

Observations and modelling of winds and waves during the surface wave dynamics experiment. Report 4, ROWS wind and wave observations, 12 February-7 March 1991/by Frederick C. Jackson; prepared for U.S. Army Corps of Engineers and National Aeronautics and Space Administration, Goddard Space Flight Center, Laboratory for Hydrospheric Processes; monitored by Coastal Engineering Research Center, U.S. Army Engineer Waterways Experiment Station.

245 p.: ill.; 28 cm. — (Technical report; CERC-93-6 rept.4) Includes bibliographic references.

Report 4 of a series.

1. Ocean waves — Atlantic Ocean — Measurement. 2. Oceanographic buoys. 3. Remote sensing — Equipment and supplies. 4. Wind waves — Atlantic Ocean — Measurement. I. United States. Army. Corps of Engineers. II. U.S. Army Engineer Waterways Experiment Station. III. Coastal Engineering Research Center (U.S. Army Engineer Waterways Experiment Station) IV. United States. National Aeronautics and Space Administration. V. Goddard Space Flight Center. VI. Laboratory for Hydrospheric Processes (U.S.) VII. Title. VIII. ROWS wind and wave observations, 12 February-7 March 1991. IX. Series: Technical report (U.S. Army Engineer Waterways Experiment Station); CERC-93-6 rept.4.

Contents

Preface
1—Introduction
2—In Situ and Model Data
In Situ Data
3—ROWS Data
ROWS Technique
4—ROWS Winds
Wave Form Fits 2 Interpolation Fields 2 ROWS Versus Buoy Winds 2
5—ROWS Spectra
Frequency-Direction Plots
6—Conclusion
References
Appendix A: Buoy Environmental Data, 11-18 February 1991 A
Appendix B: NMC Wind Fields, 14-16 February 1991
Annandis C: NOCIJES Current Fields 14 16 February 1001

Appendix	D: Buoy Spectra, 12, 14-16 February 1991DI
D2 Di D3 Di D4 Di	February 1991 D2 scus-North, 14-16 February 1991 D7 scus-East, 14-16 February 1991 D14 scus-Center, 14-16 February 1991 D21 soy CERC, 14-16 February 1991 D28
Appendix 1	E: ROWS Spectra, 12 February-7 March 1991 E1
E2 RC for the	OWS Spectra, 12 February
Appendix 1	F: Daily Weather Maps
Appendix	G: Notation
SF 298	
List of	Figures
Figure 1.	Locations and types of in situ data collection platforms in the southern Middle Atlantic Bight region during the latter part of the SWADE experiment
Figure 2.	Average 10-m neutral wind speed and average wind direction with standard deviations for the nine platforms listed in Table 1 during the St. Valentine's data collection period 6
Figure 3.	Radar Ocean Wave Spectrometer (ROWS) measurement geometry
Figure 4.	NASA's Wallops Flight Facility T-39 aircraft 12
Figure 5.	ROWS data processing flow
Figure 6.	Examples of altimeter mode average wave form data 22
Figure 7.	Scatterplot and regression analysis of full wave form fit mean square slope (MSS) data versus tail region wave form fit MSS data
Figure 8.	Fields of ROWS altimeter-mode inferred 10-m neutral wind speeds for the four St. Valentine's flights from least-square polynomial fits to the observations
Figure 9.	Buoy 10-m neutral winds versus ROWS-inferred 10-m neutral winds for the four St. Valentine's flights 26

rigure 10.	Buoy neutral wind speeds versus ROWS uncorrected full wave form fit neutral wind speeds for a 50-km proximity circle
Figure 11.	Buoy neutral wind speeds versus ROWS wind speeds from corrected wave form fit data
Figure 12.	Detailed analysis of ROWS spectrum file S11 for flight No. 1 on 14 February
Figure 13.	Custer diagrams of the mean wave vectors for the four ROWS St. Valentine's flights on a Cartesian map with idealized coastline
Figure 14.	Radar and buoy nondimensional energy and peak frequency
	data versus nondimensional fetch for 16 February 1991 with empirical growth laws
List of	empirical growth laws
List of	empirical growth laws
	Tables
Table 1.	Tables In Situ Data Collection Platforms
Table 1. Table 2.	Tables In Situ Data Collection Platforms
Table 1. Table 2. Table 3.	Tables In Situ Data Collection Platforms

Preface

The airborne Radar Ocean Wave Spectrometer (ROWS) data presented in this report were collected by the author as part of the National Aeronautics and Space Administration's (NASA's) contribution to the Surface WAve Dynamics Experiment (SWADE). Funding for the aircraft flights was provided jointly by NASA and the U.S. Army Corps of Engineers (USACE). Thanks are due Dr. C. Linwood Vincent for the USACE contribution to the funding of these flights.

The successful ROWS flight campaign in SWADE would not have been possible without the support of a number of NASA/Wallops Flight Facility (WFF) personnel. Aircraft flights were conducted over a 2-month period—days, nights, and weekends—often on short notice according to the vagaries of the weather and often under trying circumstances. Among the aircraft support personnel involved in the ROWS flights, the author acknowledges particularly the support of Mr. Peter Bradfield, the flight coordinator, and Mr. Robert Gidge, the pilot of the NASA 431 for most of the ROWS SWADE flights.

Engineering and technical support for the ROWS instrument were provided by Mr. Douglas Vandemark and Mr. Donald Hines. Mr. John Ward and Mr. Steve Bailey were responsible for developing the new PC-based data acquisition system for the ROWS. Dr. Charles Vaughn developed new ROWS preprocessing software. Mr. Doug Vandemark and Dr. Bertrand Chapron (SM Systems and Research Corporation) developed a new code for the ROWS production data processing. Ms. Karen Stewart (Computer Sciences Corporation) carried out the production data processing. Mr. David Oberholtzer helped produce ROWS flight line maps. The cooperation of all these individuals would not have been possible without the full support of the head of the Observational Sciences Branch (Code 972), WFF, Mr. David Clem. The author thanks Mr. Clem for hosting him during his year's stay at WFF. Mr. Clem is also to be acknowledged and thanked by all SWADE participants for his hosting of SWADE meetings at WFF and for his logistical support during all phases of the experiment.

ROWS data collection strategy in the early part of the mission (i.e., prior to the third Intensive Operational Period) was developed jointly between the author and Dr. Robert Jensen of the U.S. Army Engineer Waterways Experiment Station (WES). This collaboration resulted in some of

the best data collected in SWADE; namely, the ROWS data collected during the "St. Valentine's Day" wind/wave episode. Dr. Jensen provided the author with a number of data sets generated by others, including the numerical data products of Dr. William Gemmill of the National Oceanic and Atmospheric Administration/National Weather Service/National Meteorological Center (surface winds) and the U.S. Navy's Fleet Numerical Meterology and Oceanography Center (current fields). Throughout the course of this work, Dr. Jensen has provided guidance and encouragement, for which the author is most grateful. Dr. Jensen's work was carried out under the supervision of Mr. H. Lee Butler, Chief, Research Division; and under the general supervision of Dr. James R. Houston and Mr. Charles C. Calhoun, Jr., Director and Assistant Director, Coastal Engineering Research Center, respectively

At the time of publication of this report, Director of WES was Dr. Robert W. Whalin. Commander was COL Bruce K. Howard, EN.

The contents of this report are not to be used for advertising, publication, or promotional purposes. Citation of trade names does not constitute an official endorsement or approval of the use of such commercial products.

1 Introduction

The Surface WAve Dynamics Experiment (SWADE) was a large-scale, multi-platform surface wave experiment that was conducted in the southern Middle Atlantic Bight (MAB) region off the U.S. east coast during the fall and winter of 1990-1991. The purpose of the experiment was to study the dynamics and evolution of the directional wave field in response to meteorological forcing making use of recent advances in in situ data collection and data analysis, numerical wave modelling, and airborne remote sensing (Weller et al. 1991). Sponsoring agencies included the Office of Naval Research, the National Aeronautics and Space Administration (NASA), and the U.S. Army Corps of Engineers (USACE). The experiment was organized into several "Intensive Observation Periods" (IOPs). Previous USACE SWADE data reports (Caruso et al. 1993, 1994) have documented the moored buoy and other in situ data, AXBT data, and model-generated wind and current field data. A few examples of remotely sensed wave data from NASA's Surface Contour Radar and the French RESSAC instrument were included in the IOP-3 report (Caruso et al. 1994).

Of the several remote sensing instruments participating in SWADE, NASA's Radar Ocean Wave Spectrometer (ROWS) instrument was the most heavily exercised. ROWS collected approximately 45 hr of high-resolution, directional wave spectra and wind speed data on more than a dozen aircraft flights before, during, and after the last IOP (IOP-3). Funding for these flights was provided by NASA and USACE. USACE also contributed to the processing of these data with follow-on funding in fiscal year 1993. Processed data include 158 spectra files and 88 wind speed files for 12 flights conducted over the period 12 February - 7 March, 1991. A subset of these data for the "St. Valentine's Day" frontal episode (14-16 February, 1991) has been further analyzed and published as a case study (Jackson and Jensen 1995). This study demonstrated both the high quality of the ROWS data and the importance of the radar data in providing extended coverage (i.e., beyond that provided by the SWADE buoy array) in the case of large-scale wind/wave events.

This report presents all ROWS data that have been processed to date for the SWADE mission. The report also presents buoy and model data for the St. Valentine's (StV) data collection period. Appendix A contains time series of buoy environmental data (pressure, temperature, etc.) for the StV

data collection period. Appendices B and C contain analysis surface wind and current fields for the same period. Appendix D contains the buoy directional spectra for the StV period. Appendix E contains fully scaled ROWS directional spectra for both StV and IOP-3 data collection periods and log-energy and frequency-direction plots for the StV period. Interpolated values of wind speeds from the ROWS altimeter mode are presented in the directional spectra plots in Appendix E along with inferred significant wave heights. Appendix F is a collection of daily weather maps for the study period. Appendix G is a notation of symbols and abbreviations used in the report. Statistical comparisons of ROWS and buoy wind speeds are provided in Chapter 4.

2 In Situ and Model Data

In Situ Data

The buoy network in SWADE consisted of four National Data Buoy Center (NDBC) 3-m discus buoys equipped with Hippy heave-pitch-roll sensors, identified in SWADE as Discus-N(orth), Discus-E(ast), Discus-C(enter), and Buoy Coastal Engineering Research Center (CERC); four small meteorological buoys (MiniMet buoys); the operational NDBC nondirectional wave-sensing buoys in the east coast NDBC network; and several C-Man stations along the coast as described by Weller et al. (1991) and Caruso et al. (1993, 1994). The locations of these in situ data collection platforms are shown in Figure 1. The inset to Figure 1 shows the configuration of the three NDBC "SWADE buoys," viz., Discus-E, -N, and -C. These buoys were equipped with a K-Gill rapid response anemometer, the standard propeller/vane anemometer, air and water temperature sensors, and humidity and pressure sensors, as indicated in the inset. The buoy positions shown in Figure 1 are the same as at the time of deployment, except for Discus-E, which was captured by the Gulf Stream on January 24, 1991, and deposited 40 km northeast of its original position. Of the four original MiniMets, only MET-3 remained on station throughout SWADE, the others having drifted out of the area (Caruso et al. 1994).

Data from these buoys and C-Man stations have been archived at the NASA/Wallops Flight Facility (WFF) SWADE Data Archive Center (Oberholtzer and Donelan 1996) and are accessible by file transfer protocol with anonymous log on. Directional wave data from the NDBC discus buoys have been processed by the classical harmonic analysis technique (Longuet-Higgins, Cartwright, and Smith 1963), by NDBC (Steele, Teng, and Wang 1992), and by the maximum likelihood method (MLM) as described by Drennan, Graber, and Donelan (1996). In processing the heave, pitch, and roll co- and cross-spectral data for the directional distribution by MLM, the inversion occasionally fails for a particular frequency, or even for a band average. In this case, the processing reverts to the classical harmonic analysis method. The buoy spectra in this report have been produced by MLM.

Time series of in situ environmental data (temperature, pressure, etc.) for nine SWADE platforms during the StV observational period are

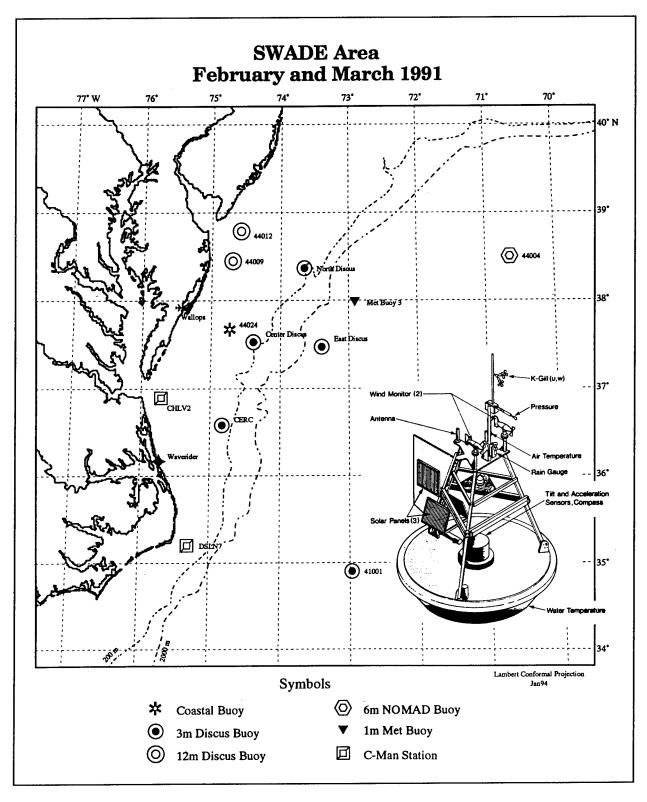


Figure 1. Locations and types of in situ data collection platforms in the southern middle Atlantic Bight region during the latter part of the SWADE experiment. The insert shows an NDBC 3-m discus directional wave sensing buoy as modified for SWADE (from Weller et al. (1991))

presented in Appendix A. Table 1 lists these platforms. Wind speeds in these plots are the raw anemometer-level wind speeds. In situ wind speeds have also been converted to neutral equivalent 10-m-level wind speeds U_{10n}^{-1} using two boundary layer models, the Cardone (1969) model, and the Large and Pond (1981) model. Average neutral wind speeds (and wind directions) for the SWADE area during the StV period are shown in Figure 2. In this figure, the St. Valentine's Day wind/wave event can be seen in the \sim 90-deg turning of the wind from southerly to westerly following the passage of a cold front on February 14.

Buoy directional spectra for the StV period 12-16 February are presented in Appendix D. Buoy spectra for the IOP-3 period (25 February - 9 March, 1991) are documented in the report by Caruso et al. (1994).

Table 1 In Situ Data Collection Platforms					
Platform	Buoy No.	Latitude	Longtitude	Type of Spectra	Note
Discus-N	44001	38°22'N	73°39'W	Direct. spectra	1,2
CERC buoy	44014	36°35'N	74°50'W	Direct. spectra	1,2
Discus-E	44015	37°29'N	73°24'W	Direct. spectra	1,2
Discus-C	44023	37°32'N	74°23′W	Direct. spectra	1,2
EXP buoy	44024	37°41'N	74°43'W	Nondir. spectra	1,2
МЕТ-3	44020	38°00'N	72°55'W	No spectra	2
NDBC buoy	44004	38°30'N	70°39'W	Nondir. spectra	1,2
NDBC buoy	44012	38°47'N	74°35'W	Nondir. spectra	1,2
C-Man Sta.	CHLV2	36°54'N	75°42'W	Nondir. spectra	1
C-Man Sta.	DSLN7	35°12'N	75°18'W	Nondir. spectra	1,2

Data used for SWADE area winds in Figure 2.
 Data used for altimeter wind speed comparisons.

Data about for animotor wind speed companies.

Model Data

Coarse-gridded National Meteorological Center (NMC) wind fields have been interpolated and regridded on a high-resolution 0.3-deg latitude by 0.5-deg longitude regional-domain grid using an objective interpolation

For convenience, symbols and abbreviations are listed in the notation (Appendix G).

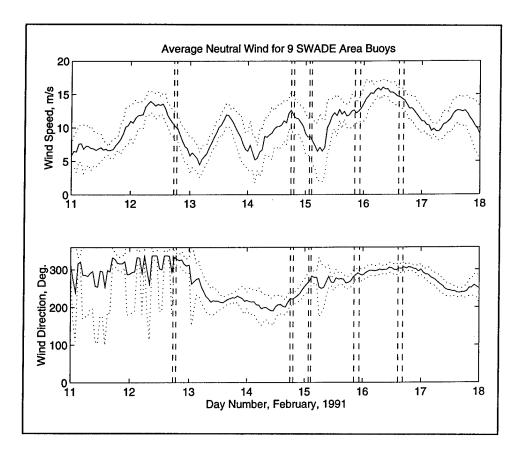


Figure 2. Average 10-m neutral wind speed (upper panel) and average wind direction (lower panel) with standard deviations (dotted curves) for the nine platforms listed in Table 1 during the St. Valentine's data collection period. The vertical dashed lines define the radar flight times. The boundary layer model used is the Large and Pond (1981) model

scheme (a conditional relaxation method) incorporating SWADE buoy data and, with lower weighting, ship reports (Gemmill 1991). In the course of the analysis procedure, the lowest-level NMC winds are reduced to surface, 10-m-level winds via a boundary-layer model. The NMC surface wind fields are shown in Appendix B for the StV period.

The current fields reported here are from the U.S. Navy Operational Gulf Stream Forecast System (NOGUFS). NOGUFS routinely provides analyses and forecasts of the current field using an eddy-resolving model incorporating optimally interpolated drifting buoy data and satellite thermal infrared sea-surface temperature and radar altimeter sea-surface topography data (Fox, Carnes, and Mitchell 1991). These surface current fields for 14-16 February are shown in Appendix C.

3 ROWS Data

ROWS Technique

The NASA/Goddard Space Flight Center's Radar Ocean Wave Spectrometer (ROWS) is a 14-GHz pulse compression radar that was initially developed as an aircraft test bed instrument for a potential satellite wave measurement system (Jackson, Walton, and Baker 1985; Jackson, Walton, and Peng 1985; Jackson 1987; Jackson 1991). Until recently, when automatic mode switching was implemented (cf. Vandemark et al. 1994a,b), the radar would have to be manually cycled between its two measurement modes: a 'spectrometer' mode and an 'altimeter' mode. Each instrument mode employs a different antenna to accomplish a specific measurement task.

In the spectrometer ('S') mode (Figure 3), a small rotary antenna whose optical axis is inclined to 16 deg from the vertical is used to measure the two-dimensional, directional reflectivity spectrum of the sea surface. At small incidence angles, the surface radar reflectivity variations are mainly due to geometrical tilting of small-scale, specularly reflecting wave facets by the underlying dominant waves. For wind speeds in excess of several meters per second, the slope variance of the smaller scale waves is generally large compared to the slope variance of the dominant waves. In this case the reflectivity modulation process can be assumed to be approximately linear on the slopes of the dominant, energy-containing waves. At high aircraft altitudes, the antenna's two-dimensional footprint on the surface is generally large compared to the scale of the dominant waves. (This is the feature of ROWS that makes it directionally sensitive). In the limiting case of large footprints, it can be shown that the wave number spectrum of the surface reflectivity modulation as seen by the radar for any particular azimuth ø of the antenna is directly proportional to the directional wave slope spectrum as

$$P_m(k,\phi) = \alpha k^2 F(k,\phi) \tag{1}$$

where

k = (radian) wave number

 α = measurement sensitivity coefficient

F = directional wave-height variance, or energy, spectrum

At microwave frequencies, the reflecting wave slope elements are approximately normally and isotropically distributed (Jackson et al. 1992). The sensitivity coefficient can then be expressed simply in terms of a single scalar surface parameter, the diffraction-effective mean square slope (MSS), as

$$\alpha = \left(\sqrt{2\pi} / L_y\right) \left(\cot \theta_e + 2 \tan \theta_e / MSS\right)^2 \tag{2}$$

where

 L_y = lateral, 1-sigma, antenna footprint dimension

 θ_e = effective incidence angle

This angle is usually taken to be 13 deg, which is the nominal incidence angle for the maximum power return within the radar range, or elevation angle, data window. The isotropy assumption is generally good to within \pm 10 percent or so in terms of the inferred directional spectrum of the energy-containing waves. However, anisotropy of the small-scale slope elements can be accounted for by using the MSS in Equation 2,

$$1/MSS \rightarrow 0.5 \left[\cos^2(\phi - \phi_1)/MSS_1 + \sin^2(\phi - \phi_1)/MSS_2\right]$$
 (3)

where the one- and two-subscripted MSSs are the principal mean square slope components, and where \emptyset_1 is the major axis direction. The slope anisotropy aspect ratio, $R = MSS_2/MSS_1$, may range from a low of $R \approx 0.8$ in strongly wind-driven cases to the isotropic limit of R = 1 in cases of low and variable winds (Jackson et al. 1992). The major axis direction generally lies close to the local wind direction.

Assuming the linear, deep-water, gravity-wave dispersion relationship, viz., $f = (gK/2\pi)^{1/2}$

where

f =frequency in hertz

K = wave number in cycles per meter

g = acceleration of gravity

Equation 1 can be rewritten for the directional height, or energy spectrum, in the frequency domain,

$$E(f,\phi) = (\pi \alpha f)^{-1} P_m(K,\phi)$$
(4)

The energy spectrum E is defined so that the significant wave height SWH,

$$SWH \equiv 4 E_0^{1/2} \tag{5}$$

where the wave height variance $E_0 = \iint E(f,\emptyset) df d\emptyset$. Normally, ROWS is operated at altitudes between 5 km and 10 km. The half-power antenna footprint dimensions are then of the order of 350-700 m in azimuth and 750-1,500 m in surface range. The combination of the finite sample window in surface range and azimuth and the finite azimuth swept out during the system integration time results in directional and wave number resolutions, respectively, on the order of 30 deg or better and 20 percent or better for waves shorter than 200 m. Statistical stability requires the averaging of spectra from a number of antenna rotations. Usually 10 rotations are averaged. When the spectra are symmetrized by averaging the spectral estimates 180 deg apart in azimuth, the resulting directional spectrum estimates have 40 degrees of freedom per elementary wave number and direction band.

Ideally, the MSS components and sensitivity coefficient α would be computed from the average power received in the spectrometer mode. However, because of the steep incidence angle (16 deg) and the relatively narrow elevation beam width (10 deg) of the antenna, the spectrometer mode power return is quite sensitive to aircraft altitude and antenna pointing errors, and so reliable estimates of the MSS and sensitivity coefficient are not easily obtainable in this system mode. This is one reason why the system is switched intermittently to the altimeter ('A') mode (Figure 3). This mode uses a relatively broad-beam antenna; hence the return power is relatively insensitive to aircraft altitude and antenna alignment errors. Estimation of the MSS parameter and the surface wind speed from the ROWS altimeter mode data is discussed in Chapter 4.

SWADE Mission

In SWADE, ROWS was operated on a small, twin-engine, T-39 training jet (Figure 4). The aircraft has a maximum altitude of about 12 km and a range of about 3 hr (about 2,200 km). Most of the SWADE flights reported here were at a constant standard pressure altitude of 7,625 m. The aircraft is less stable than the larger platforms used previously, and aircraft pitch, roll, and yaw motions affect the data reported here to an extent that has not been well determined. One effect of the aircraft motions is to cause an error in the assumed azimuth of the antenna pointing of the order of yaw angle + (antenna rotation axis tilt) $X \cot \theta_e$ where θ_e is the nominal incidence angle. To the first order, this will not affect the measurement of mean wave directions from the symmetrized spectra, but it will

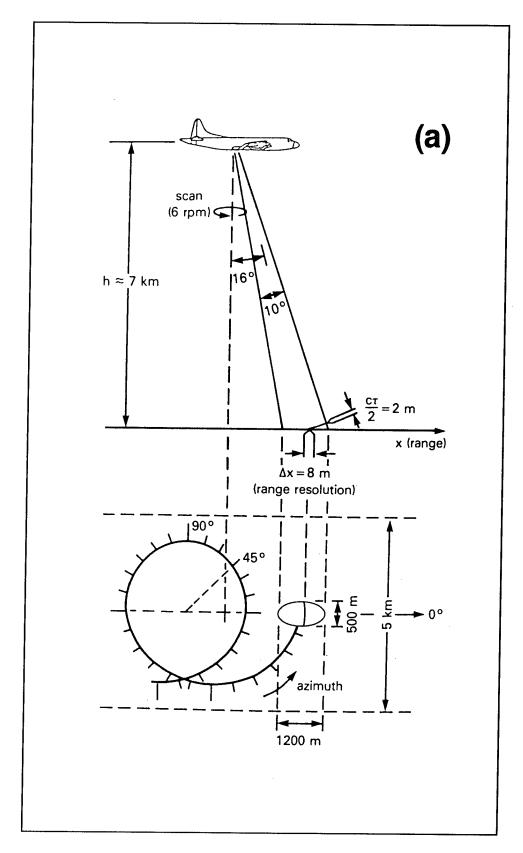


Figure 3. Radar Ocean Wave Spectrometer (ROWS) measurement geometry, (a) spectrometer ('S') mode (Continued)

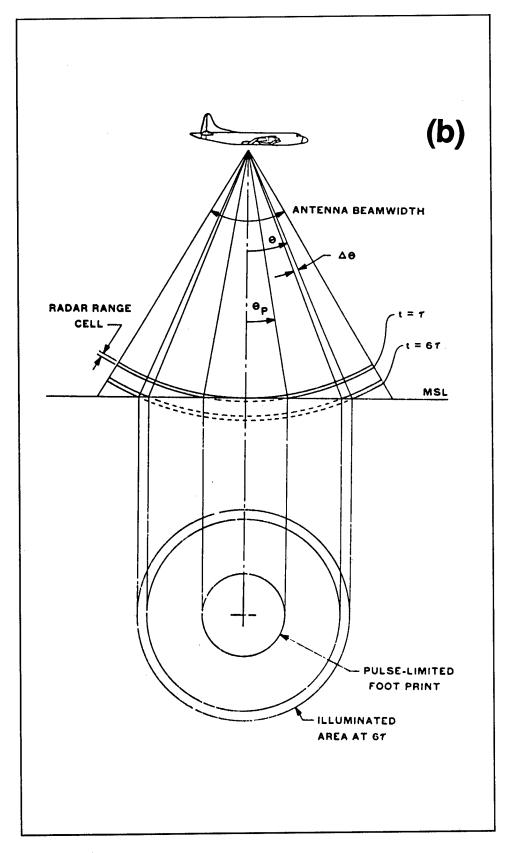
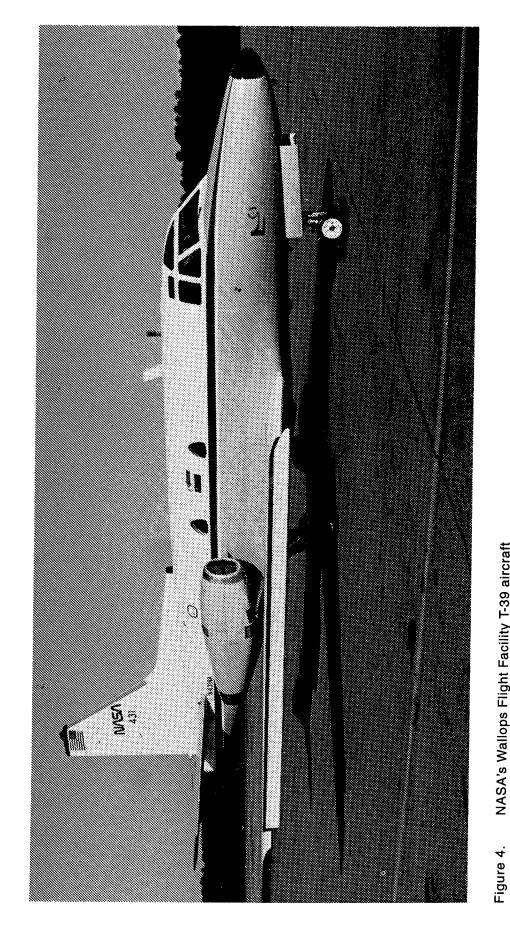


Figure 3. (b) altimeter ('A') mode (Concluded)



NASA's Wallops Flight Facility T-39 aircraft

broaden the apparent directional spreading beyond that associated with the finite directional resolution of the system.

For SWADE, ROWS was configured with a new PC-based data acquisition system that could store up to 2.5 hr of 10-ns-sampled, 100-Hz pulsereturn data on a single video cassette tape (Exabyte recording system; cf. Ward 1992). Recording resolution was eight bits and the frame size was 1,024 bytes. The pulse return data occupy the first 700 bytes of the frame; the remainder of the frame is reserved for housekeeping data. Unfortunately, it was not possible to implement automatic navigation data logging-in time for the experiment. Hence, all navigation data had to be hand-logged and flight lines and file locations manually reconstructed post-flight from the radar log, pilot's flight plan, and other sources.

In all, 17 ROWS/T-39 data flights were made between 22 January and 25 March, 1991. The dates and times of these flights are given in Table 2. Selected data from 13 of these flights have been processed; but, because adequate scaling data for the 11 February flight are lacking, data from only 12 flights are presented here. These include data from five flights in the StV period (12-16 February) and from seven flights in the IOP-3 period (27 February - 7 March). Only a small fraction of the total amount of data recorded could be processed owing to time and funding limitations. The data presented herein represent a survey of the data for each flight consisting of some 10-20 S-mode files and 5-10 A-mode files per flight. The S-mode data were processed as 100- or 150-s subfiles of the original data files, which are typically 3-5 min in length. The 100-s record lengths can correspond to anywhere between 15 km and 30 km of flight track, depending on the aircraft ground speed. The A-mode data, as a rule, were processed in 10-s subfiles. These files were generally recorded alternately with the S-mode data so as to provide scaling coefficients for the S-mode data as discussed in Chapter 4. The reconstructed flight lines accompanying the ROWS spectra in Appendix E are simplified versions of actual ground tracks which are meant only to establish the overall flight pattern. Thus, turning maneuvers, special flight patterns over buoys, and reverse courses are not shown on these maps.

SWADE Data Processing

Data processing consisted of three stages, as shown in Figure 5.

a. Preprocessing. The QUICKBASIC program PREROWS2 (Vaughn 1993) is used to (1) generate tapescans (Exabyte logs) of the flight data tapes, (2) determine the 0 deg antenna shaft encoder bit change record location, and (3) assure data quality. The Exabyte logs are used together with radar logs of navigation and file data to generate a list of files with starting frame locations for processing (N*.ASC files, * = date). The selected S-mode and A-mode data sequences (or subfiles) are then read by

Chapter 3 ROWS Data 13

Table 2 ROWS Flight Summary				
Date (1991)	Hours (LST) (UT - 5)	No. Spectra Processed	Remarks	
Jan 22	14:20-16:10	None	Poor ancillary data	
Feb 11	15:45-17:30	5	Unscaled spectra	
Feb 12	12:05-14:00	11		
Feb 14 #1	12:20-14:31	15	Start St. Valentine's	
Feb 14 #2	20:10-22:00	11		
Feb 15	15:12-17:53	19		
Feb 16	09:10-11:55	22	End St. Valentine's	
Feb 27	18:15-20:30	9	Start IOP-3 flights	
Feb 28	14:15-17:27	18		
Mar 02	15:27-18:30	10		
Mar 04	16:10-18:45	18		
Mar 05	11:43-14:14	11	SWADE priority day	
Mar 06	14:02-15:38	7		
Mar 07 #1	16:40-19:40	11		
Mar 07 #2	22:00-00:20	None	End IOP-3 flights	
Mar 11	17:25-18:57	None		
Mar 25	10:50-12:30	None		

PREROWS2 and transferred to hard disk and stored as 10-MB (S-mode) and 1-MB (A-mode) files.

b. Processing. The selected data files on hard disk are input to the C programs SAXALTD (A-mode data) and SAXSPEC (S-mode data), the original versions of which were developed for SAXON-FPN data (Jackson et al. 1993). The output of SAXSPEC (Version 2.1) consists of ASCII hard disk files (*.SRF files) of peak-value scaled directional modulation spectra P_m and ancillary data listings of the processing statistics (*.LST files). These files, along with the A-mode output files (*.OUT files), have resided at the WFF SWADE Data Archive Center since early 1993 in flight day directories (where the file tags * = local times).

Some routines in SAXSPEC differ from the routines described in Jackson, Walton, and Baker (1985) and Jackson, Walton, and Peng (1985).

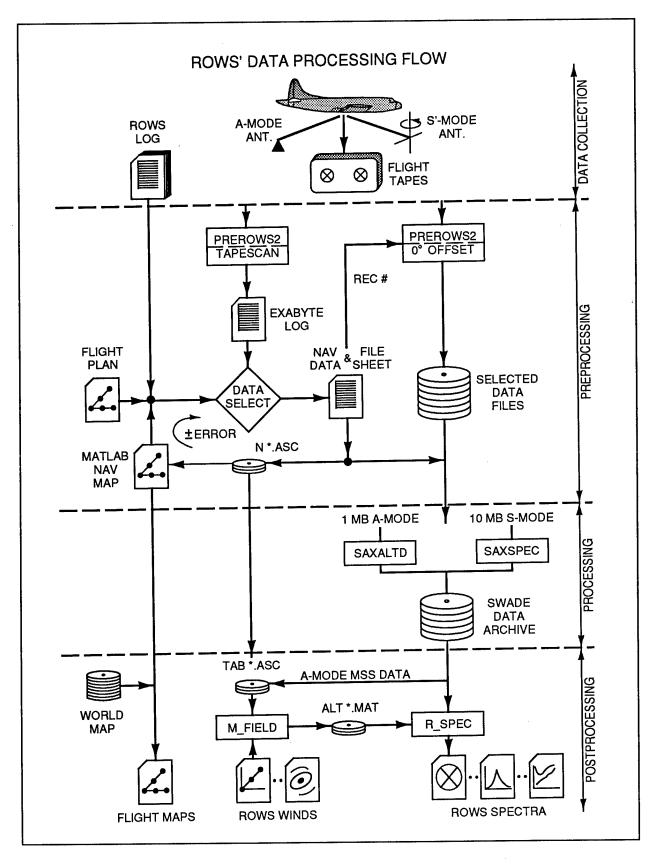


Figure 5. ROWS data processing flow

- (1) Range data window: Inner and outer incidence angle limits are 7 deg and 20 deg, but the window may be smaller if the 10 percent of peak power points lie interior to this interval.
- (2) Delay time to surface range transformation: The 10-ns time bins are rebinned into 8-m surface range bins using a 16-m boxcar smoother.
- (3) Azimuth sectors: An 18-deg sector is chosen for the basic pulse integration (50 pulse average). The spectra for these sectors are then interpolated and output in 12-deg azimuth bins in a true north-oriented reference frame.
- (4) Average power estimation and normalization: The average power envelope estimate for any sector is given by a model function fit based on a skewed normal quasi-specular scattering cross section. Four parameters are derived from the average power envelope fit using a third degree polynomial approximation to the logarithm of the return power for each sector. While the fit is generally excellent, there is some low-frequency content that is not accounted for, and so some of these data (particularly for low sea states) may have a fair amount of 'dc' component. From the cubic fit parameters we may recover pitch and roll and surface slope distribution skewness (the last only if external altitude data are available), surface mean square slope, and principal axis direction. The fit parameters are listed in the last four columns of the sector summary data in the *.LST files. After power normalization, the usual Hanning window is applied to the wave modulation signal.
- (5) Noise background subtraction: The average value of the spectrum in the last 32 bins is used as a preliminary estimate of the noise background.

The surface range window for FFT is 2,048 m. When this exceeds the actual range extent of the pulse return data, the record outside of the actual data window (e.g., as determined by the 7-deg and 20-deg points) is padded with zeros. Accordingly, the spectral resolution will generally be less than that indicated by the elementary wave number bin size and there will be some correlation overlap between spectral estimates. For data compression, the spectrum data are block averaged in logarithmically spaced intervals to produce 35 output bins. In the frequency domain, the rebinned data range from f = 0.055 Hz to f = 0.31 Hz.

c. Postprocessing. All successfully executed A- and S-mode output files for each flight are ordered sequentially as Smmdd.nn and Ammdd.nn files, where mmdd = month and day and nn = file sequence number. The header data for the *.SRF files are stripped and the peak normalization constant is inserted into the (1,1) matrix element of the 36 X 31 arrays (row 1 = azimuth in degrees, column 1 = frequency in Hz). The navigation and file tables N*.ASC (* = mmdd) are augmented with A-mode altitude and MSS data and stored as TAB*.ASC files.

All postprocessing software is written in MATLAB for PC:

(1) The program M_FIELD reads TAB*.ASC data and interpolates A-mode MSS and U_{10n} data to the S-mode file locations as described in Chapter 4. The output data for each flight are stored as ALF*.MAT files (* = mmdd). Table 3 describes these data files.

Table 3 ALF*.MAT File Contents		
Column	Data Element	
1	File sequence number	
2	Month	
3	Day	
4	Hours, UT	
5	Minutes	
6	Latitude, degrees north	
7	Longitude, minus degrees west	
8	Aircraft altitude, m	
9	Aircraft ground speed, m/s	
10	Aircraft heading, degrees true	
11	Neutral 10-m wind speed U _{10n} , m/s	
12	Mean square slope (MSS) parameter	
13	Minimum degrees of freedom	

(2) The program R_SPEC reads the S*.nn (* = mmdd) header-stripped spectral matrices and scales the spectra using the interpolated MSS data in ALF*.MAT. A correction factor, FAC = 4*delx*256 (delx = 8 m) is applied to the spectra to correct a scaling error in SAXSPEC. The routine SENS is then called on to compute the sensitivity coefficient _ from the MSS data according to Equations 1-3. For all data except the StV data, an isotropic MSS is used; for the StV data, the anisotropic form (Equation 3) is used. In SENS the measured MSS is subject to a correction based on the difference between the MSS versus wind speed relationship in the original ROWS training data set for wave spectra (Jackson, Walton, and Baker 1985) and the altimeter wind speed versus MSS relationships (Equation 10). The correction is

$$MSS_{\alpha} = 1.22 \ MSS_{Measured} - 0.007 \tag{6}$$

R_SPEC performs several other postprocessing functions as well, including a final noise background subtraction and a point target response correction. The noise background is approximated by a smoothed estimate of the minimum in the measured directional power spectrum as a function of frequency. The point target response is taken to be the same as in Jackson, Walton, and Baker (1985) and Jackson, Walton, and Peng (1985). Most of the data processed in this manner exhibit f^4 power-law behavior in the rear-face region of the wind-sea spectrum out to 0.2 Hz or more (ca. 40-m wavelength), whereafter a spectral roll-off occurs (cf. Figure 12, panel 'd'). To account for this roll-off, the observed nondirectional spectrum for f > 0.2 Hz is replaced by a f^4 power-law spectrum with a spectral constant that is determined by the value of the observed spectrum at 0.2 Hz.

R_SPEC generates polar contour and scaled nondirectional spectra plots by calling on the routine S_PLOT, a modified version of the plotting software used for buoy spectra. R_SPEC also contains a directional analysis package that computes the mean direction and directional spreading as a function of frequency (see Chapter 5). R_SPEC outputs the array DEL*.MAT (or the array EPS*.MAT for the anisotropic StV data) containing derived spectral products as shown in Table 4. Chapter 5 discusses these data products in more detail.

(3) The program WA_FIELD reads DEL*.MAT (or EPS*.MAT) files and plots "Custer" diagrams of the wave field and other derived data products as discussed in Chapter 5.

Table 4 DEL*.MAT and EPS*.MAT File Contents		
Column(s)	Data Element	
1-13	Alpha vector as described in Table 3	
14	Cutoff frequency, f_min	
15	Peak frequency of nondirectional spectrum, f_pknd	
16	Peak period, 1/f_pknd	
17	Mean period, T_bar	
18	Peak of nondirectional spectrum, s_pknd	
19	Confidence interval for peak, ci_pk	
20	Significant wave height of tail patch region, Hs_tail	
21	Significant wave height, Hs (SWH)	
22	Direction at peak of directional spectrum, phi_pk	
23	Peak direction at f_pknd, phi_pknd	
24	Mean direction, phi_bar, according to WAM Group definition	
25	Spread parameter, sig_phi, according to WAM Group definition	
26-35	Blanks (NaNs)	
36-70	Frequency, f	
71-105	Fully scaled nondirectional spectrum, s_nd	
106-140	Mean direction versus f from 2nd harmonic phase, dirs(:,4)	
141-175	Half power full-width directional spread from s2 parm dirs(:,5)	

Chapter 3 ROWS Data 19

4 ROWS Winds

ROWS was switched periodically from the instrument's spectrometer ('S') mode to the instrument's nadir-looking altimeter ('A') mode to collect data on:

- a. Significant wave height (SWH) and wind speed (U_{10n}) .
- b. Mean square slope (MSS) for scaling the ROWS spectra.
- c. Mean altitude (H) to correct the aircraft pressure altitude.

The A-mode data takes were generally around 1 min in duration as compared to 3-5 min for typical S-mode data takes. As a rule, the data takes for the two modes were alternated, or interleaved (see flight line maps in Appendix E). A problem with the triggering of the digitizer has precluded the recovery of meaningful SWH estimates from the wave form data in the leading edge region. Thus, wave height data for SWADE are only available via the scaled ROWS spectra.

A total of 88 selected A-mode files have been prepared for the 12 processed SWADE flights listed in Table 2. The locations of these files are shown on the flight line maps in Appendix E by 'X's' and the files are denoted 'A1', 'A2', etc. in the chronological order of the data takes. As a rule, the A-mode data were processed as 10-s subfiles, one subfile per file of raw data, using a four-parameter wave form fit to the average pulse return data as described below.

Wave Form Fits

As shown in Figure 3, the altimeter mode uses a relatively broad beamwidth (32.4 deg) fixed, nadir-pointing antenna to collect surface information beneath the aircraft. The antenna pattern in the main lobe is approximately Gaussian. The ROWS pulse shape is also approximately Gaussian. Since the sea surface slope distribution is quasi-isotropic and approximately normally distributed, it follows from the quasi-specular scattering model that the average altimeter power return wave form W(t) is given by (Jackson et al. 1992):

$$W(t) = (A/2) \left\{ 1 + erf \left[(t - t_o) / 2^{1/2} \sigma \right] \right\} \exp \left[-(t - t_o) / \tau \right]$$
(7)

where A is the wave form amplitude, t_o is the time of return from the mean sea surface (epoch), and σ and τ are the leading and trailing edge wave form parameters, respectively, given by

$$\sigma = \left[(SWH / 2c)^2 + \sigma_p^2 \right]^{1/2}$$
 (8a)

$$\tau = (H/c)(1/MSS + 1/\sigma_b^2)^{-1}$$
(8b)

where c is the speed of light, H is the aircraft altitude, and σ_p and σ_b are respectively the 1-sigma radar pulse width and antenna beam width parameters as given in Jackson et al. (1992).

Processing of A-mode data consists of: (a) bias estimation and subtraction, (b) epoch (t_0) estimation and pulse realignment based on 50-pulse (0.5-s) averages, and (c) four-parameter iterative least square fitting of the model wave form (Equation 7) to 2.5-s averages of the realigned pulse returns, where the fit is limited to nadir angles \leq 15 deg. The output of SAXALTD consists of four estimates each of the MSS, the epoch t_0 (or mean altitude H), and the SWH for every processed 10-s subfile. Output also includes wind speed estimates, which are derived from the MSS estimates according to the algorithm described below. If no inordinate fluctuation in any of the fit parameters occurs, the four values of mean altitude, wind speed, and MSS are averaged and entered into the table TAB*.ASC (* = mmdd) as discussed in Chapter 3.

Figure 6 is an example of the altimeter average wave form data (10-s averages) from the March 2 flight. The power in the tail region is seen to be well approximated by exponential decay as predicted by the Gaussian specular point model (Equation 7). A linear log-power dependence on delay time holds for nearly 20 dB of dynamic range.

A posteriori wave form fit correction

Direct wind speed comparisons with the SWADE buoys (see below) show a significant bias in the ROWS wind speeds inferred from the SAXALTD full wave form fit MSS data. A study of the ROWS altimeter-mode wave form data from the recent HIRES mission (Vandemark et al. 1994b) shows that there is a bias between the MSS inferred from the full wave form fits and the MSS inferred by a fitting of the wave form trailing edge region

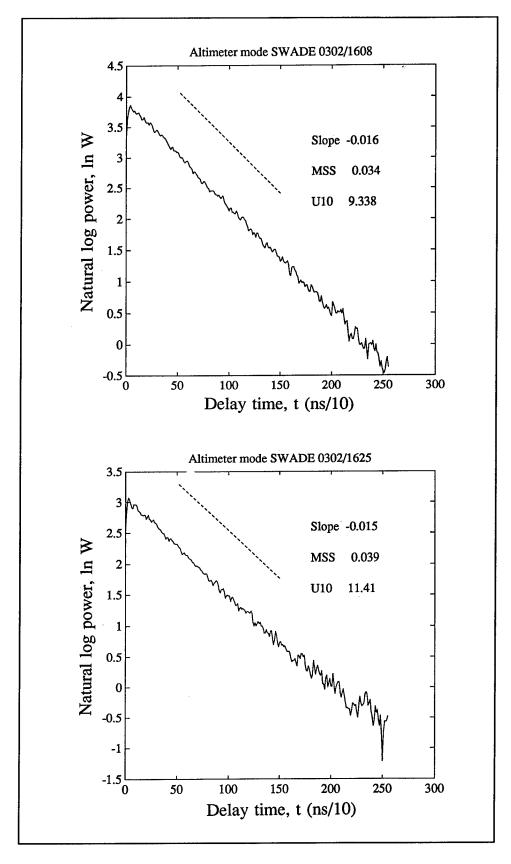


Figure 6. Examples of altimeter mode average wave form data

alone. Figure 7 is a scatterplot of these data. A linear regression of MSS from the tail region fit on the full wave form fit MSS gives

$$MSS_{Tail\ Fit} = 1.0523\ MSS_{Full\ Fit} + 0.00022$$
 (9)

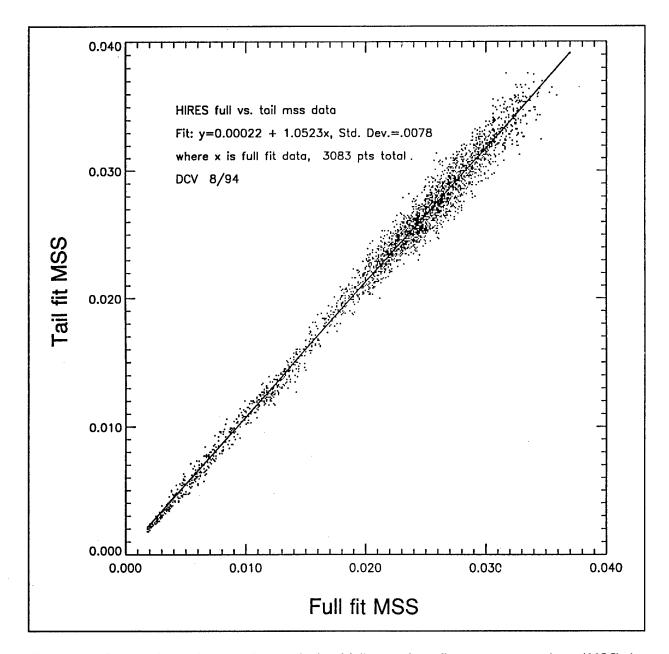


Figure 7. Scatterplot and regression analysis of full wave form fit mean square slope (MSS) data versus tail region wave form fit MSS data

Chapter 4 ROWS Winds 23

Personal communication, D. Vandemark, NASA, Wallops Flight Facility, Wallops Island, Virginia.

The scaled spectra and wind speed data presented in Appendix E are based on SAXALTD full wave form fit MSS. These stastical buoy wind speeds have been corrected according to Equation 9.

Wind speed algorithm

For wind/wave conditions not too far removed from equilibrium, the MSS can be expressed in terms of the 10-m-level neutral equivalent wind speed U_{10n} according to the quasi-empirical relationships found in Jackson et al. (1992). The ROWS wind speed algorithm consists of the inverse of these relationships, viz.,

$$U_{10n} = \exp(100*MSS - 1.1), \qquad 0 \le MSS \le 0.028$$
 (10a)

$$U_{10n} = (MSS - 0.013) / 0.0023, \qquad MSS \ge 0.028$$
 (10b)

Although the relationships of Equation 10 were developed from ROWS aircraft data alone, they provide excellent predictions for satellite altimeter wind speed data (Jackson et al. 1992).

Interpolation Fields

As discussed in Chapter 3, ROWS spectra in SWADE are scaled using A-mode estimates of the MSS. Because the A-mode data do not always neatly bracket the S-mode data, a simple linear interpolation between adjacent data points is generally not possible. Instead, two-dimensional least squares interpolating polynomials of the MSS and U_{10n} are constructed as functions of latitude and longitude using the A-mode data input from TAB*.ASC. The degree of the fit polynomial is taken to be the highest possible consistent with the limited number of A-mode data points. The interpolating polynomials are then evaluated at the S-mode locations (principally for the MSS scaling data) and at the buoy locations (principally for wind speed comparisons). The fits are accomplished using the MATLAB program M_FIELD. The interpolated MSS and U_{10n} data at S-mode file locations are output in the MATLAB data file ALF*.MAT.

Evaluation of the 2-D fit polynomials at the A-mode locations shows a fit error of at most 1 ms⁻¹ rms in terms of wind speed. Thus we expect a fairly good representation of the local MSS at the S-mode file locations, except perhaps in cases of rapid wind/wave field changes (for example, near currents); or, in cases where there are only a few A-mode data points to define the field; or, in cases where the S-mode and A-mode files are geographically widely separated. Figure 8 shows the constructed fields of altimeter-mode U_{10n} for the four StV flights between 14 and 16 February. The highest degree fit polynomial is n = 3 (for 16 February; total of 11 data points) while the lowest is n = 1 (for 14 February, flight No. 2; five

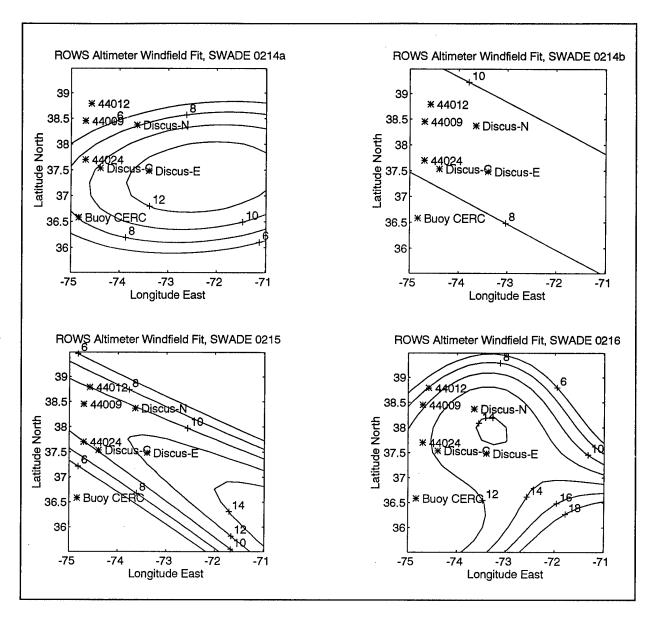


Figure 8. Fields of ROWS altimeter-mode inferred 10-m neutral wind speeds for the four St. Valentine's flights from least-square polynomial fits to the observations

valid data points). Note that in these plots, the uncorrected full wave form fit MSS data have been used.

ROWS Versus Buoy Winds

Indirect wind speed comparisons

Figure 9 compares the altimeter-inferred U_{10n} from the interpolation fields of Figure 8 with buoy wind speeds. The altimeter U_{10n} evaluated at

Chapter 4 ROWS Winds 25

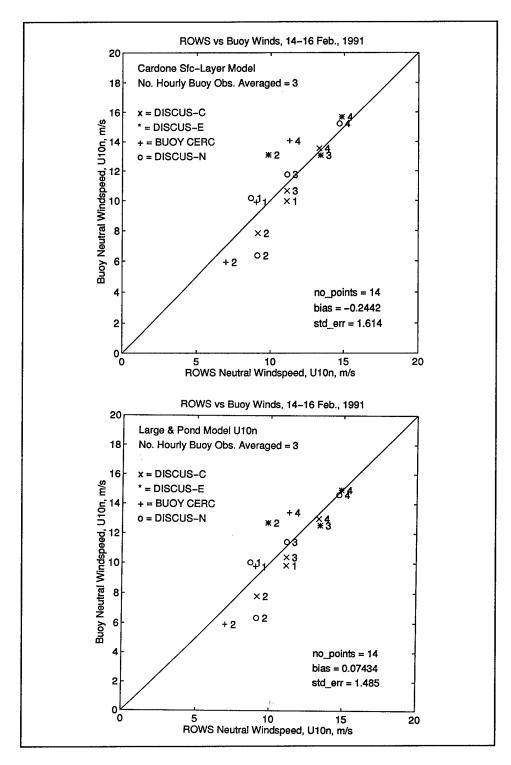


Figure 9. Buoy 10-m neutral winds versus ROWS-inferred 10-m neutral winds for the four St. Valentine's flights. The ROWS winds are from the corrected wave form fit interpolation fields corresponding to the fields of Figure 8. The buoy winds are conputed using the Cardone (a) and the Large and Pond (b) boundary layer models. The numbers 1-4 indicate the ROWS flight number.

the buoy locations are compared to the mean buoy U_{10n} observed within \pm 1 hr of the nominal flight time. The buoy U_{10n} are computed according to the Large and Pond (1981) boundary layer model using the buoy-measured air-sea temperature differences. The agreement is seen to be generally quite good. For StV flight No. 4 on 16 February, the flight with the highest degree polynomial fit, the agreement is better than $\pm 1 \text{ ms}^{-1}$ for the three SWADE buoys, Discus-N, Discus-E, and Discus-C. For all flights there is excellent agreement with centrally located Discus-C. The data contain only one outlier, the CERC point for flight No. 2. In this case the winds were low and variable and the CERC buoy lay fairly well outside the low degree fit region of the radar flight plan. If this point (and the Discus-E null data point for flight No. 1) are excluded from the comparison, then 14 data points remain; these show a bias of + 0.8 ms⁻¹ (buoy minus ROWS wind speed) and a standard error of 1.8 ms⁻¹ over the observed range of $\sim 7-15 \text{ ms}^{-1}$. We note again that the comparison here for the four flight days of the StV event is based on the uncorrected full wave form fit MSS data. If the wave form fit correction (Equation 9) were used. the bias might be reduced somewhat (see below).

Direct wind speed comparisons (all data)

ROWS-inferred U_{10n} for the 12 SWADE flights in the period 12 February-7 March are compared to buoy wind speeds in Figures 10 and 11. The comparisons are made for ROWS-buoy separation distances (proximity circles) of 10 km, 25 km, and 50 km. The temporal window in each case is taken to be the ROWS data take time \pm 0.55 h. If two hourly buoy observations fall within this window, these observations are averaged. In all cases the in situ neutral wind speeds are computed according to the Large and Pond (1981) boundary layer model.

Figure 10 compares the full wave form fit ROWS U_{10n} estimates (as output from SAXALTD) to in situ U_{10n} estimates for the 50-km proximity circle case. The comparison consists of 49 "hits" on 9 different platforms. These platforms are listed in Table 1. The ROWS full wave form fit U_{10n} are seen to be biased low with respect to the buoy U_{10n} by about 1.5 ms Figure 11a shows the same comparison, but for the ROWS MSS data corrected according to Equation 9. With this correction, the bias in inferred U_{10n} is reduced to -0.5 ms⁻¹ (ROWS - buoy). The linear regression of the in situ U_{10n} on the ROWS U_{10n} is now very close to the line of perfect agreement. Going to the smaller separation distances (Figures 11b and 11c), one sees a decrease in the standard deviation from 2 ms⁻¹ in the 50-km case to 1.8 ms⁻¹ in the 25-km case (22 hits) and 1 ms⁻¹ in the 10-km case (7 hits). These standard deviation errors are comparable to those found in satellite altimeter versus buoy wind speed comparisons involving similar temporal and spatial offsets (Dobson, Monaldo, and Goldhirsh 1987).

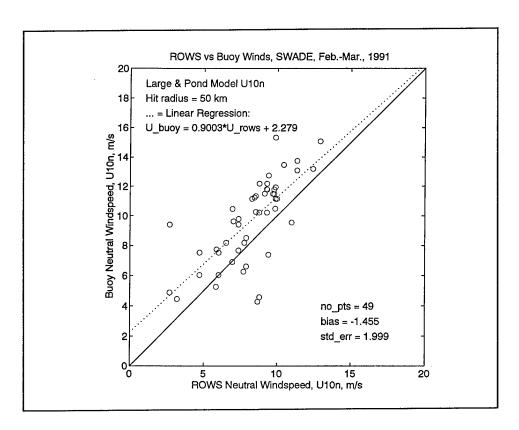


Figure 10. Buoy neutral wind speeds (Large and Pond model winds) versus ROWS uncorrected full wave form fit neutral wind speeds for a 50-km proximity circle

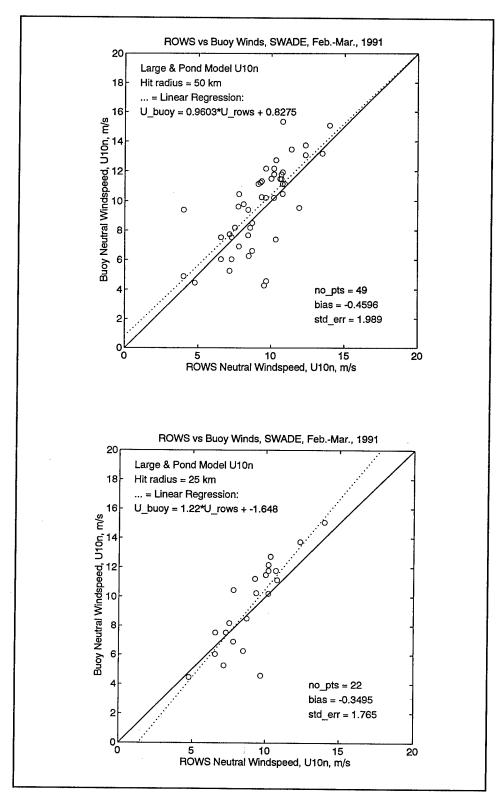


Figure 11. Buoy neutral wind speeds (Large and Pond model winds) versus ROWS wind speeds from corrected wave form fit data:
(a) 50-km proximity circle, (b) 25-km proximity circle (Continued)

29

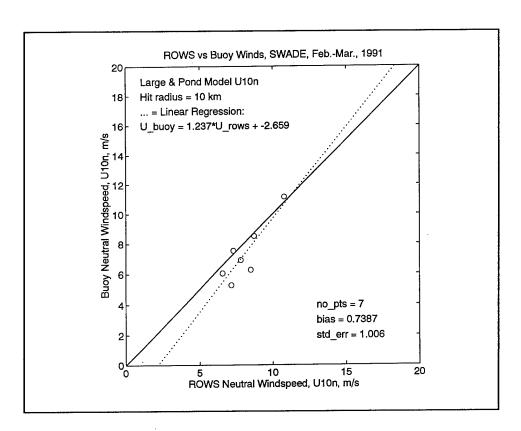


Figure 11. (c) 10-km proximity circle (Concluded)

5 ROWS Spectra

Appendix E contains ROWS directional and nondirectional spectra plots for the 12 T-39 flights in the period 12 February - 7 March, 1991. The appendix also contains flight line maps, navigation and file location data sheets, and weather maps (Appendix F) for each flight day. The spectra are plotted in the same format as the buoy spectra in Appendix D. This has resulted in some loss of detail in many of the spectra because of the high frequency range of the plots (outermost frequency ring = 0.4 Hz). For the SWADE priority day (March 5), however, plots with a maximum frequency of 0.2 Hz have been included to permit a better display of the complex modal structure in the energy-containing region of these spectra. All spectra in Appendix E have been produced using an isotropic sensitivity coefficient α based on interpolated A-mode MSS data as discussed in Chapters 3 and 4.

Each directional spectrum plot in Appendix E is accompanied by a wind speed (W) and a peak and mean direction (pd and md) estimate; each non-directional spectrum plot is accompanied by a wave height (Hs) and a peak period (Tp) estimate. The wind speed estimates are from the A-mode interpolation fields of neutral wind speed as discussed in Chapter 4. The spectral peak direction is the directional maximum at the peak frequency f_pknd of the nondirectional spectrum as obtained from a parabolic fit to the binned data. Similarly, f_pknd is obtained by parabolic fit to the nondirectional spectrum peak and the peak period is taken as $Tp = 1/f_pknd$. The mean direction and mean period are computed from the binned spectrum data according to the definitions

$$\overline{\phi} = a \tan \left(\langle \sin \phi \rangle / \langle \cos \phi \rangle \right) \tag{11a}$$

$$\overline{T} = \langle f^{-1} \rangle \tag{11b}$$

where the moment $<...> \equiv E_o^{-1} \iint (...) E(f,\phi) df d\phi$. A low-frequency cutoff is imposed to ensure that spurious low-frequency content in the measured spectrum does not corrupt these estimates. All these derived products are contained in the DEL*.MAT files as shown in Table 4. Note that the peak period and direction data for the buoy spectra in Appendix D are simple bin values as defined in the original S_PLOT program. Thus they cannot be expected to agree with the more precise ROWS values.

Frequency-Direction Plots

Appendix E also contains frequency-direction plots for the four StV flights. The directional analysis consists of the following: After prewhitening the directional spectrum by multiplying by f^5 and smoothing the data in frequency in the rear-face region, the measured first and second angular harmonics for each frequency band are equated to the corresponding first and second harmonic values of an assumed cosine-power model directional distribution function

$$D(f,\phi) = D_o(s) \left[\cos((\phi - \phi_o)/2)\right]^{2s}$$
(12)

where D_o is a normalization constant (cf. Longuet-Higgins, Cartwright, and Smith 1963). Two estimates of the spread parameter, $s \equiv s_{\alpha}(f)$, and mean direction, $\phi_o \equiv \phi_{o\alpha}(f)$ ($\alpha = 1,2$) result from equating the first two measured harmonics to the first two harmonics of Equation 12. From the estimated spread parameters, the corresponding half-power directional spreads are calculated according to

$$\Delta \phi = 4a \cos \left[\left(1/2 \right)^{1/2s} \right] \tag{13}$$

The analysis approach was arrived at after testing a number of estimators for the mean direction as a function of frequency. These tests showed the phase angle of the second angular harmonic of the symmetrical radar directional spectrum to be the most stable estimator of mean direction; also, the second harmonic mean direction estimates were found to be very close to the average of the mean direction estimates from two alternative estimators. In the case of the polar-symmetric radar data, a meaningful, nonzero first harmonic can be inferred from the radar angular distribution only if the 180-deg directional ambiguity is removed. For the present analysis, a likely direction of travel is chosen on the basis of meteorology and buoy observations. The radar spectrum is then redefined as being nonzero only in the 180-deg direction band between the absolute minima in the symmetric spectrum in the appropriate half space (see also Jackson, Walton, and Peng (1985)). Restricting the direction band to 180 deg results in an isotropic limit for the first harmonic half-power spread of $\pi/(\pi-2)$, or $\Delta \phi_{iso} = 112.1$ deg.

The mean directions so computed tend to be unstable at higher frequency when the standard isotropic sensitivity is used. Thus for the directional analyses, we use an anisotropic sensitivity based on an anisotropic MSS as defined by Equation 3. For the aspect ratios and principal directions, the values given in Table 5 are assumed. The principal axis direction is taken be the average wind direction as represented in Figure 2. The aspect ratios are essentially educated guesses.

Table 5 Assumed Anisotropy for St. Valentine's Data			
Flight	Time ¹ , UT	Direction, ϕ_1	Aspect Ration, R
No. 1 (Feb. 14a)	17:59-19:09 (14 Feb.)	039°	0.85
No. 2 (Feb. 14b)	01:28-02:41 (15 Feb.)	102°	0.95
No. 3 (Feb. 15)	20:34-22:34 (15 Feb.)	102°	0.80
No. 4 (Feb. 16)	14:33-16:27 (16 Feb.)	122°	0.80

Example Data Products

Figure 12 is an example of the kind of ROWS data products that are available with post-processing. The example file S11 is from the southern leg of the first StV flight on 14 February (see Appendix E flight maps for file locations). Here, the spectrum is represented in both polar (panel 'a') and rectangular forms (panel 'c'). Contouring is logarithmic. The directionally integrated spectrum is given in both linear-linear form (panel 'b') and in log-log form (panel 'd'). Panel 'f' is a frequency-direction plot for the spectrum. Panel 'e' shows the cosine-power model fit to the directional distribution at the spectrum peak.

The spectrum example is for a nearly fully developed sea (Jackson and Jensen 1995). As with most observed unimodal spectra, the directional distribution is well fitted by the model function (Equation 12). From the frequency-direction plot in panel 'f,' it is seen that the mean direction is nearly constant with frequency and equal to 4 deg true azimuth. The directional spreading (which, we note, has not been corrected here for finite system resolution) is about 60 deg at the spectral peak. The first harmonic spreads saturate at the isotropic limit of 112.1 deg around 0.2 Hz. From panel 'd' it is seen that the rear face of the nondirectional spectrum follows a f^4 power law out to about 0.2 Hz, beyond which frequency a spectral roll-off is evident. The f^4 power law behavior in the rear face region is typical of the ROWS data collected in SWADE.

Custer Diagrams

Synoptic views of the wave field in the SWADE area at the times of the four StV flights are presented in Figure 13 in the form of "Custer" diagrams, in which the ROWS and buoy-observed mean wave periods and directions are represented by arrows of various lengths and directions. In

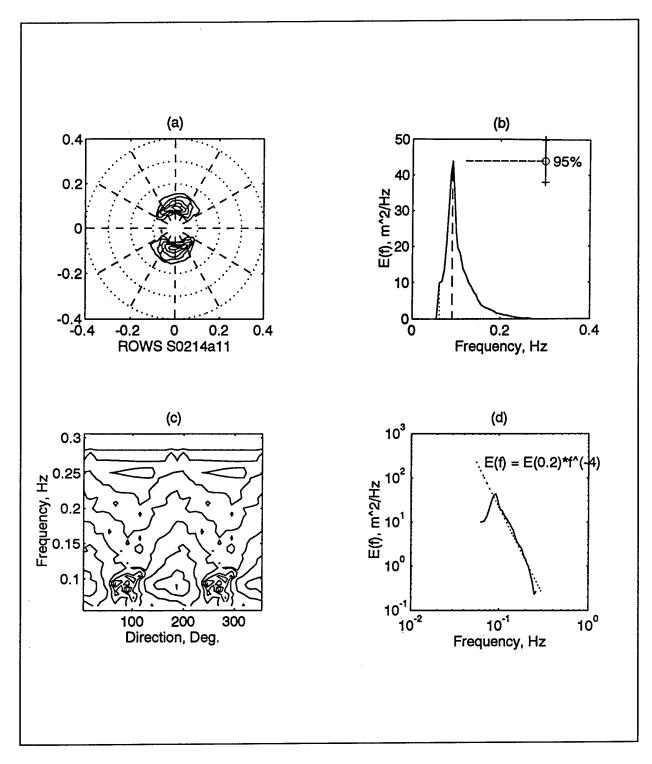


Figure 12. Detailed analysis of ROWS spectrum file S11 for flight No. 1 on 14 February: (a) Polar contour plot of directional energy spectrum, contour levels in 2.5-dB decrements from spectral peak and frequency axis scales in Hz, (b) Nondirectional energy (height-variance) spectrum, with 95-percent confidence interval for peak as indicated, (c) Rectangular contour plot of the directional spectrum with logarithmic contour spacing, (d) Log-log plot of nondirectional height spectrum with f⁻⁴ power-law (dotted line) (Continued)

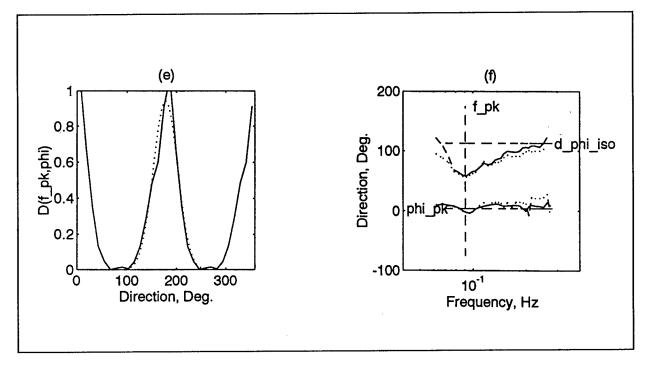


Figure 12. (e) Cosine-power model function fit (dotted curve) to the directional distribution at the peak of the nondirectional spectrum (solid curve), (f) Directional analysis: Lower curves are first (dotted lines) and second (solid line) harmonic phase angles; upper curves are the model function half-power full-widths (dotted line, first harmonic fit; solid line, second harmonic fit). f_pk is the frequency of the peak of the nondirectional spectrum; phi_pk is the peak direction at f = f_pk; and d_phi_iso is the isotropic limit for the first-harmonic directional half-power spreading (Concluded)

these figures, the coastline of the southern MAB is idealized as two straight lines, one running north and one south from Cape Henry, VA. The notch in the northern coastline is meant to represent the added fetch area associated with the Delaware Bay. Mean wave directions and periods are computed from the radar and buoy directional spectra according to the definitions in Equation 11.

Fetch-Limited Data

The StV wind-turning event concludes on 16 February with strong, steady northwesterly winds. By the time of the fourth StV flight on the 16th, the wave field has adjusted to the new fetch-limited conditions. The Custer diagram for this flight shows the mean wave vectors on the southern flight leg to be aligned with the mean wind direction of 122 deg (direction to). On the northern flight leg, the mean wave directions are rotated some 10-30 deg northward of the wind direction. This may be an effect of the Delaware Bay (Jackson and Jensen 1995).

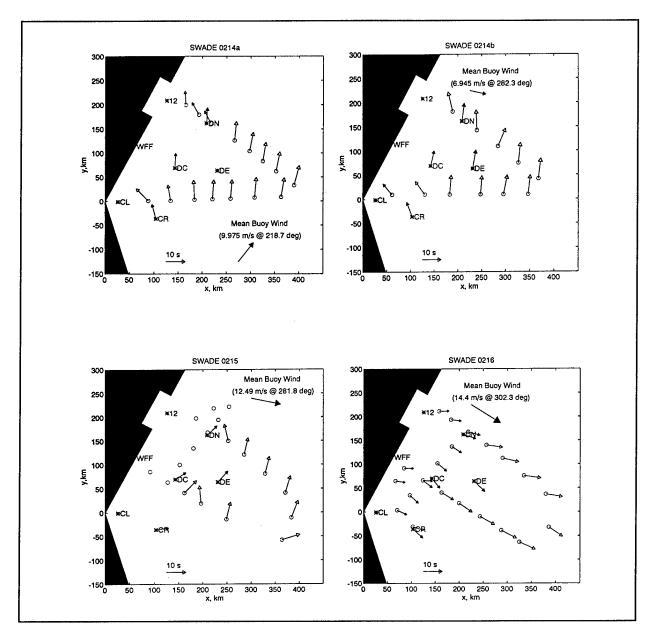


Figure 13. Custer diagrams of the mean wave vectors (mean directions and periods) for the four ROWS St. Valentine's flights (o = radar data; * = buoy data) on a Cartesian map with idealized coastline. The notch in the northern coastline represents an added fetch area associated with the Delaware Bay

In Figure 14, the wave energy and peak frequency for all radar and buoy observations at the time of the fourth StV flight on 16 February are plotted in nondimensional form as a function of the fetch normal to the idealized northern coastline. Data for both frequency and energy show an approach to the Pierson-Moskowitz (PM) limits around the largest observed fetch of about 375 km. These limits are computed assuming a wind speed of $U_{10n} = 13.7$ m/s, which is the mean wind speed for ROWS files S05-12. The buoy and radar data agree fairly well, except near the

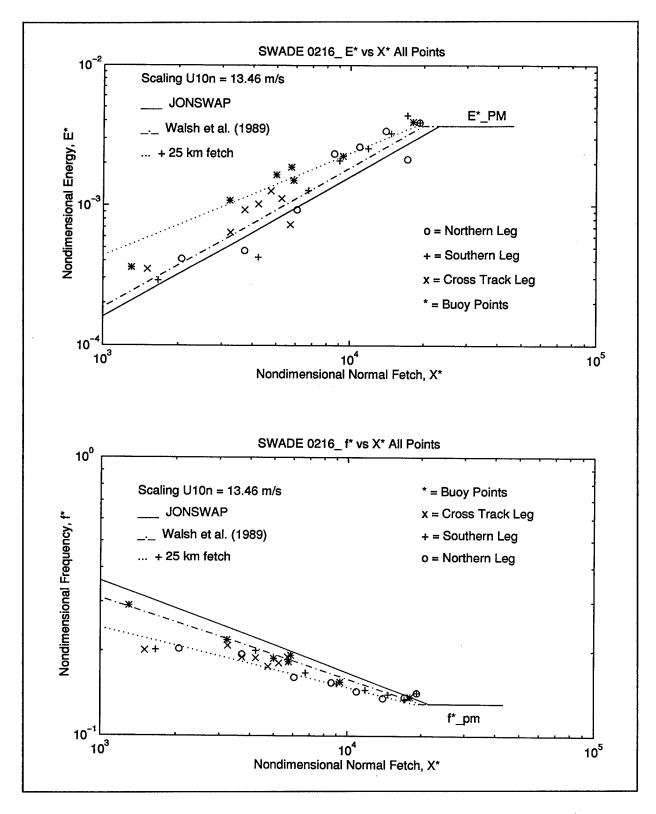


Figure 14. Radar and buoy nondimensional energy (upper panel) and peak frequency (lower panel) data versus nondimensional fetch for 16 February 1991 with empirical growth laws. The curve for the extra 25-km fetch is intended to model the possible effect of the added fetch region around the mouth of Delaware Bay

shelf break, where the buoys are relatively high in both energy and frequency compared to the radar observations. The discrepancies here may be due to poor ROWS response in low sea states. They may also be due to wave field variability in the vicinity of the shelf break. However, similar discrepancies have been observed with the SCR¹; thus, it is quite possible that the buoy data are in error.²

Nondimensional fetch, frequency, and energy are given, respectively, by

$$X^* = (g / U_{10n}^2) X \tag{14a}$$

$$f^* = (U_{10n} / g) f \tag{14b}$$

$$E^* = (g^2 / U_{10n}^4) E \tag{14c}$$

where $E \equiv \text{SWH}^2$. A scaling wind speed of $U_{10n} = 13.7$ m/s is assumed. As seen in Figure 14, the nondimensional energy data agree fairly well with the JONSWAP linear fetch law, $E^* = 1.60 \times 10^{-7} X^*$, but the peak frequency data differ significantly from the JONSWAP fetch law, viz. $f^* = 3.5 \times 10^{-3} X^*$ (Hasselmann et al. 1973). The ROWS data in both energy and frequency are seen to agree better with the modified fetch laws proposed by Walsh et al. (1989), namely, $E^* = 1.86 \times 10^{-7} X^*$ and $f^* = 2.3 \times 10^{-2} X^*$

38

Personal communication, E. Walsh, NASA/Wallops Flight Facility, Wallops Island, Virginia. On assignment at the NOAA/ERL Wave Propagation Laboratory, Boulder, CO.

Note in proof: recently reprocessed data for discus E and C show better agreement with the data; however, the buoy wave heights and frequency data remain higher than the ROWS data.

6 Conclusion

This report presents all ROWS wind and wave data that have been processed for SWADE. The production of more data is unlikely given that the author is no longer with NASA. ROWS data reduction for SWADE was unusually demanding. Over 3 months were taken in the manual reduction of the navigation and file data alone. The data processing itself required manual intervention to establish the zero degree azimuth offset. Scaling of the spectra required interpolation of altimeter mode data to the spectrometer mode file locations.

Since the SWADE experiment, work on the ROWS system has eliminated the sources of the aforementioned difficulties in data collection and data reduction. Antenna shaft encoder data are now properly recorded; navigation data are now electronically logged; switching to the altimeter mode now is automatic so that the spectrum data can be easily scaled; the digitizer is now properly synchronized with the radar so that wave height data are available directly from the altimeter mode data (albeit with only 10 ns resolution; cf. Vandemark et al. (1994a,b)).

ROWS data quality for SWADE is generally quite good. The only problems encountered with the data are: (a) 'dc' contamination of the spectra in low sea state cases (wave heights less than 2 m) and (b) directional broadening of the spectra caused by aircraft altitude variations. It is possible also that some of the spectra are poorly scaled. Poor scaling may occur in cases where large wind and/or wave field gradients exist between the spectra observations and the altimeter mode observations used to scale the spectra. These problems should not detract from the usefulness of the data for a number of possible SWADE investigations. The most interesting set of ROWS data collected in SWADE is from the St. Valentine's Day wind/wave event. The fetch diagrams of Figure 14 from the fourth St. Valentine's flight provide an example of the usefulness of the ROWS SWADE data for wave research.

Chapter 6 Conclusion 39

A ferrite switch switches between the two ROWS antennas on an alternate pulse basis. Thus ROWS operates continuously with a 50 percent duty cycle, that is with 50 pulses per second for each ROWS mode.

Since 1993, ROWS spectra (*.SRF files) and altimeter data (*.OUT files) have been archived at the NASA/WFF SWADE Data Archive Center. With the publication of this report, additional ROWS data such as the spectrum scaling data will be made available to the public in electronic format.

References

- Cardone, V. J. (1969). "Specification of the wind distribution in the marine boundary layer for wave forecasting," Technical Report TR-69-01, Geophys. Sciences Lab., New York Univ.
- Caruso, M. J., Graber, H. C., Jensen, R. E., and Donelan, M. A. (1993). "Observations and modelling of winds and waves during the Surface Wave Dynamics Experiment; Report 1, Intensive Observation Period IOP-1, 20-31 October 1990," Technical Report CERC-93-6, U.S. Army Engineer Waterways Experiment Station, Vicksburg, MS.
- Dobson, E. B., Monaldo, F., and Goldhirsh, J. (1987). "Validation of Geosat altimeter-derived wind speeds and wave heights using buoy data," J. Geophys. Res. 92, 10,710-10,731.
- Drennan, W. M., Graber, H. C., and Donelan, M. A. (1996). "On the measurement of directional wave spectra from pitch-roll buoys," journal article in preparation,
- Fox, D. N., Carnes, M. R., and Mitchell, J. T. (1991). "Gulf Stream mesoscale forecasting." *Proc. MTS '91 Conf.*, Marine Technology. Soc., New Orleans, LA, 411-414.
- Gemmill, W. H. (1991). "High-resolution regional ocean surface wind fields." Ocean Data Products Center Contrib. No. 54, National Meteorol. Center., Boulder, CO, 190-192.

- Hasselmann, T. P., Barnett, E., Bouws, H., Carlson, D.E., Cartwright, K., Enke, J. A., Ewing, H., Gienapp, D. E., Hasselmann, P., Kruweman, A., Meerburg, P., Muller, K. J., Olbers, K., Richter, W. Sell, and Welden, W. H. (1973). "Measurements of wind-wave growth and swell decay during the Joint North Sea Wave Project (JONSWAP)," Ergang. Deut. Hydrogr. Zeit. A(8^O), Deut. Hydrogr. Institut (in English).
- Jackson, F. C., Walton, W. T., and Baker, P. L. (1985). "Aircraft and satellite measurement of ocean wave directional spectra using scanning-beam microwave radars," J. Geophys. Res. 90, 987-1004.
- Jackson, F. C., Walton, W. T., and Peng, C. Y. (1985). "A comparison of in situ and airborne radar observations of ocean wave directionality," J. Geophys. Res. 90, 1005-1018.
- Jackson, F. C. (1987). "The radar ocean wave spectrometer," Johns Hopkins APL Tech. Digest 8, 116-127.
- _____. (1991). "Directional spectra from the radar ocean wave spectrometer during LEWEX." Directional ocean wave spectra. R. Beal, ed., The Johns Hopkins Univ. Press, Baltimore, MD, 91-97.
- Jackson, F. C., Walton, W. T., Hines, D. E., Walter, B. A., and Peng, C. Y.
 (1992). "Sea surface mean square slope from Ku-band backscatter data,"
 J. Geophys. Res. 97, 11,411-11,427.
- Jackson, F. C., Vandemark, D., Bailey, S., Vaughn, C., Hines, D., Ward, J.,
 Stewart, K., and Chapron, B. (1993). "ROWS wave spectral data
 collected in SAXON-FPN, November, 1990," NASA Technical
 Memorandum 104582, Goddard Space Flight Center, Greenbelt, MD.
- Jackson, F. C., and Jensen, R. (1995). "Wave field response to frontal passages during SWADE," J. Coastal Res. 11, 34-67.
- Large, W., and Pond, S. (1981). "Open ocean momentum flux measurements in moderate to strong winds," *J. Phys. Oceanogr.* 11, 324-336.
- Longuet-Higgins, M. S., Cartwright, D. E., and Smith, N. D. (1963). "Observations of the directional spectrum of sea waves using the motions of a floating buoy." *Ocean wave spectra*, Prentice-Hall, Englewood Cliffs, NJ, 111-136.
- Oberholtzer, D., and Donelan, M. A. "SWADE data guide," in preparation, Goddard Space Flight Center, Greenbelt, MD.
- Steele, K. E., Teng, T. C., and Wang, C-C. (1992). "Wave direction measurements using pitch-roll buoys," *Ocean Engineering* 19, 349-375.

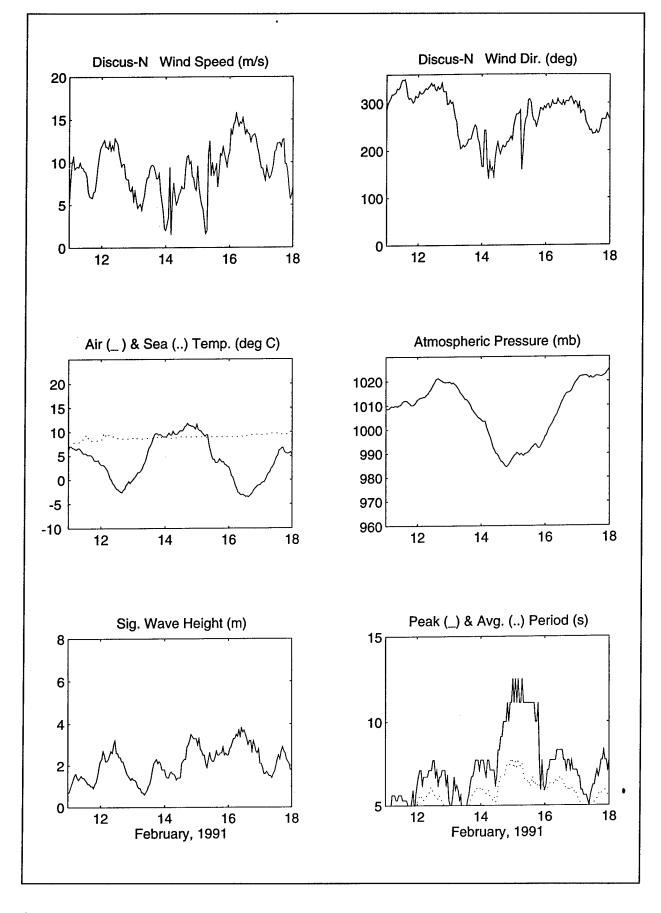
- Vandemark, D., Jackson, F. C., Walsh, E. J., and Chapron, B. (1994). "Airborne radar measurements of ocean wave spectra and wind speed during the Grand Banks ERS-1 SAR Wave Experiment," Atmosphere-Ocean 32, 143-178.
- Vandemark, D., Jackson, F. C., Walsh, E. J., Chapron, B., Hines, D., Bailey, S., and Stewart, K. (1994). "Airborne ROWS data report for the High Resolution Experiment, June 1993," NASA Technical Memorandum 104609, Goddard Space Flight Center, Greenbelt, MD.
- Vaughn, C. (1993). "Radar Ocean Wave Spectrometer (ROWS) preprocessing program (PREROWS2.EXE)," NASA Technical Memorandum 104579, Goddard Space Flight Center, Greenbelt, MD.
- Walsh, E. J., Hancock, D. W. III, Hines, D. E., Swift, R. N., and Scott, J. F. (1989). "An observation of the directional wave spectrum evolution from shoreline to fully developed," J. Phys. Oceanogr. 19, 670-690.
- Ward, J. (1992). "A PC-based data acquisition system as applied to the Radar Ocean Wave Spectrometer," NASA Technical Memorandum 104560, Goddard Space Flight Center, Greenbelt, MD.
- Weller, R. A., Donelan, M. A., Briscoe, M. G., and Huang, N. E. (1991). "Riding the crest: A tale of two wave experiments," *Bull. Am. Mereorol. Soc.* 72, 163-183.

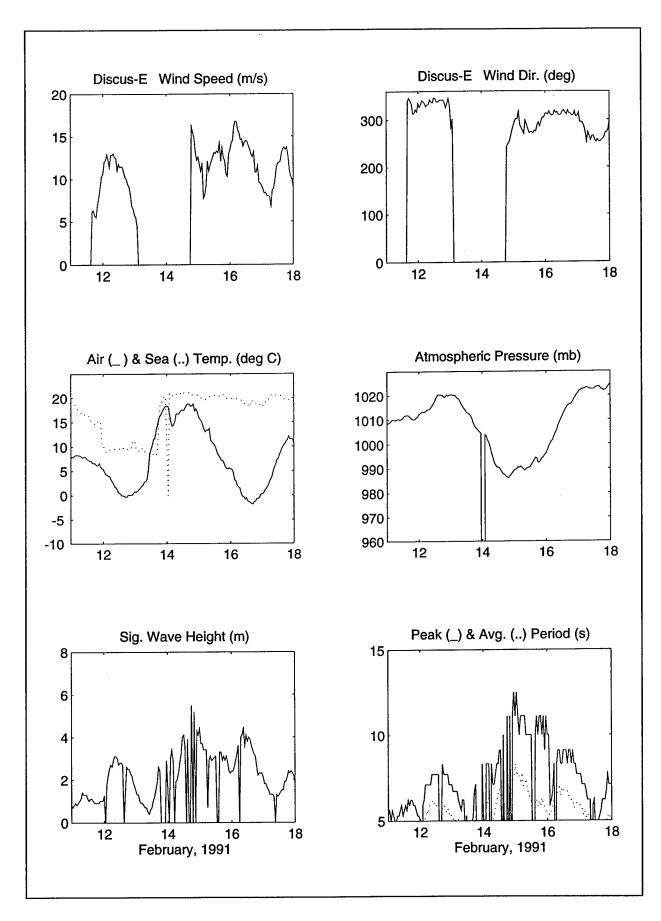
References 43

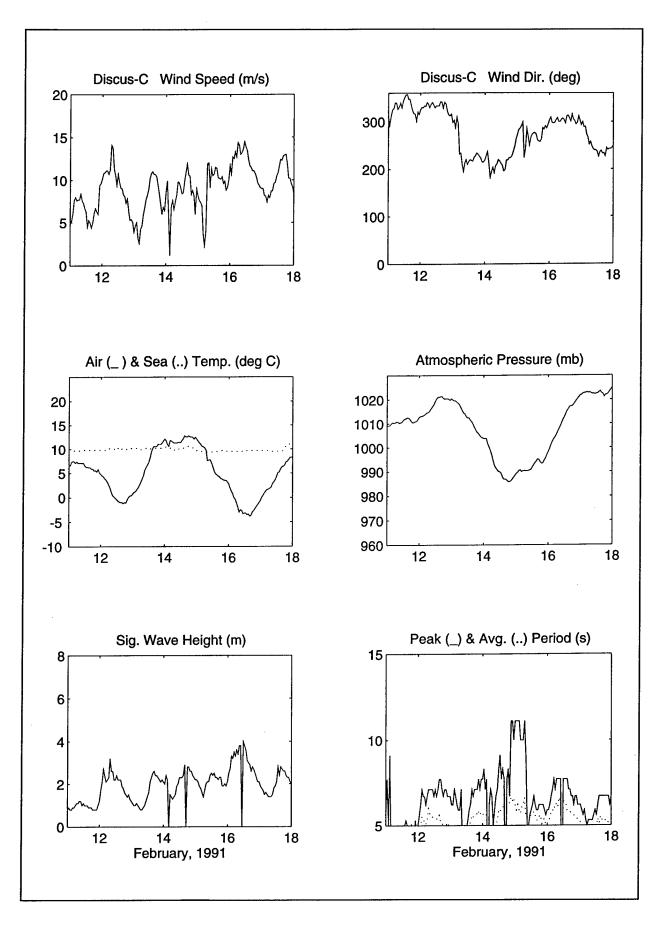
Appendix A Buoy Environmental Data, 11-18 February 1991

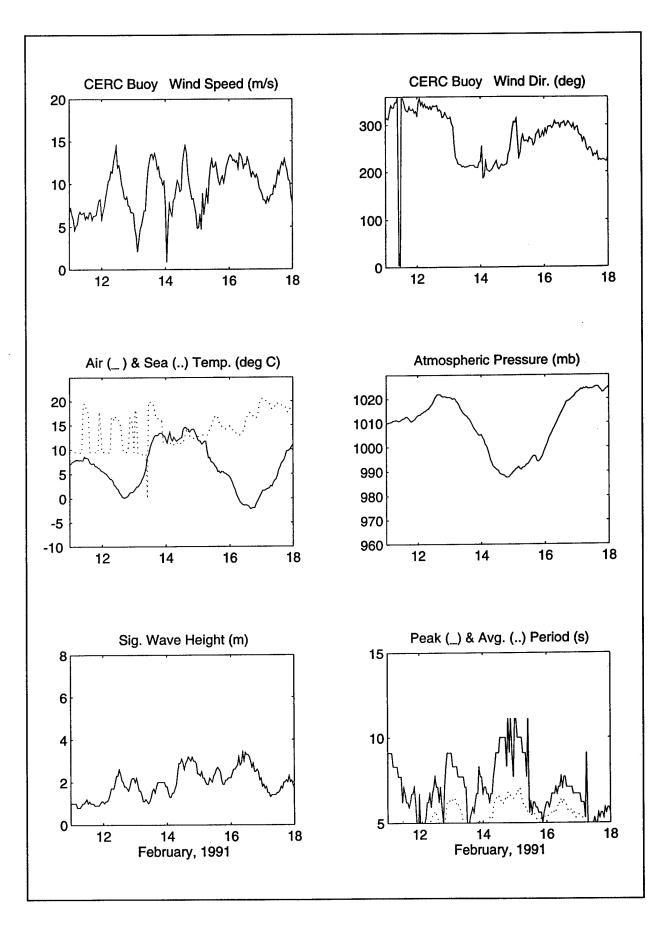
This appendix contains time series of buoy environmental data for the St. Valentine's observational period. These data are also contained in the report by Caruso et al. (1994); however, the time scale there is compressed, making the data for this interesting period difficult to read. The data presented here are for nine platforms. The locations of these data collection platforms are given in Table 1 in the main text.

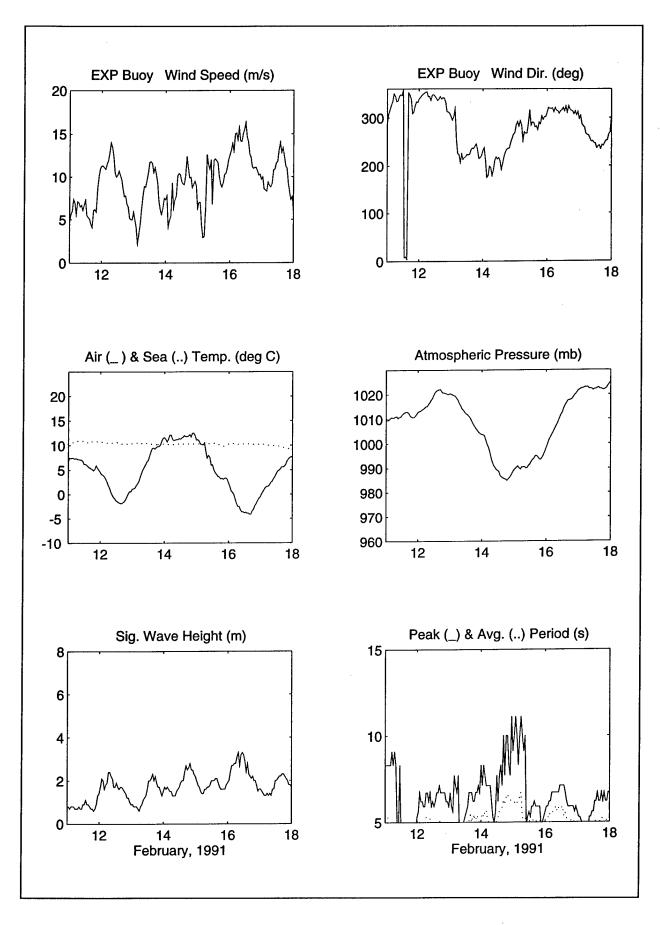
Note that the buoy mean periods are plotted here according to the second moment definition. Buoy mean periods for the Custer diagrams of Figure 13 are according to the first moment definition, Equation 11b.

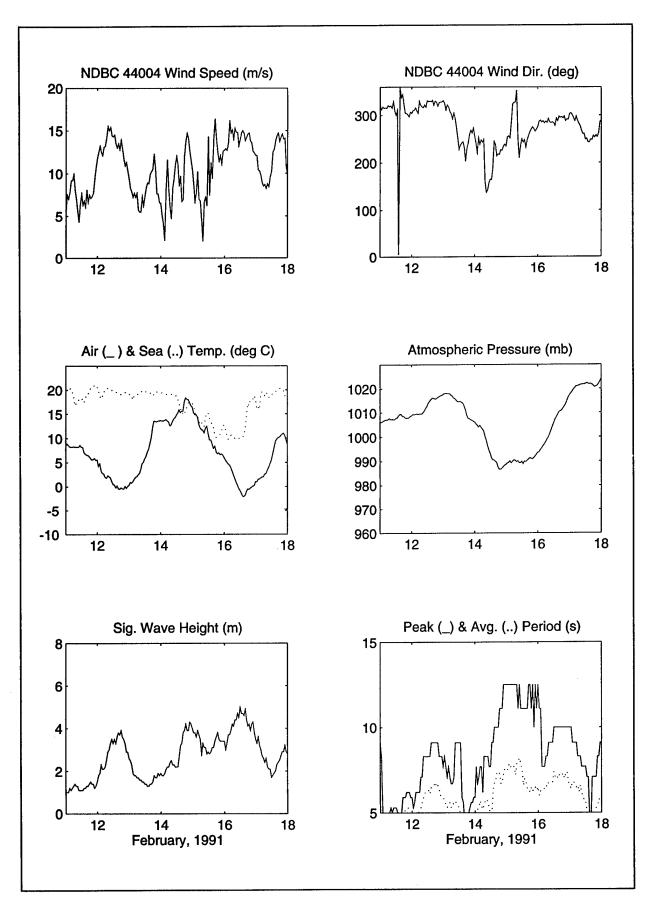


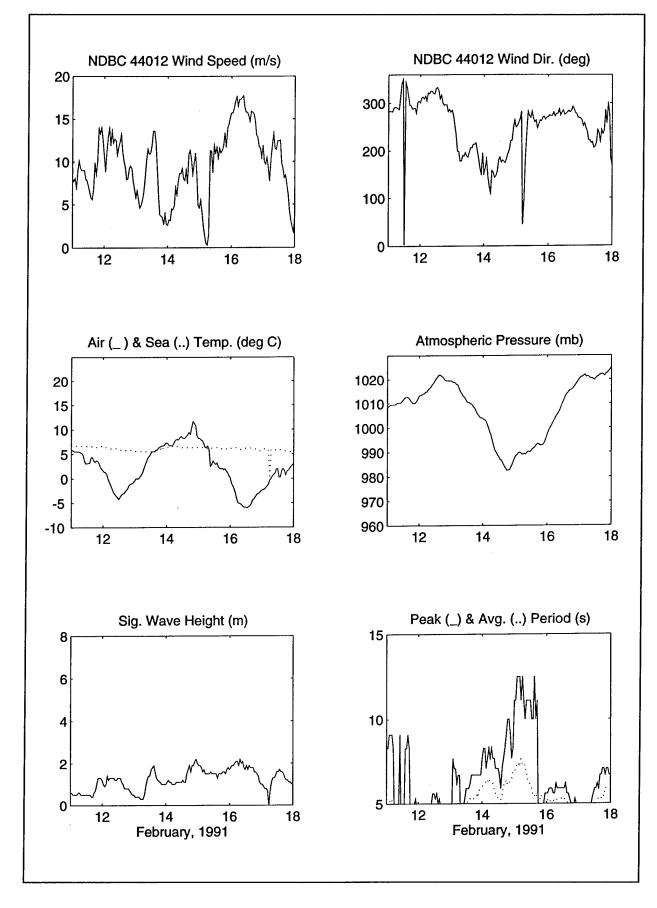


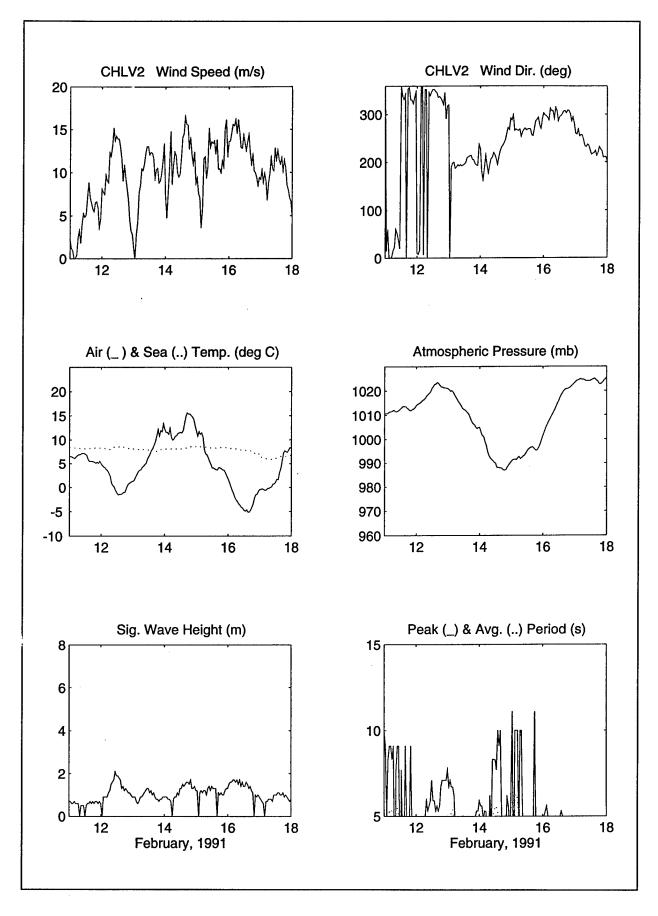


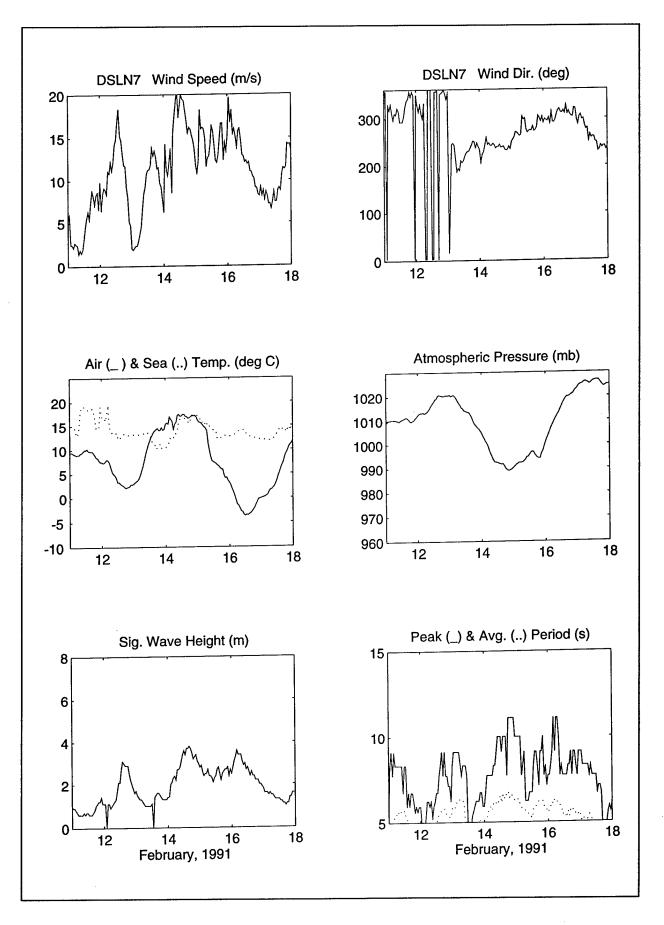




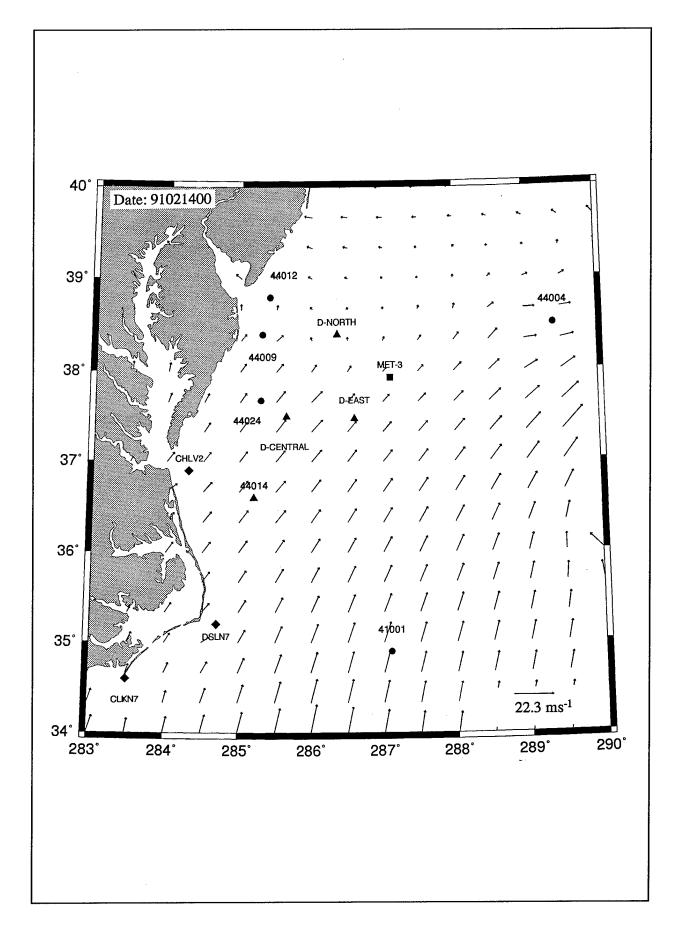


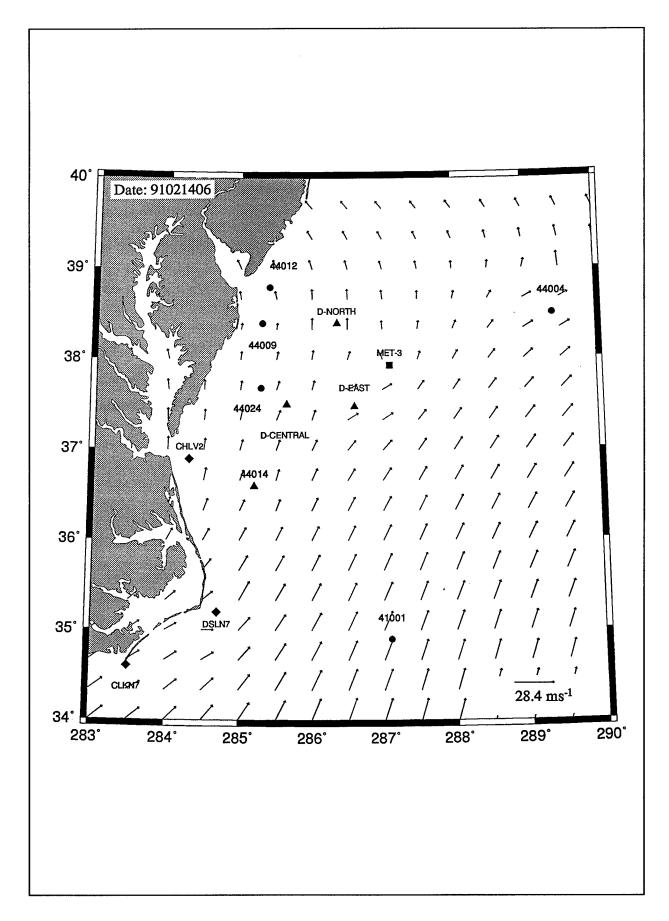


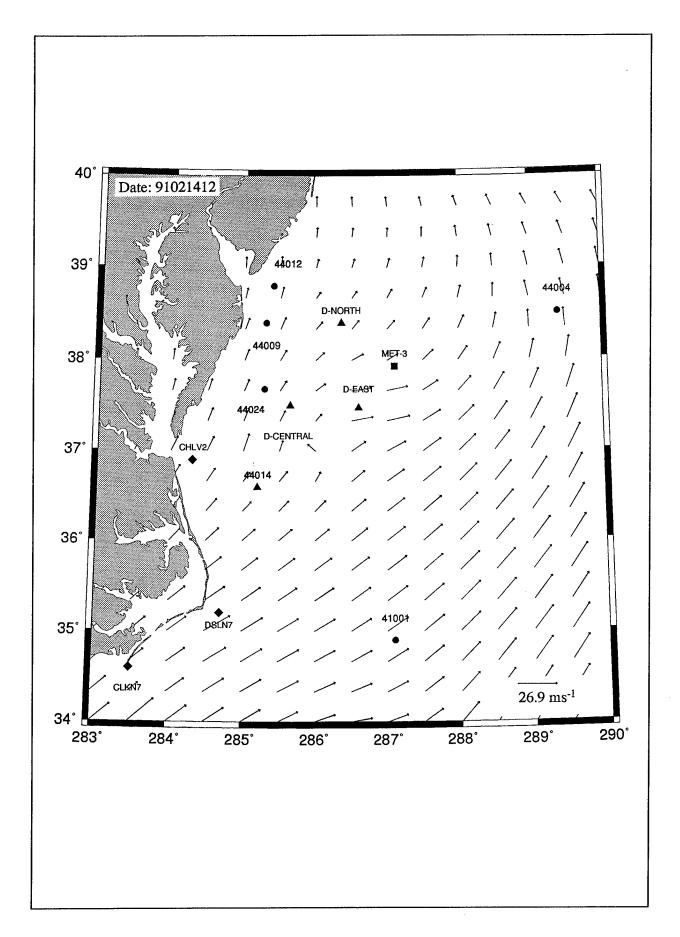


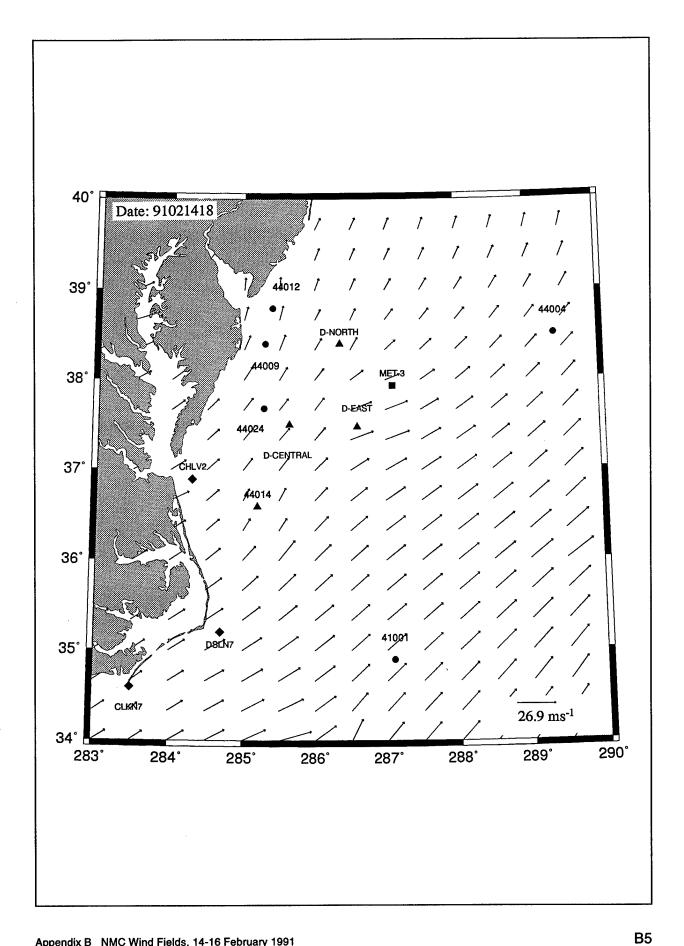


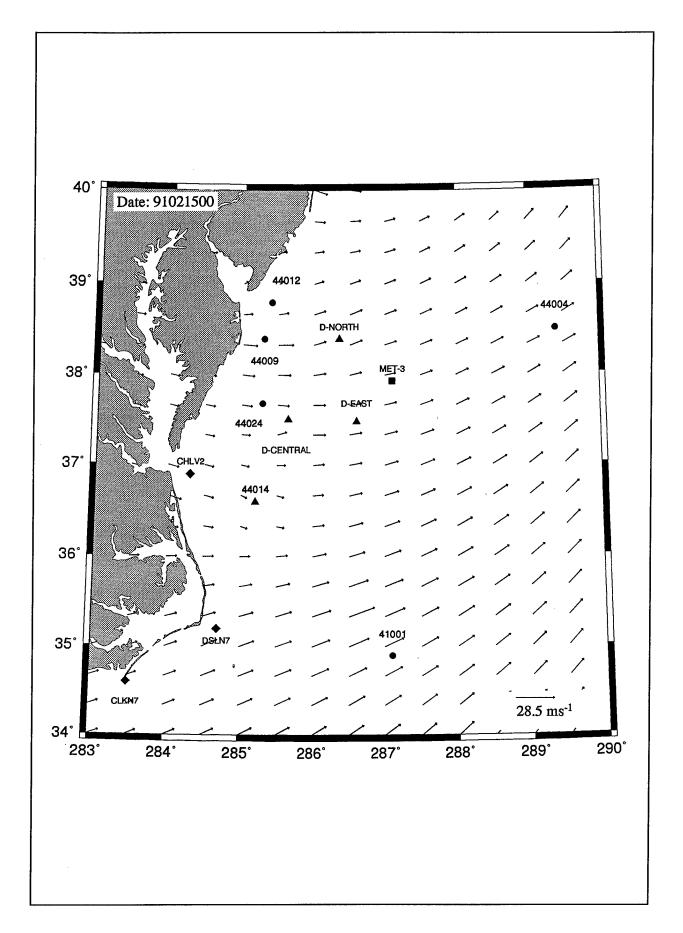
Appendix B NMC Wind Fields, 14-16 February 1991

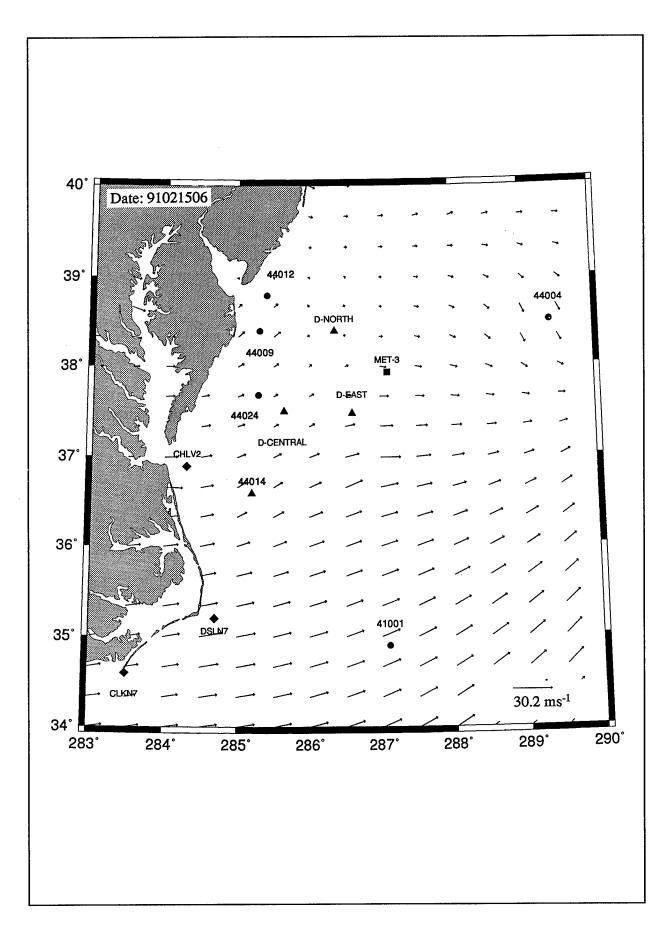


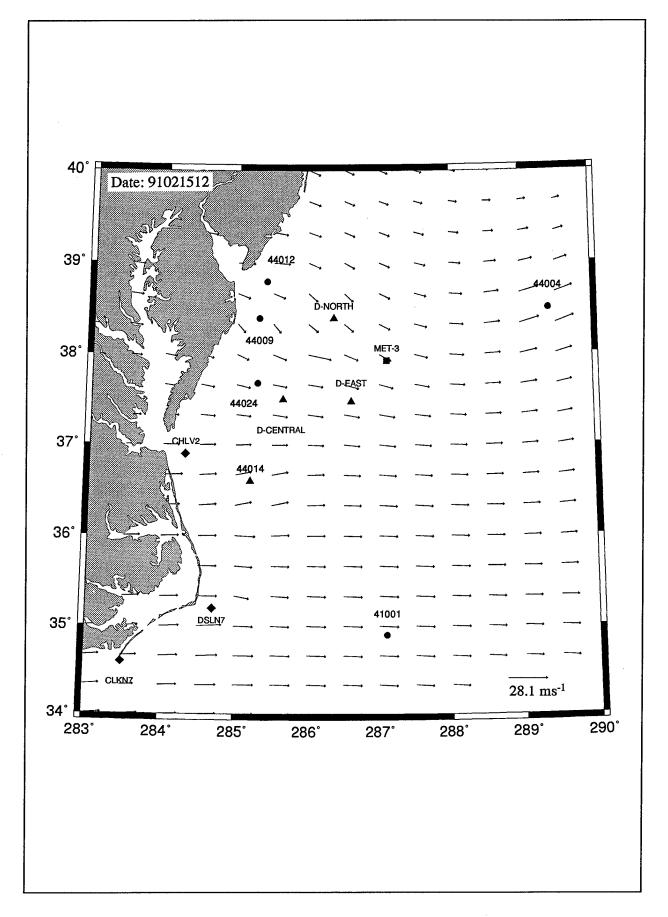


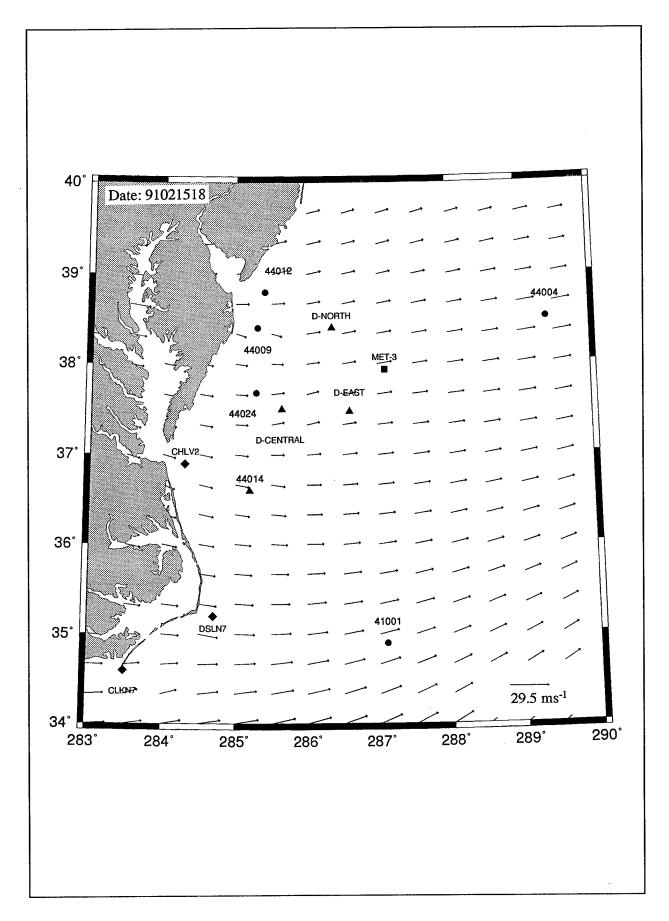


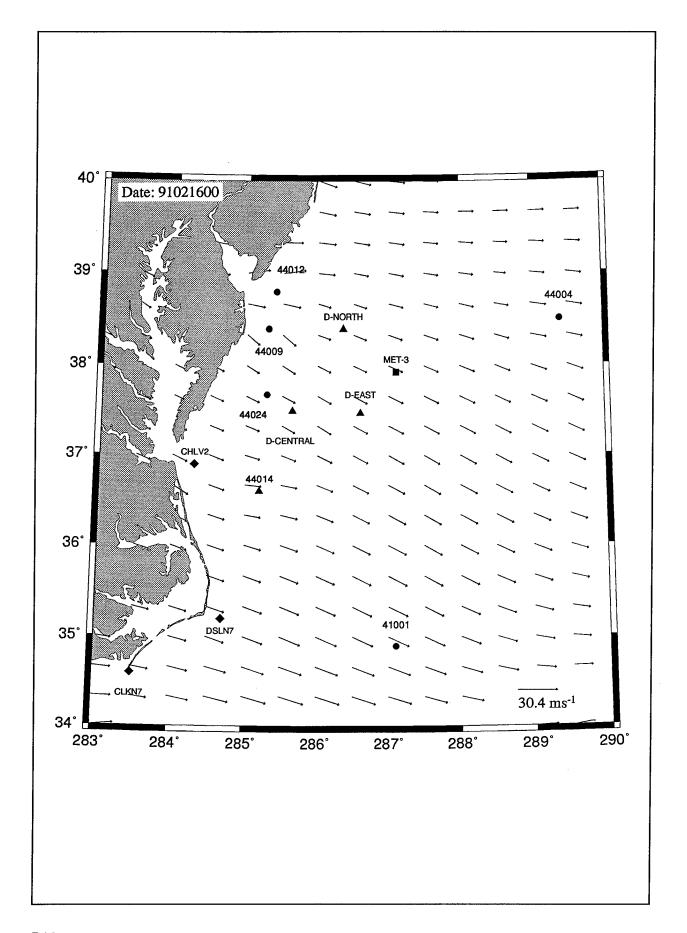


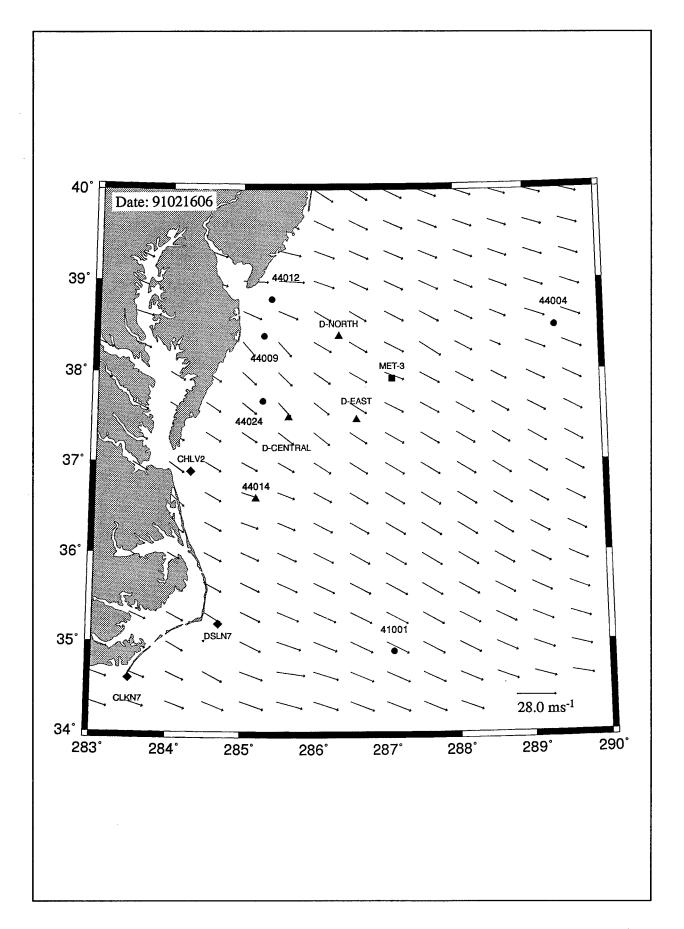


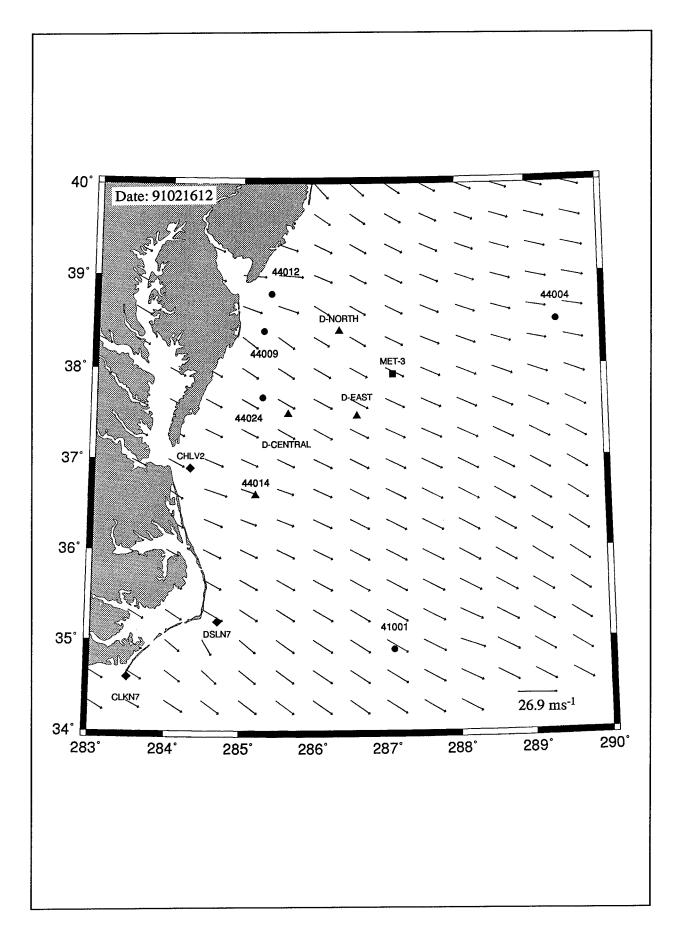


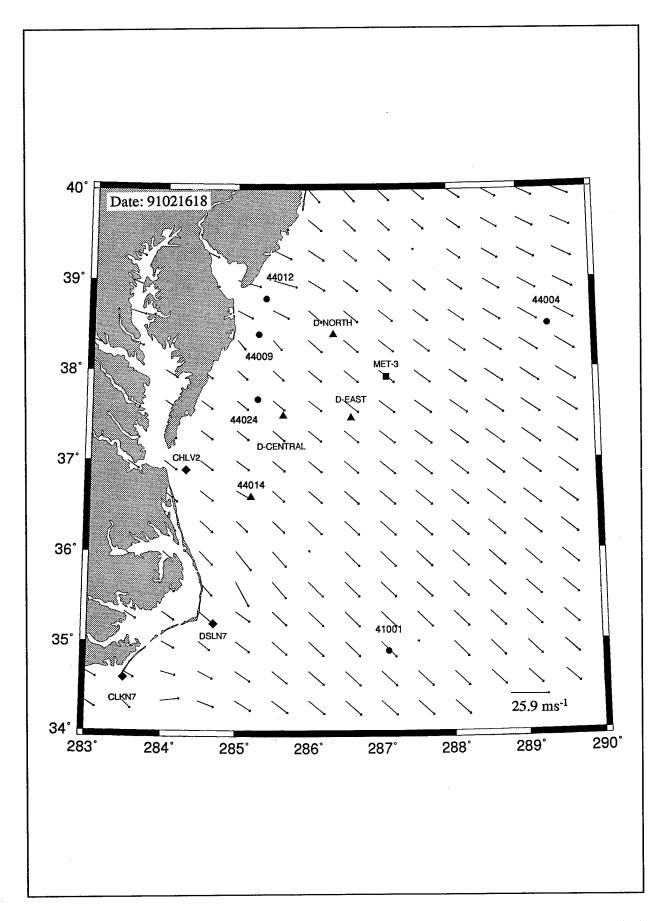


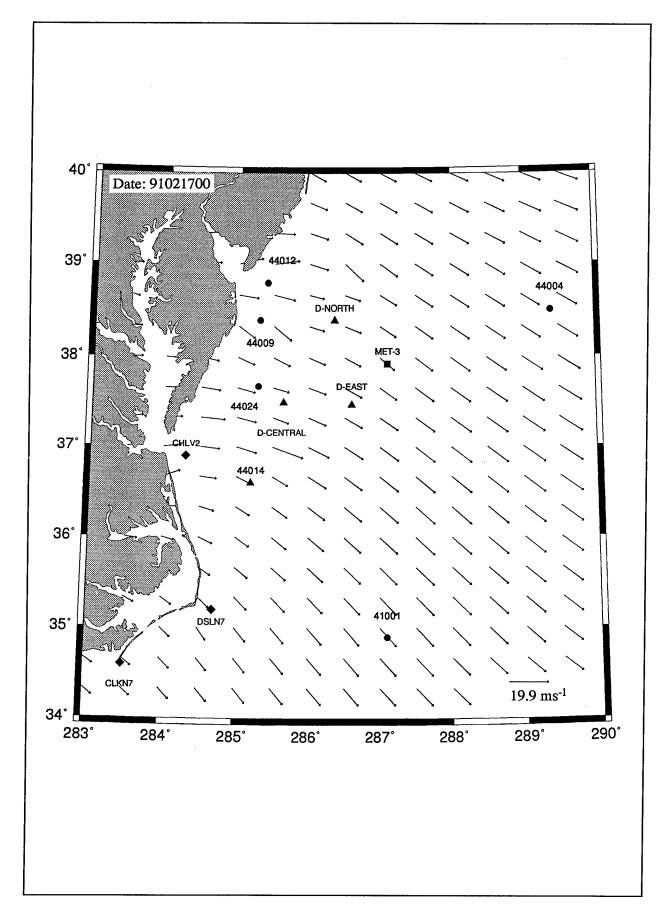




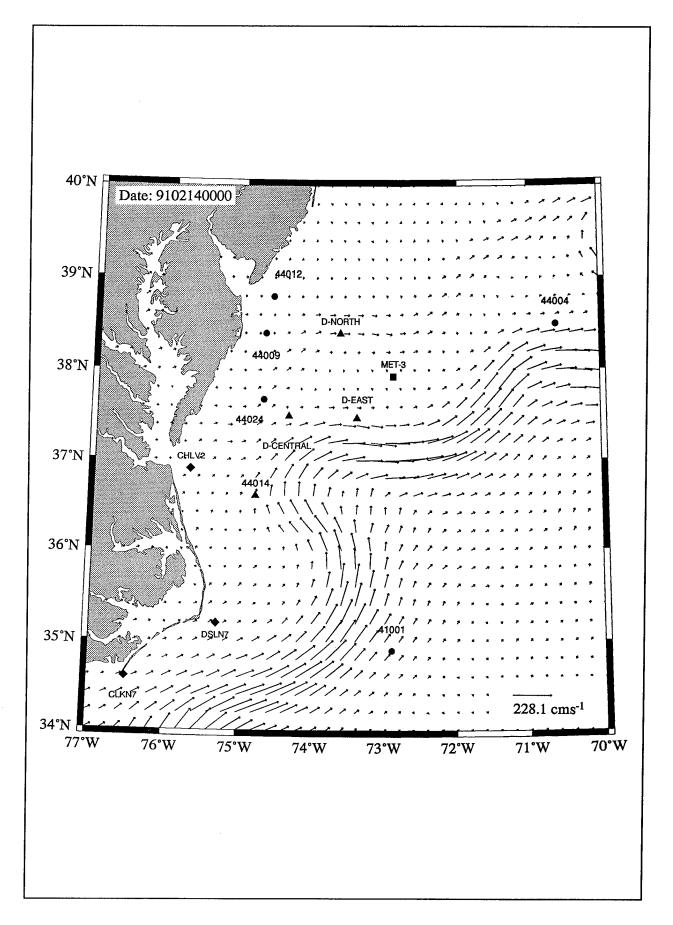


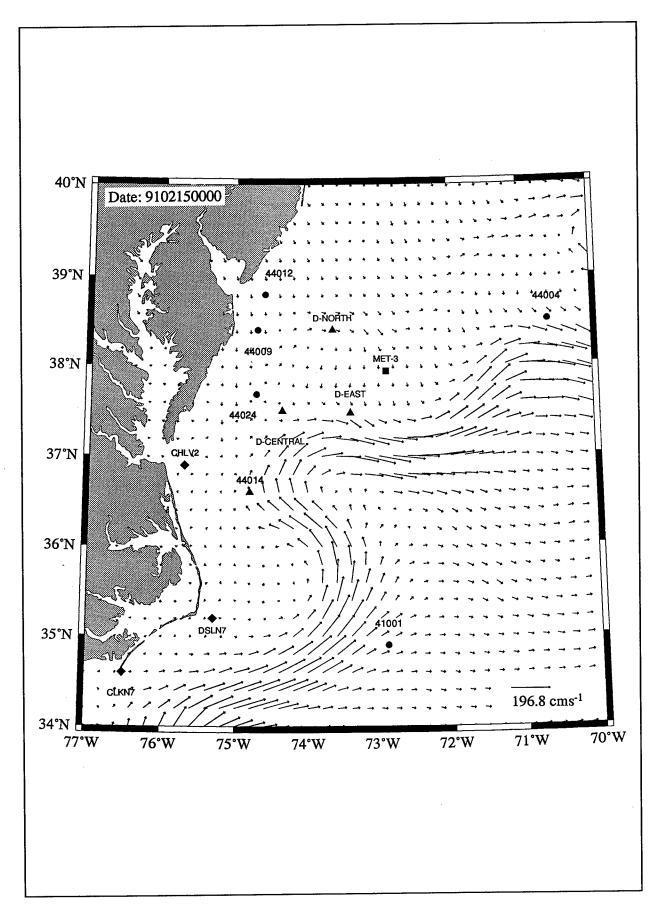


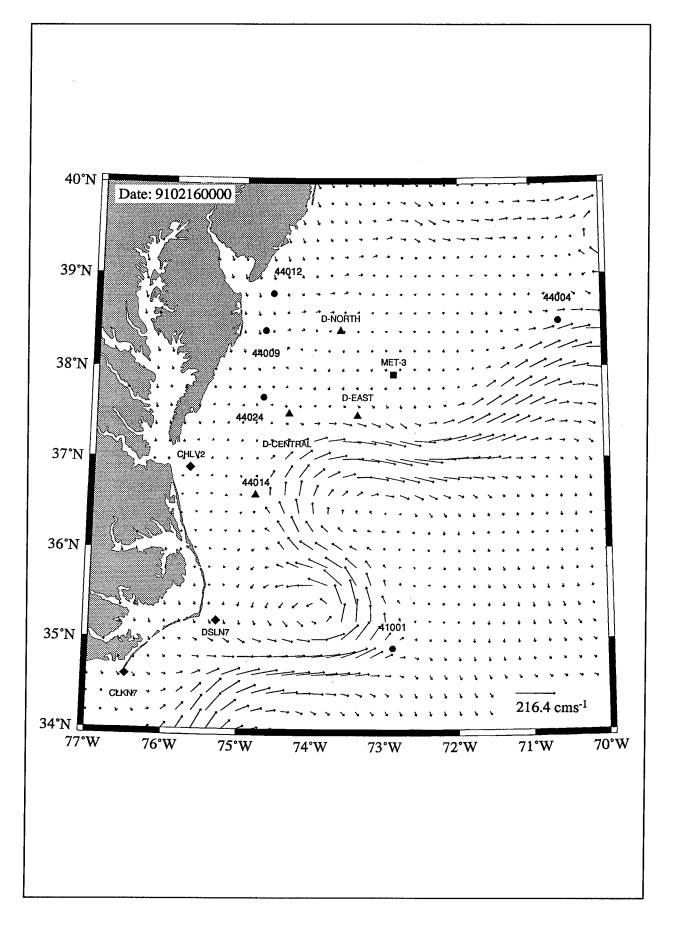


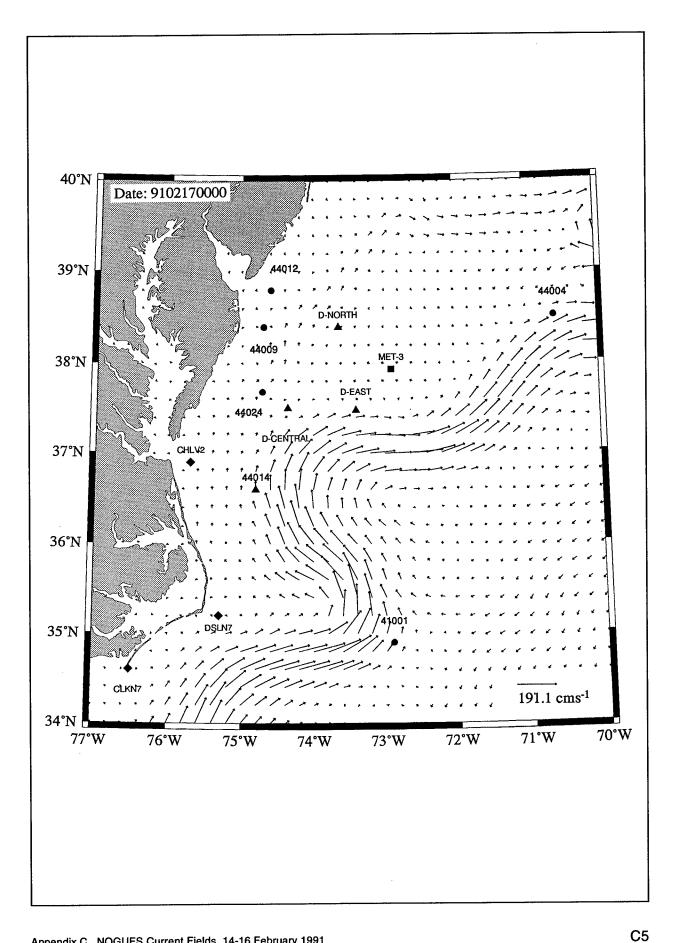


Appendix C NOGUFS Current Fields, 14-16 February 1991









Appendix D Buoy Spectra, 12, 14-16 February 1991

This appendix contains three-hourly directional spectra from the four SWADE directional wave buoys, viz., Discus-North, Discus-East, Discus-Center, and Buoy CERC. The time period covered is 14-16 February. This is the main data collection period for the ROWS for the St. Valentines wind/wave event.

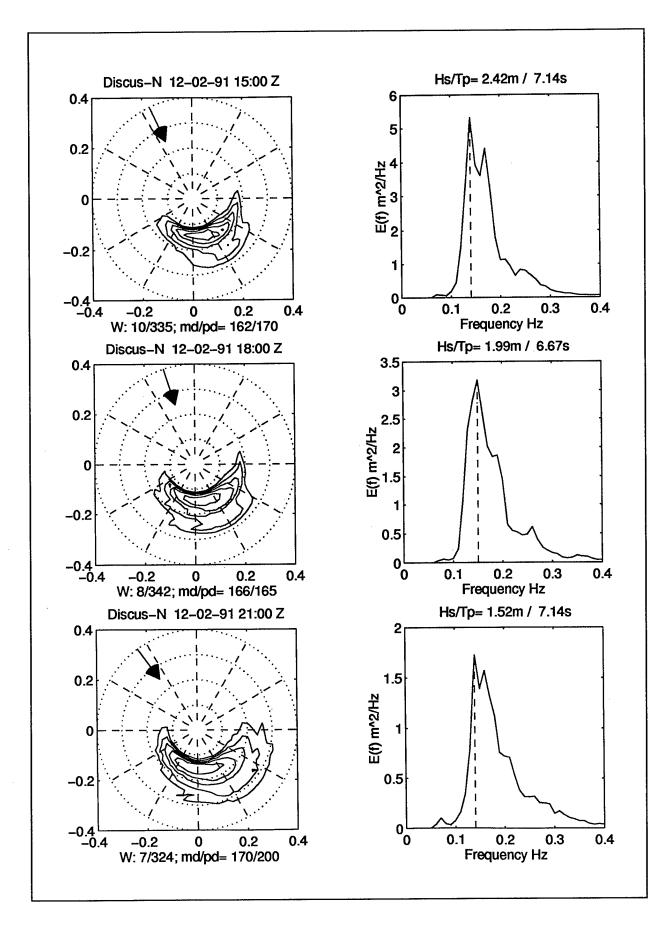
The directional wave energy spectra $E(f,\phi)$ in m²/Hz/rad are plotted in polar coordinates with logarithmically spaced contours. The contour interval is 2.5 dB. The frequency rings are spaced 0.1 Hz; the highest frequency is 0.4 Hz.

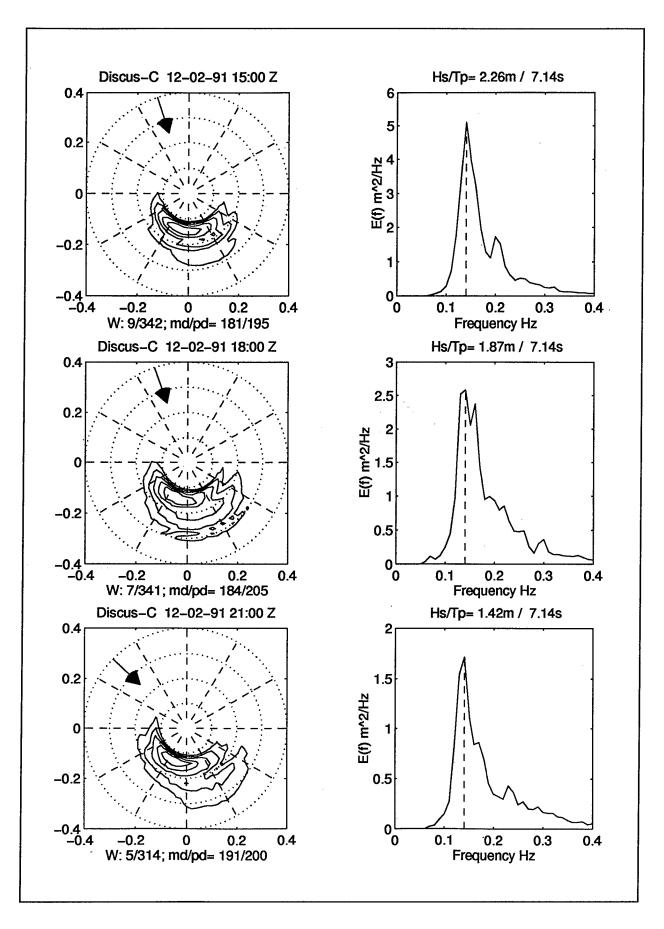
Below each directional spectrum plot are the buoy wind speed (in ms⁻¹) and direction (in degrees true according to meteorological convention) and the peak and mean wave directions (directions to). Peak directions are approximate since they are only bin values.

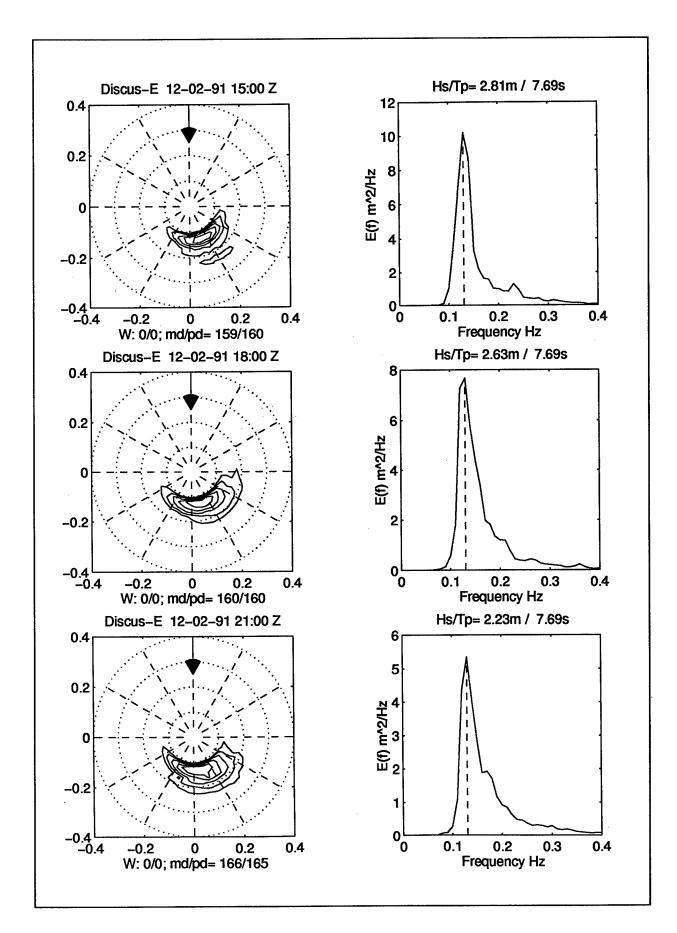
The nondirectional spectrum is given to the right of each directional spectrum. At the top of the nondirectional spectrum plot are the significant wave height (Hs) and the peak period (Tp). Note that the Tp are bin values, and thus imprecise.

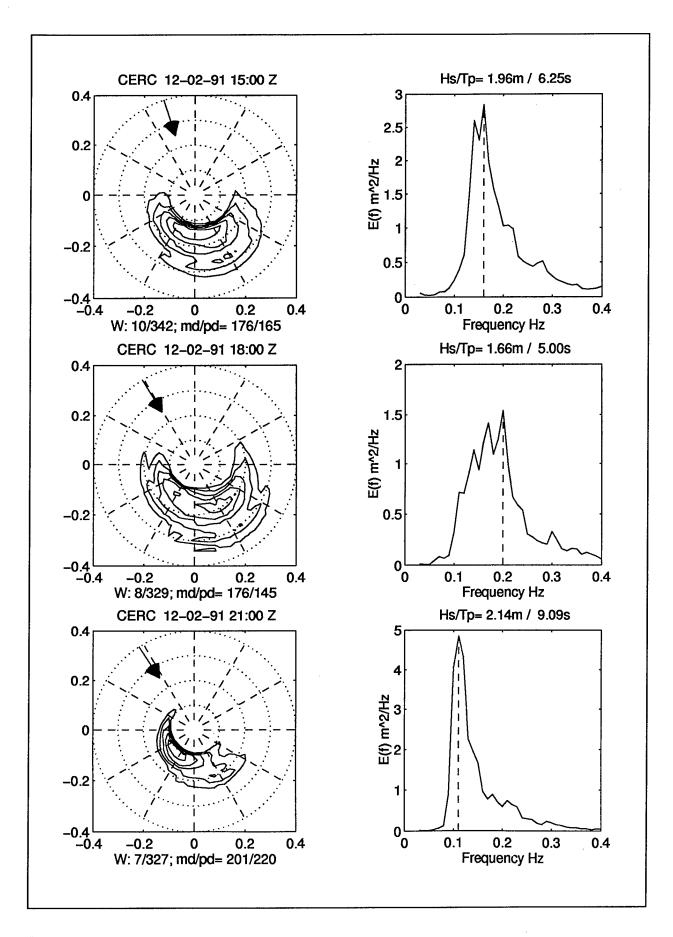
Appendix D1: 12 February 1991

Discus-N Discus-E Discus-C Buoy-CR

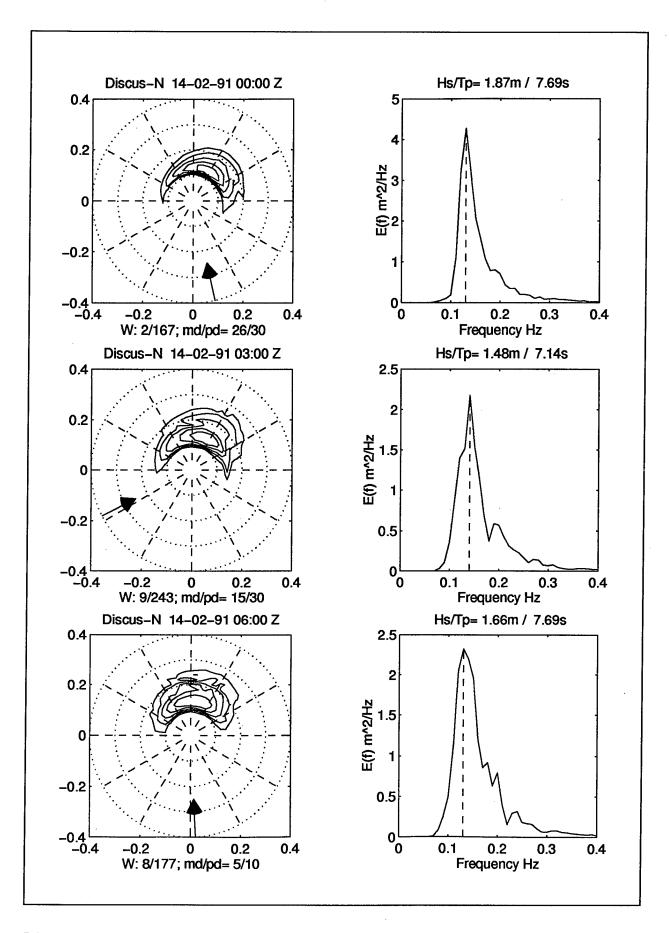


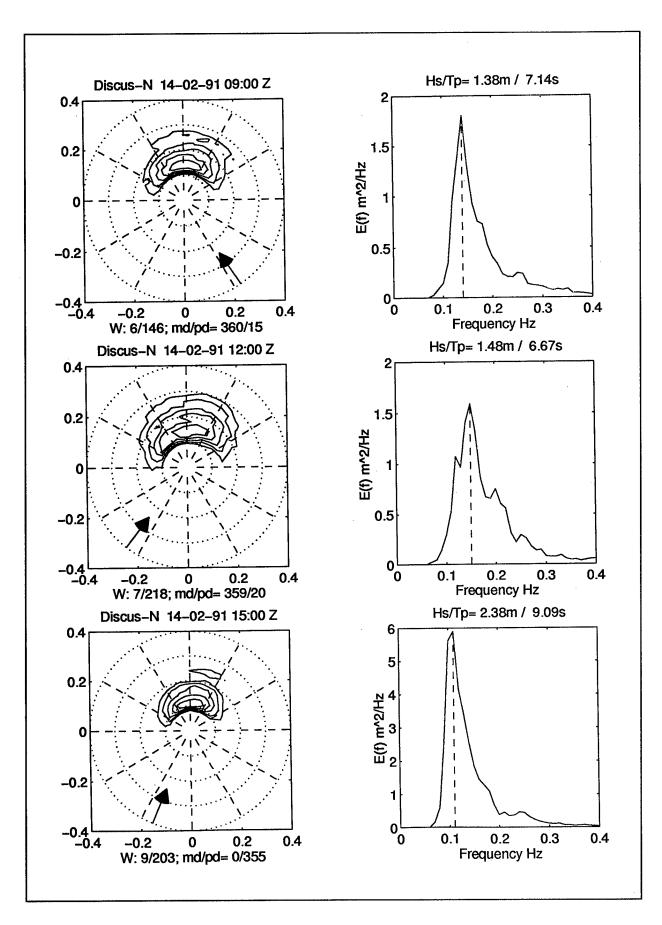


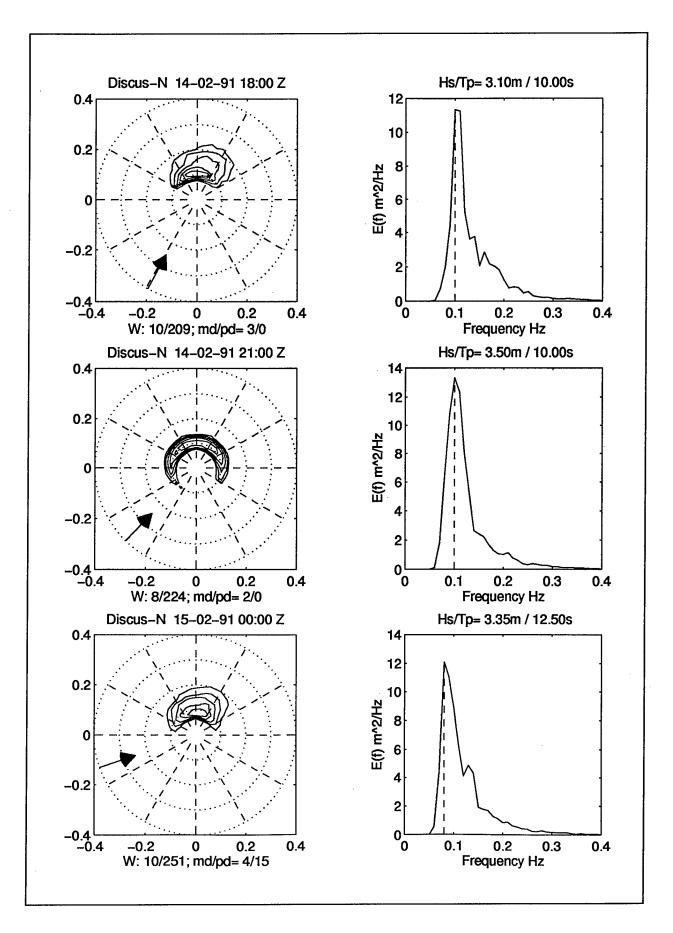


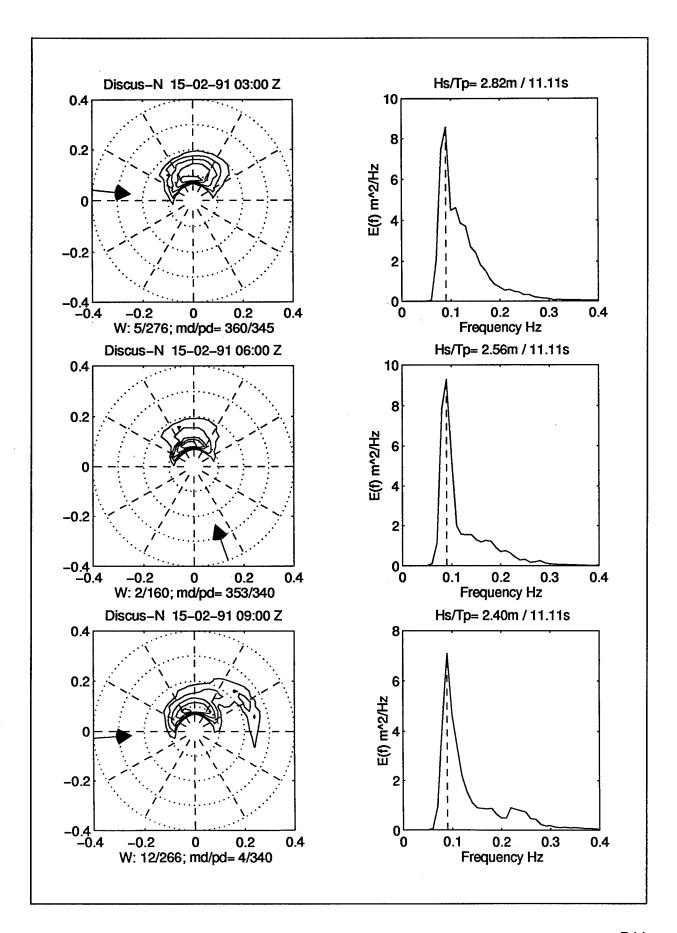


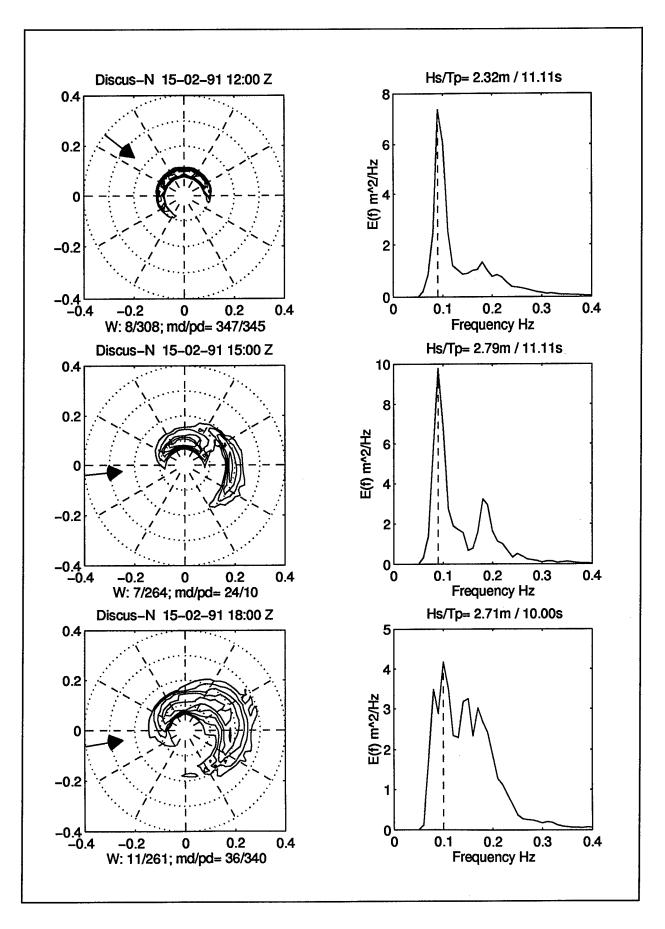
Appendix D2: Discus-North 14-16 February 1991

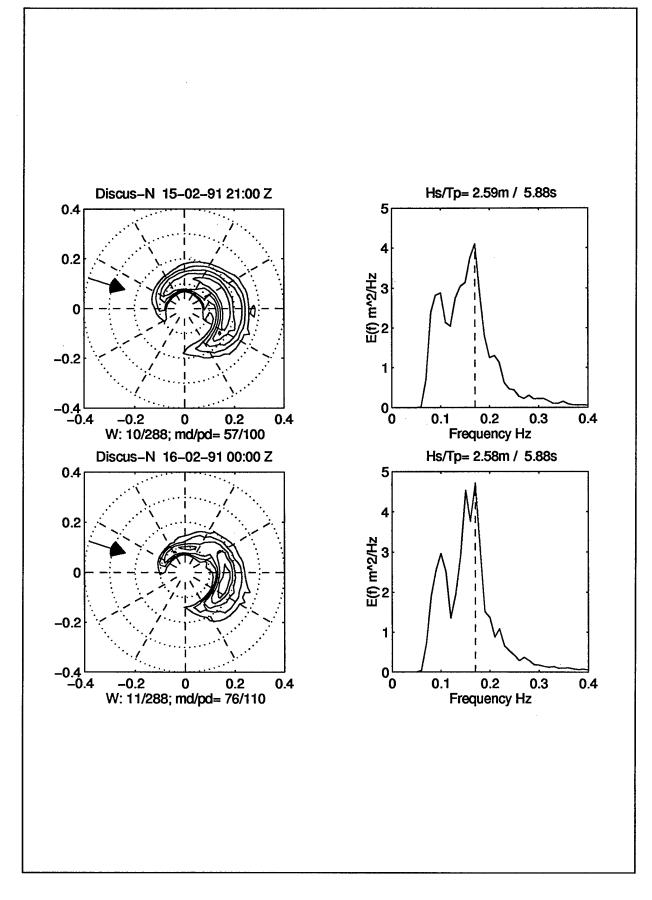




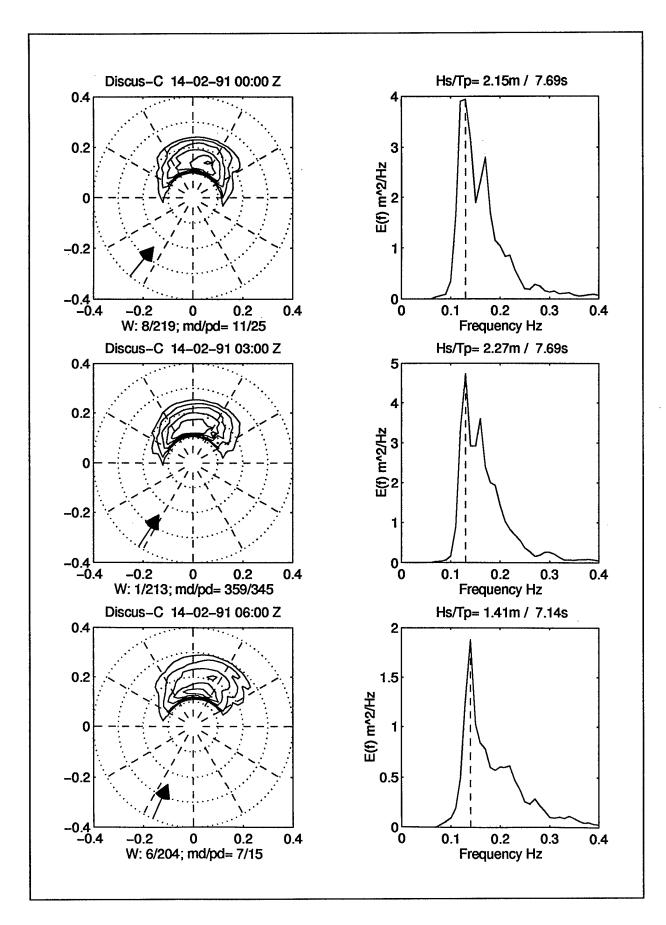


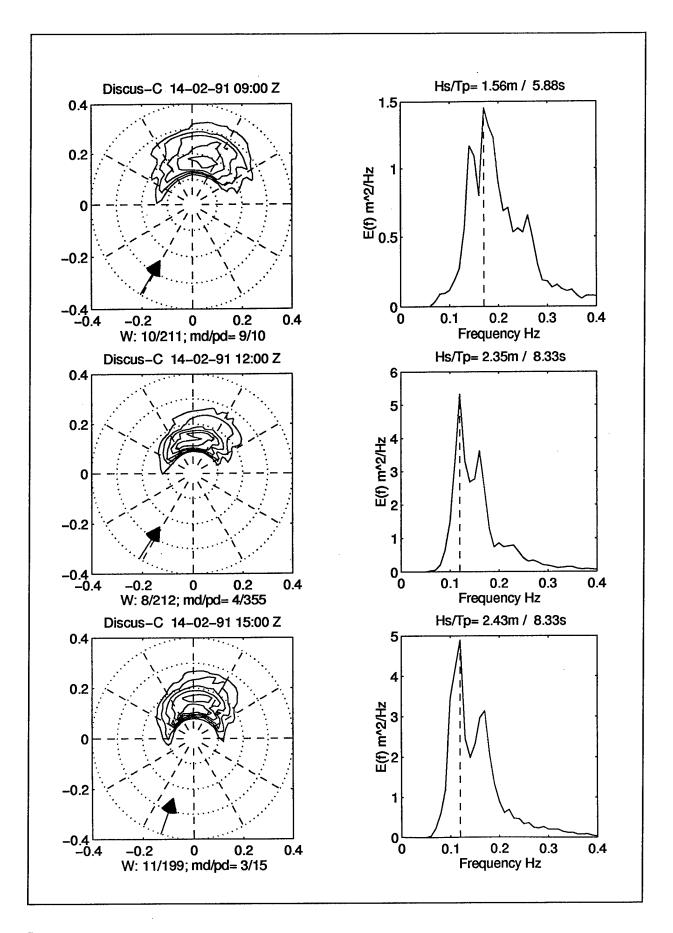


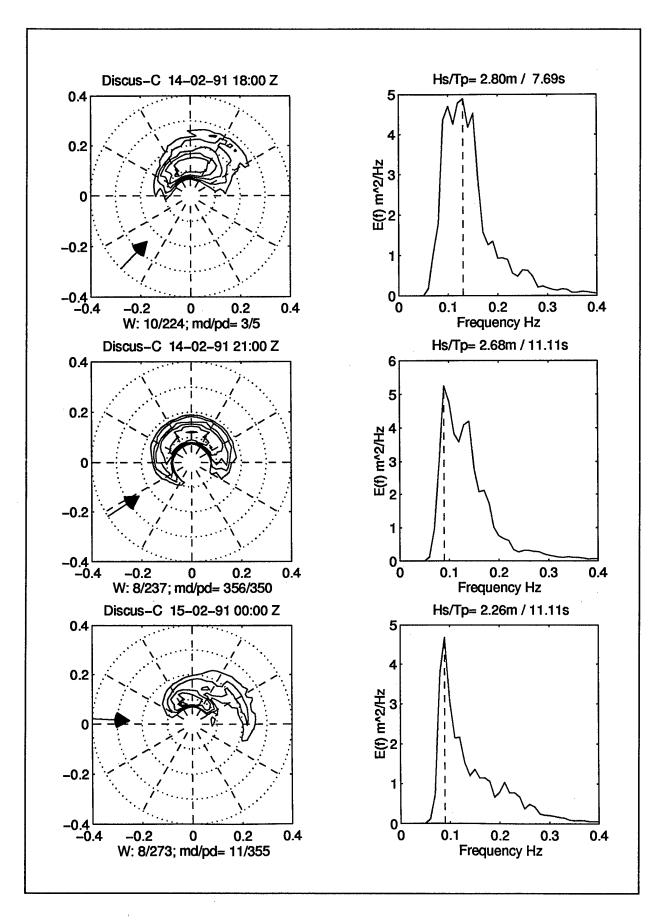


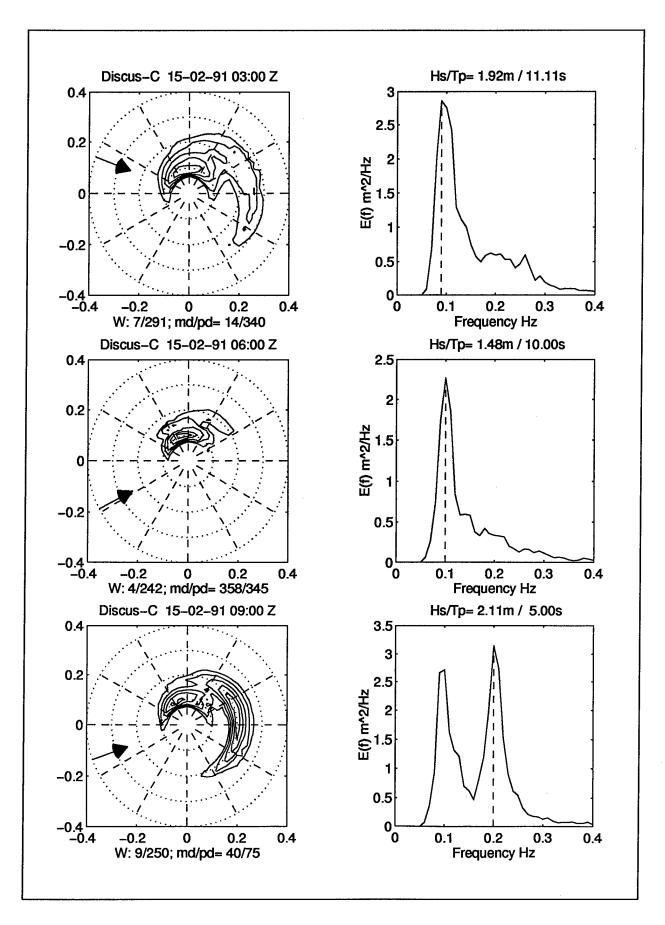


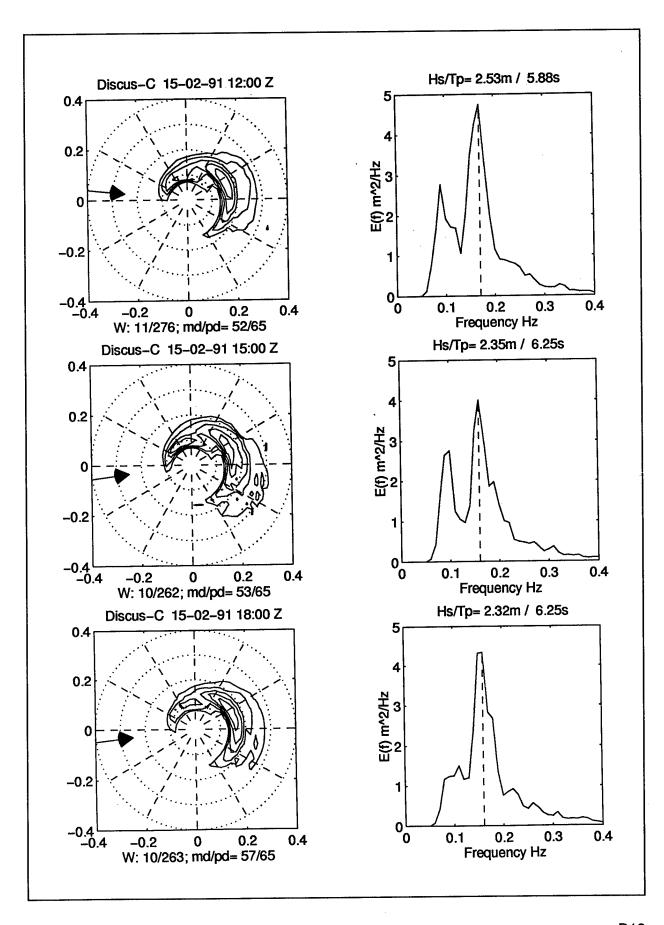
Appendix D3: Discus-East 14-16 February 1991

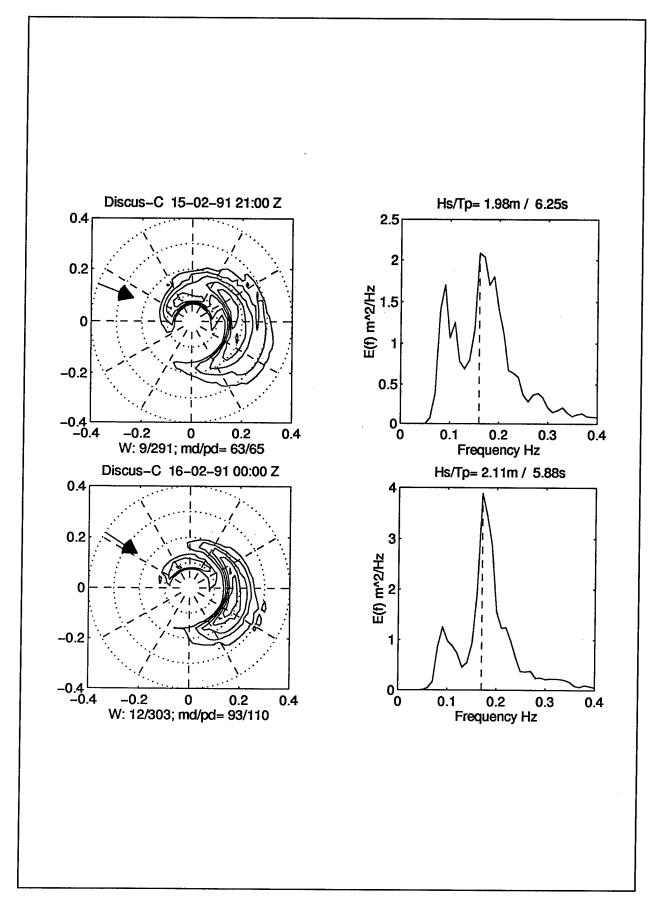




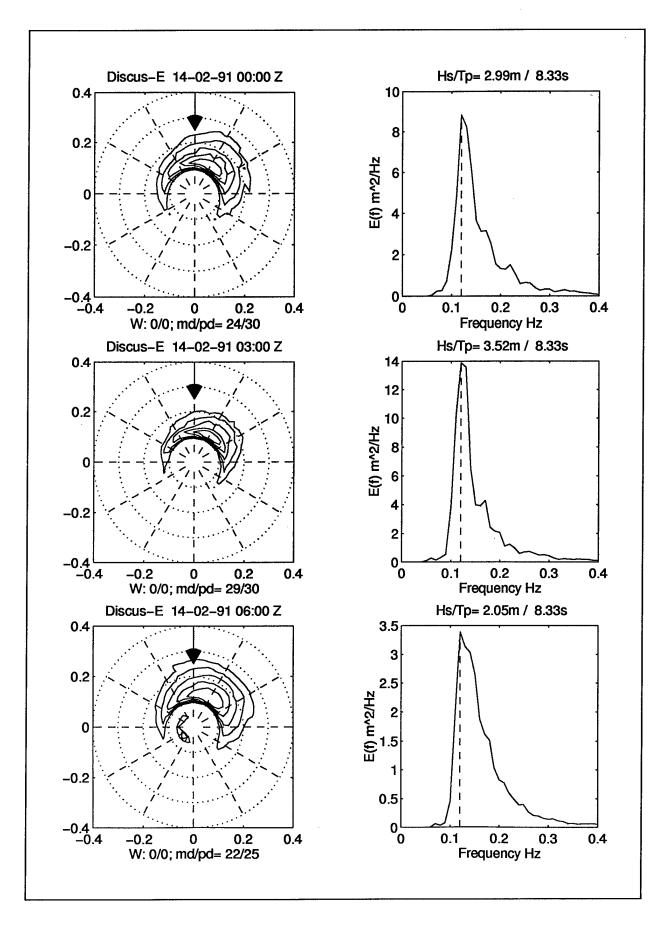


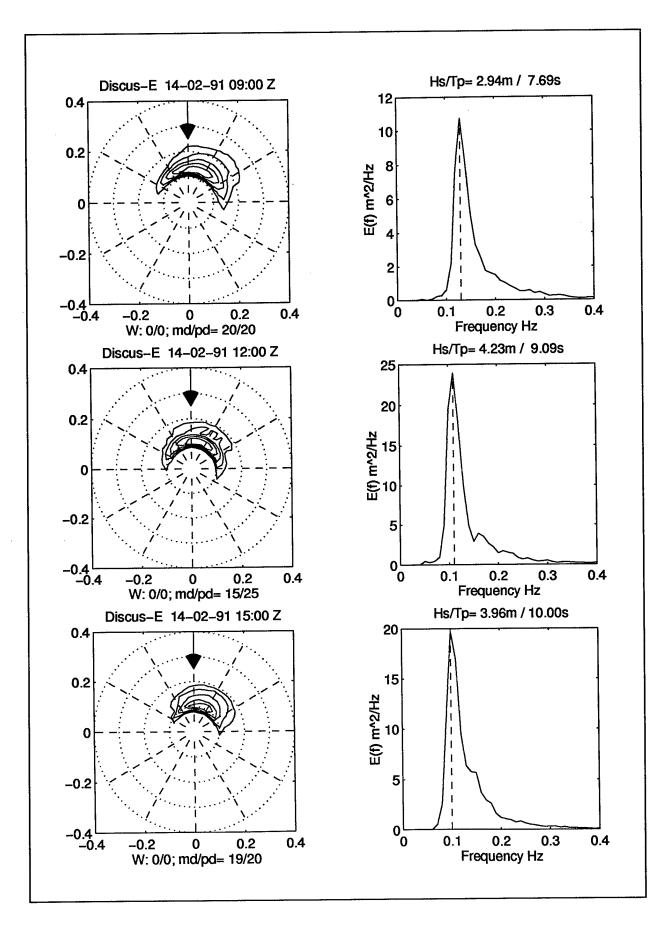


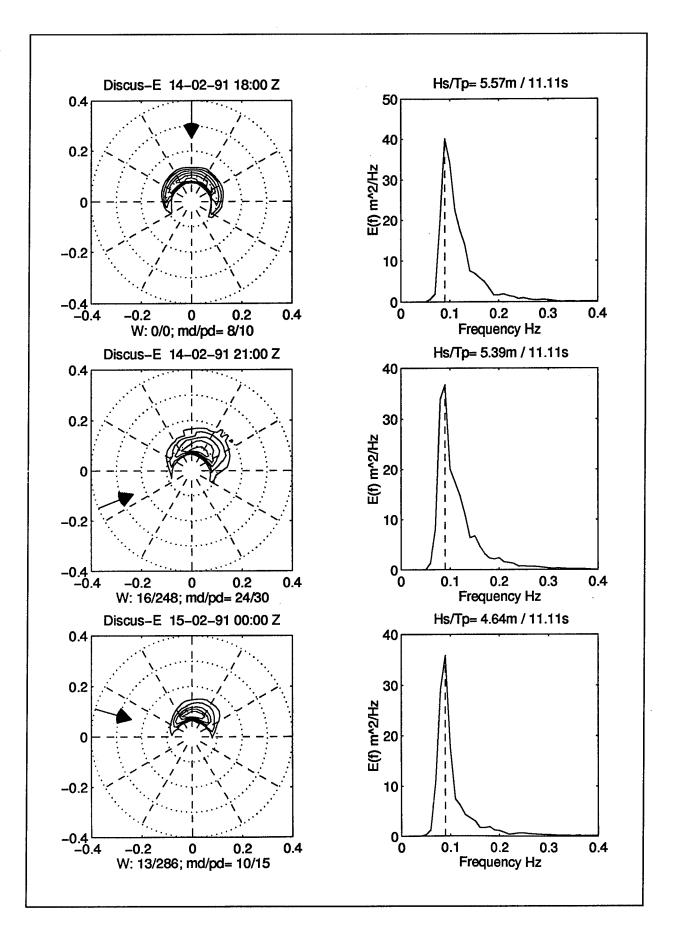


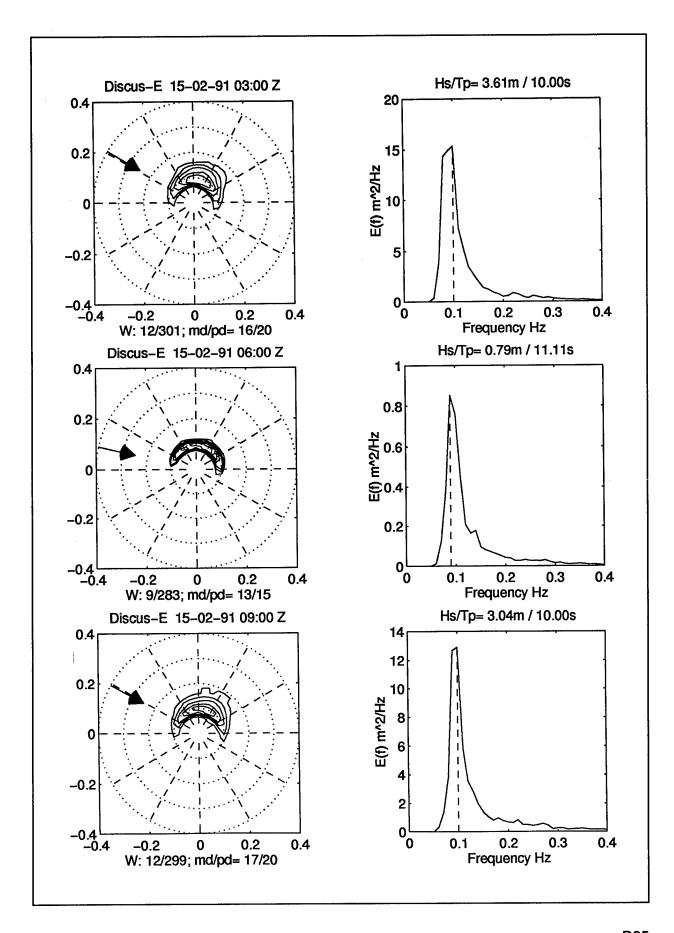


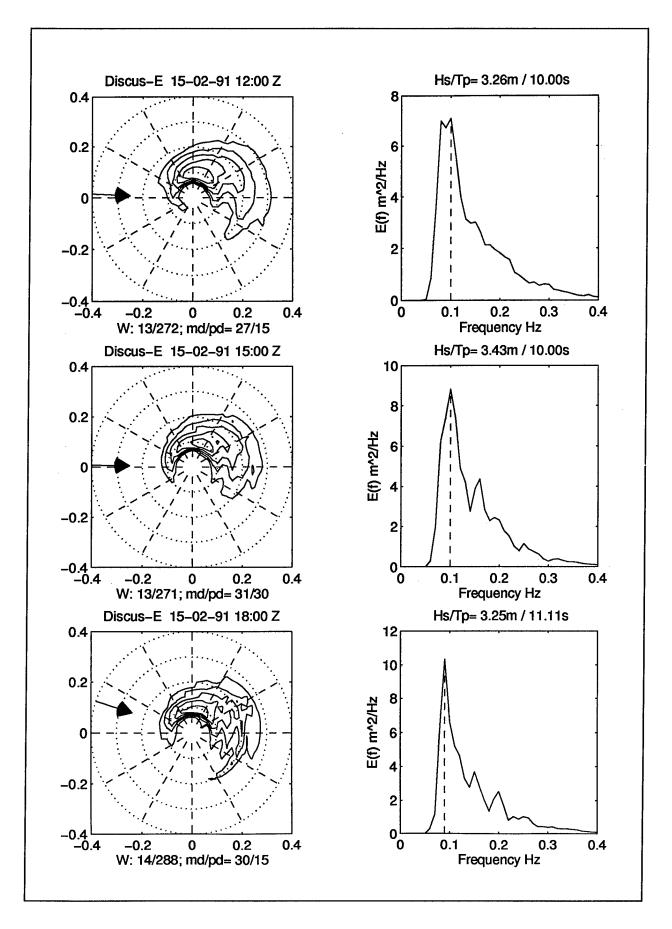
Appendix D4: Discus-Center 14-16 February 1991

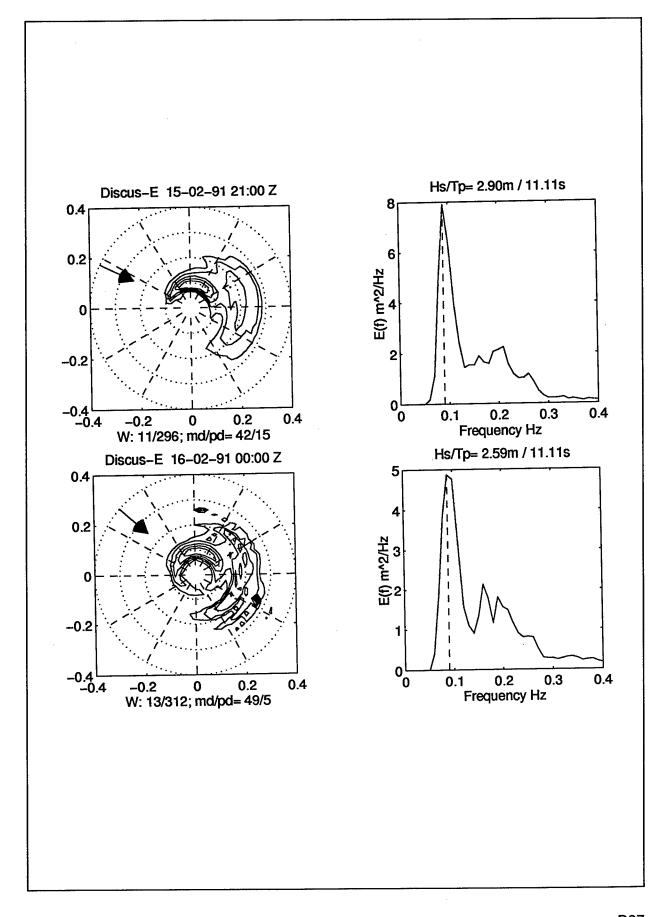




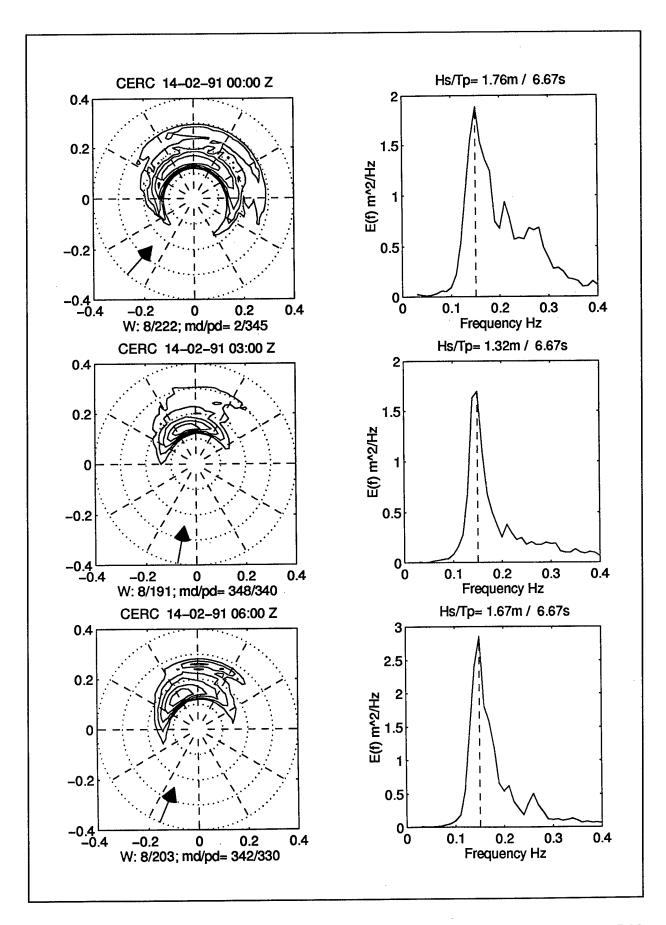


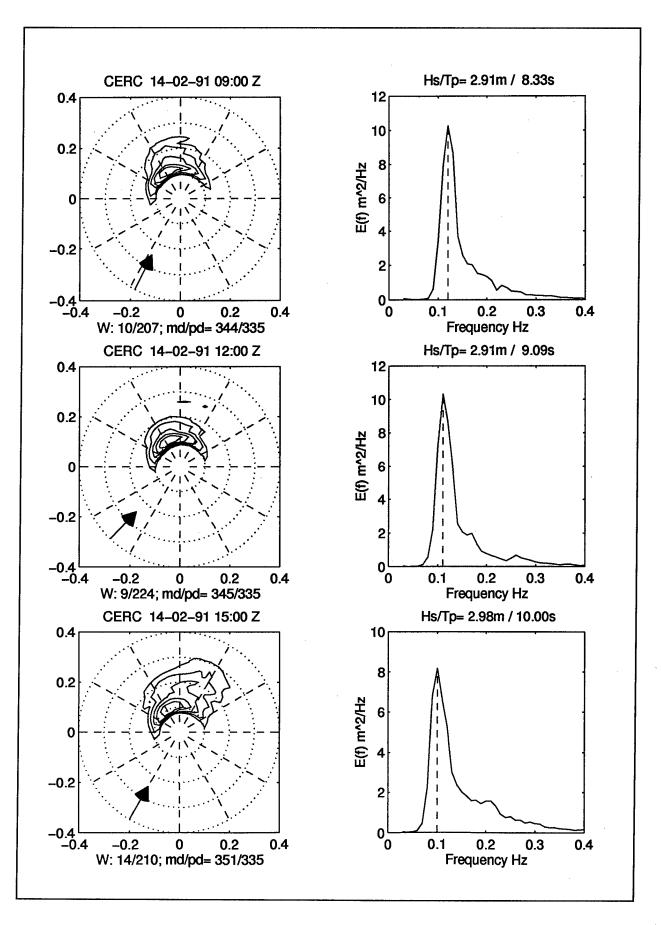


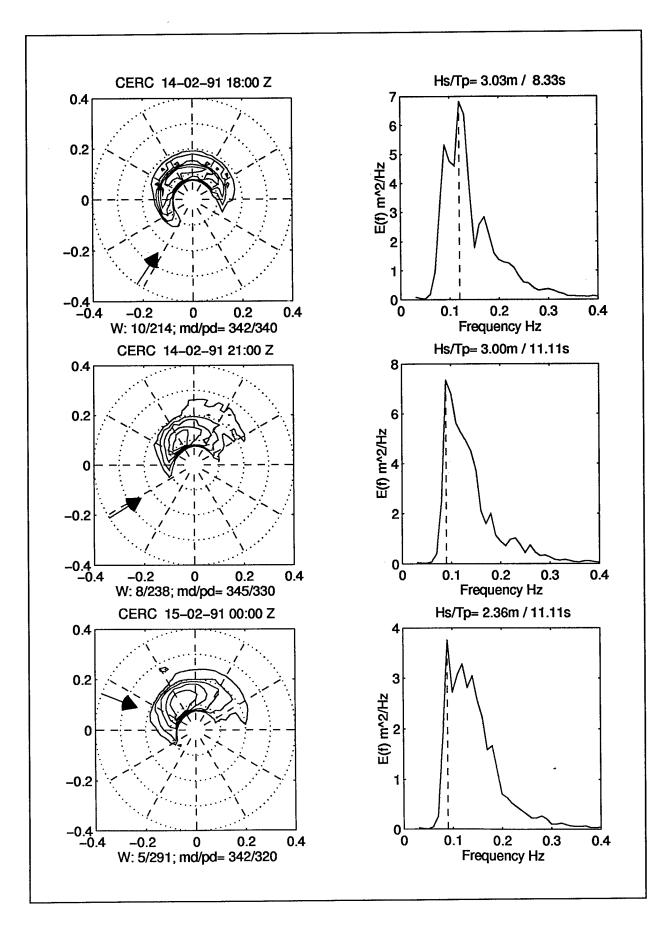


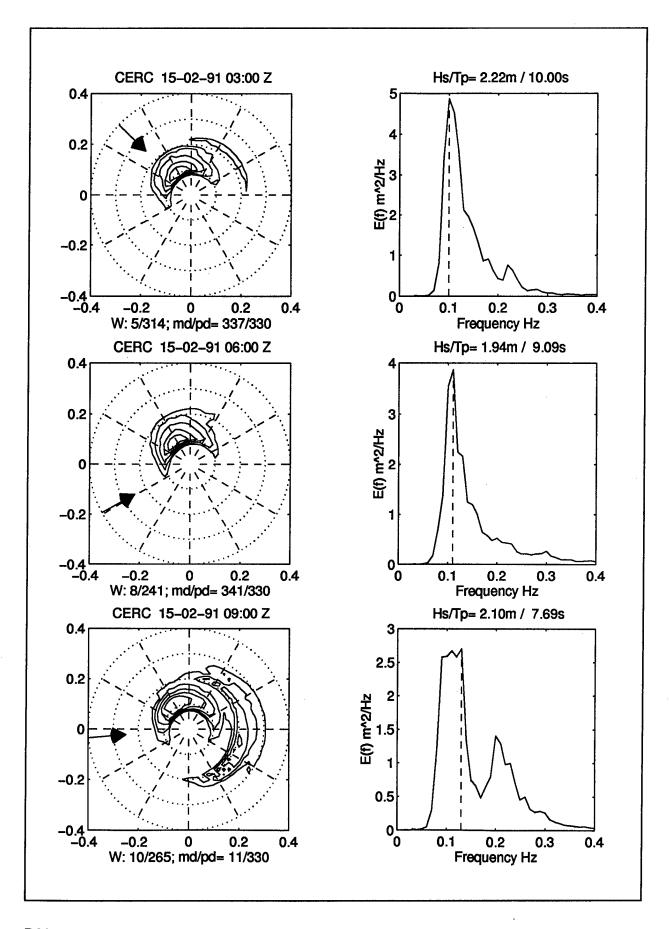


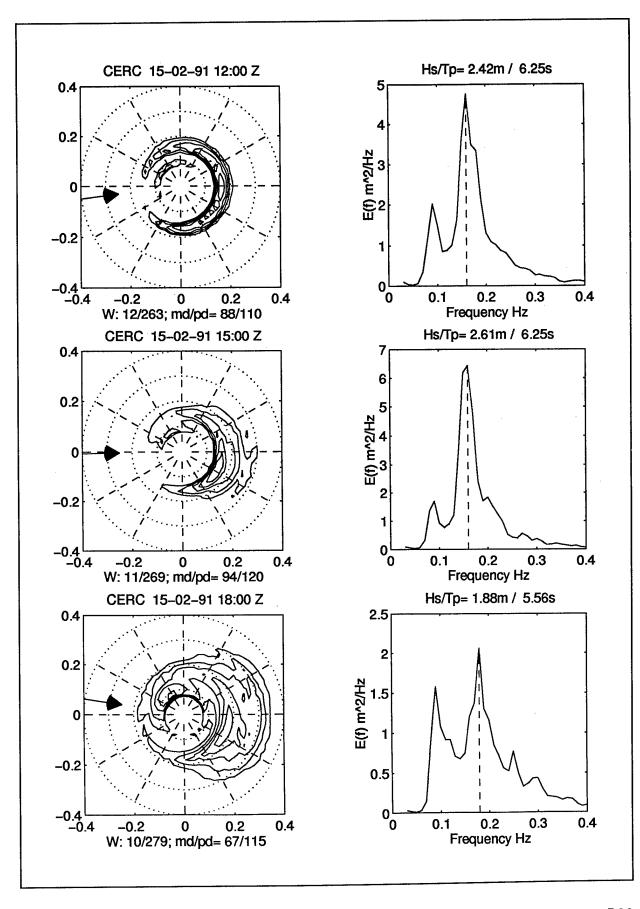
Appendix D5: Buoy CERC 14-16 February 1991

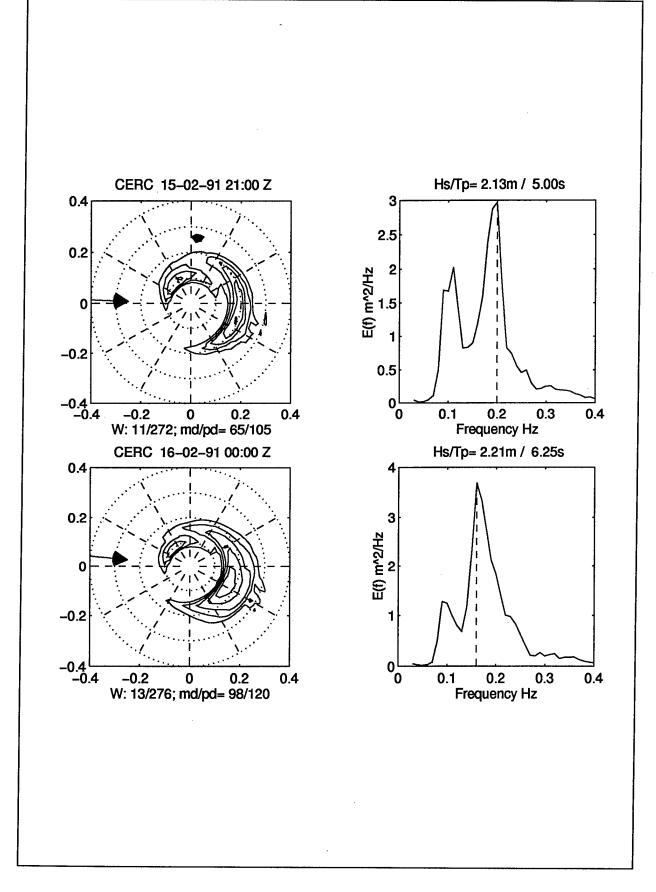












Appendix E ROWS Spectra, 12 February - 7 March 1991

ROWS directional and nondirectional spectra are presented in this appendix in a format identical to that used for the buoy spectra in Appendix D. Note, however, that in the case of these spectra the peak period and direction data are precise, each having been obtained by parabolic fit to the binned spectrum data.

In low sea state cases (SWH _ 2 m), the ROWS spectra may be subject to a fair amount of 'dc' contamination. The nondirectional spectrum and inferred SWH will then depend critically on the imposed low-frequency cutoff. In some cases the choice of cutoff frequency is obvious from the directional spectrum. In others, the choice of cutoff frequency is rather arbitrary. Often the nondirectional spectrum will have no clearly defined peak. The apparent peak in the nondirectional spectrum plot will then simply reflect the choice of cutoff frequency.

Note that the ROWS wind speeds are from the interpolation fields based on uncorrected full waveform fit altimeter data; thus they are biased low by about 1 ms⁻¹ on average.

The spectra plots for each flight are preceded by a flight map and navigation and file data table. On the flight maps the spectra files are denoted by 'S1.' 'S2,' etc. and the altimeter mode files are denoted by 'A1,' 'A2,' etc. The flight data table column entries are:

TAPE/FILE Original tape number for flight and processed file number

POS FIX Position fix (used to construct flight maps)

ROWS MODE 1 = Spectrometer mode; 2 = Altimeter mode

BUOY/WP Identifies buoy overflown or way point reached

EST Center time for particular file in Eastern Standard Time

LAT, LON Latitude (north) and longitude (east) in degrees and

decimal

ALT Aircraft standard pressure altitude in meters

SPD Aircraft ground speed in m/s

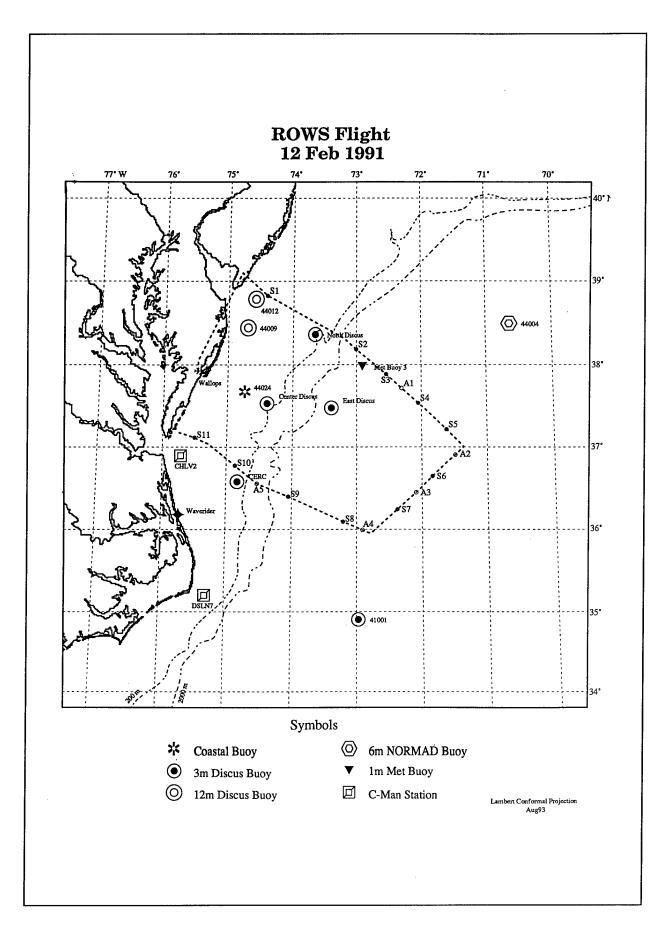
HDG True heading

PC-TIC Onboard computer 'tic' time on data tape (hhmmss)

REC # Start record number on flight data tape

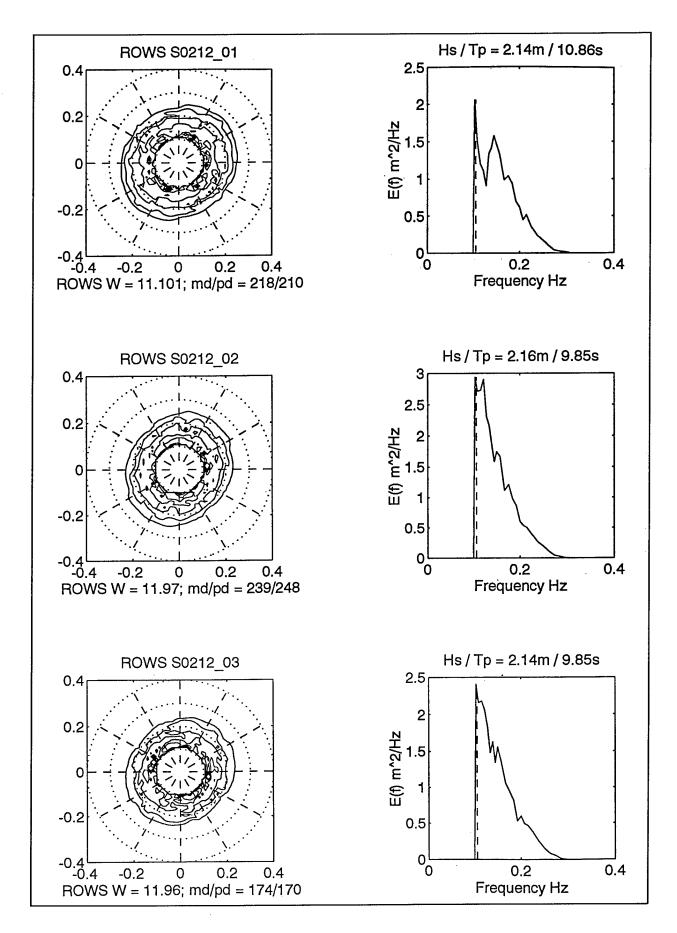
LEN Length of file to be processed in MB

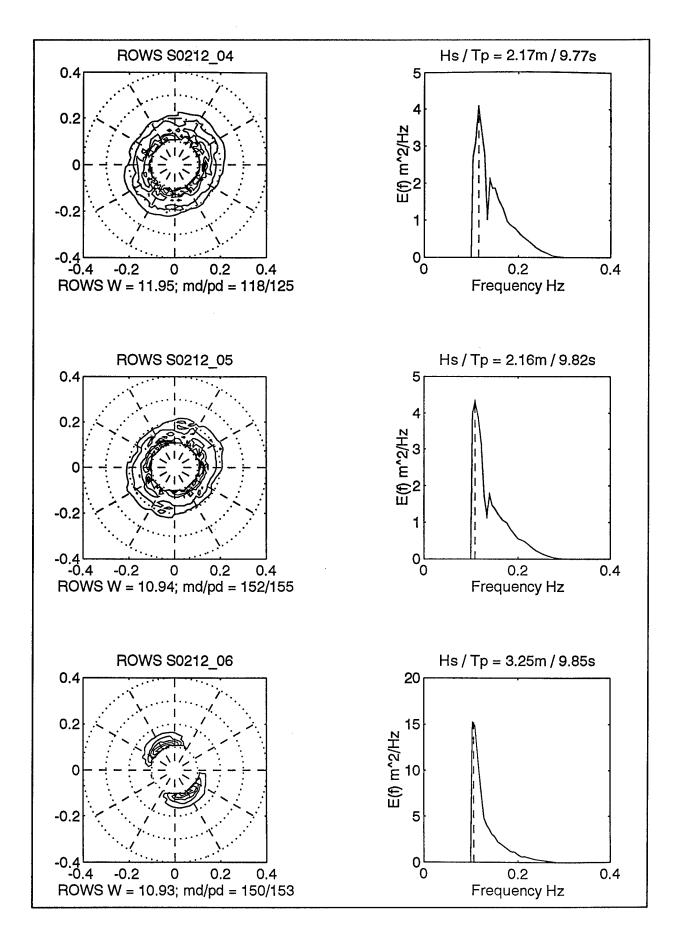
Appendix E1: ROWS Spectra, 12 February 1991

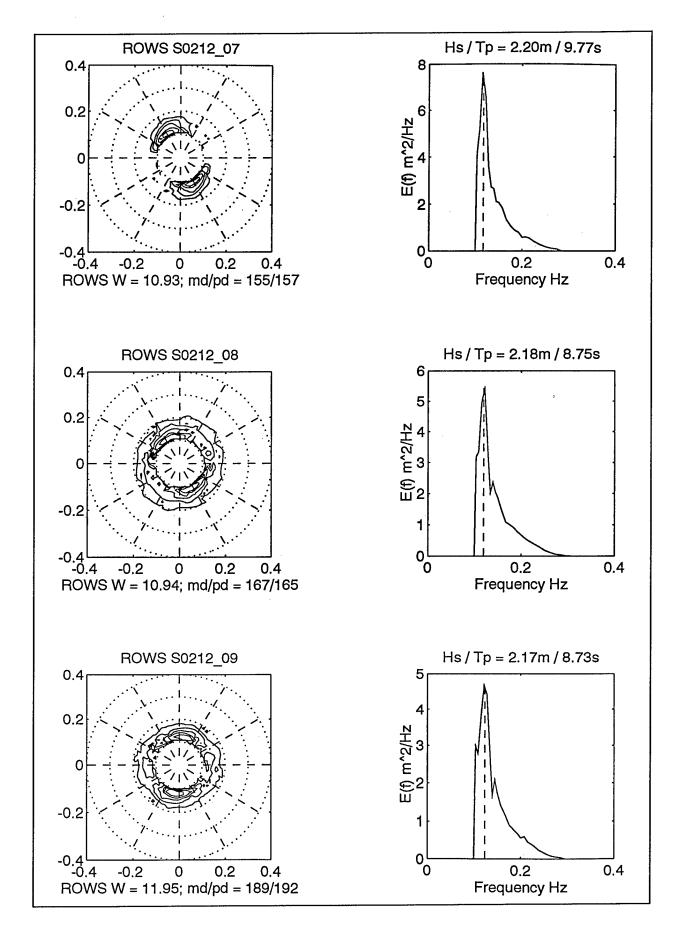


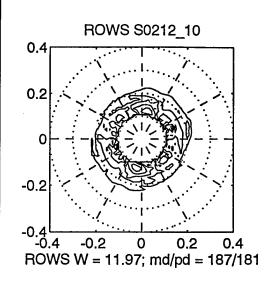
ROWS SWADE FLIGHT NAVIGATION AND FILE DATA FEB 12, 1991

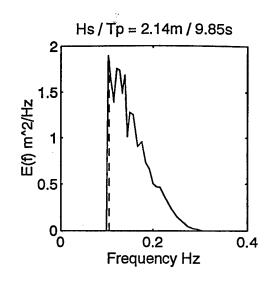
TAPE1/1 FILE	POS FIX	ROWS MODE	BUOY, WP	HH	EST MM	r ss	LAT	LON		M/S	TRU	START	REC # START	O DEG DELTA	LEN MI
	 1		WFF					-75.47							
		_	^	40	22	20	20 06	-75 A7							
	1	0	2	12	23	30	30.00	-74 80	7620						
aa.	1	1	3	10	27	0.4	33.10	-74.00	7620	231	140	122525	5301		13
S01		1		12	2/	20	30.03	-74.40	7020	231	140	122525	0002		_
	1	0	5 ′	12	20	50	20.00	-73.20	7320	238	125	122525			
	1		2.	12	33	20	20 10	-73.20	7320	235	128	123527	40801		1
S02	0			12	3/	20	27 07	-72.67	7320	233	132	12332,			
	1	0 1		12	40	00	37.27	-72.07	7320	232	132	123902	62201		1
S03	Ü	Ţ		12	41	00	37.03	-72.33	7320	232	132	124203	76101		_
A01	0	2		12	43	10	37.74	-72.05	7320	232	135	124203 124315	80201		1
S04	U	1		12	45	10	37.54	-72.05	7320	233	135	124313	00201		_
	1	0		12	40	00	37.47	-71.95	7320	233	135	124712	103901		1
S05	1	Ţ	_	12	49	20	37.22	-71.02	7320	234	133	124712	100001		_
3.00	1	Ü	6	12	50	25	36 01	-71.62 -71.36 -71.49	7320	165	242	125134	118501		
A02	1	2		12	54	15	36 82	-71.62	7320	167	242	125134 125420			
S06	7	1		12	54	52	36 65	-71.84	7320	168	241	125420	132001		1
500	1	7		12	50	30	36 48	-72.05	7320	169	240				
A03															
	0	1		13	03	30	36 24	-72.38	7320	166	240	130057	166001		1
S07	1	7		13	05	40	36 11	-72.56	7320	166	240				
	0	0	7,	13	03	40		-72.78							
	1	0	,	12	00	20	35.33	-72.87	7320	134	290				
201	0	2		13	10	00	35.37	-72.91	7320			130848	202301		
A04	.1	1		13	13	50	36.09	-73.21	7320	130	298	131111	208401		1
S08 S09	1	1		13	24	10	36.40	-74.05	6405	143	300	132130	244801		1
A05	ō	2	סואיזיים	13	29	53	36.56	-74.53	6405			132834	284201		
AUS	1			13	23	30	36.75	-74.83	6405	142	309				
S10	ō			13	34	00	36.78	-74.87	6405	142	309	133115	287001		1
210	1	Ď	Ω	13	37	43	36.95	-75.14	6405	142	310				
	. 0							-75.28							
	. 1	۸		13	41	45	37.11	-75.48	6405	147	294				
S11	Ō	1		13	42	06	37.12	-75.50	6405	147	294	133914	327501		1
STT	1			13	11	43	27 10	-75.74	6405						

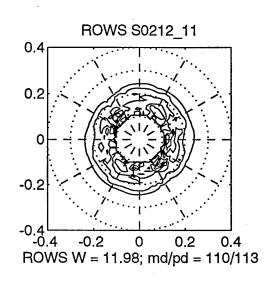


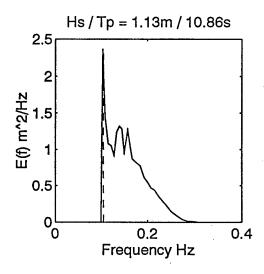








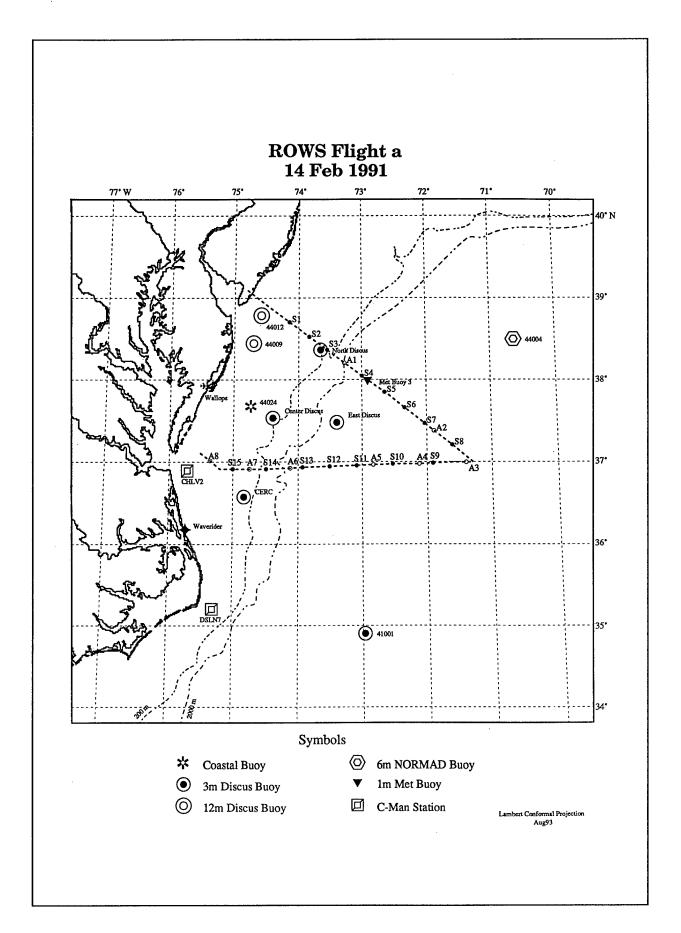




Appendix E2: ROWS Spectra and Frequency-Direction Plots for the St. Valentine's Period, 14-16 February 1991

Directional spectra for the four flights of the St. Valentine's observational period are accompanied here by plots of mean direction and directional spreading as functions of (log) frequency.

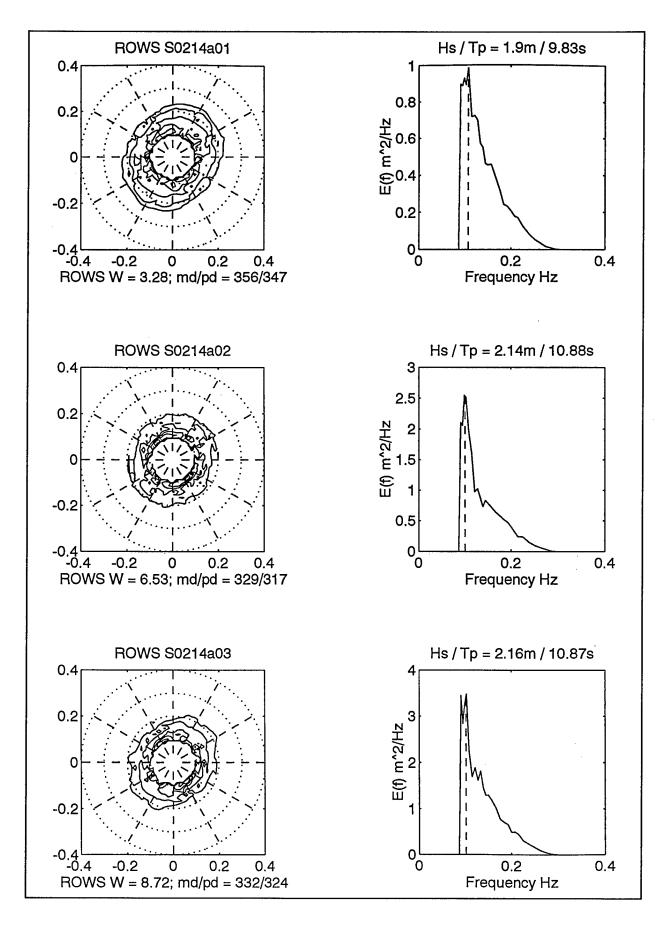
What are generally the lower of the two sets of curves are the mean directions as given by the first (dotted curve) and second (solid curve) harmonic phase angles; the upper curves are the first and second harmonic directional half power spreads. The vertical dashed line is the nondirectional spectrum peak frequency and the horizontal dashed line is the isotropic limit for the first harmonic directional half-power spread.

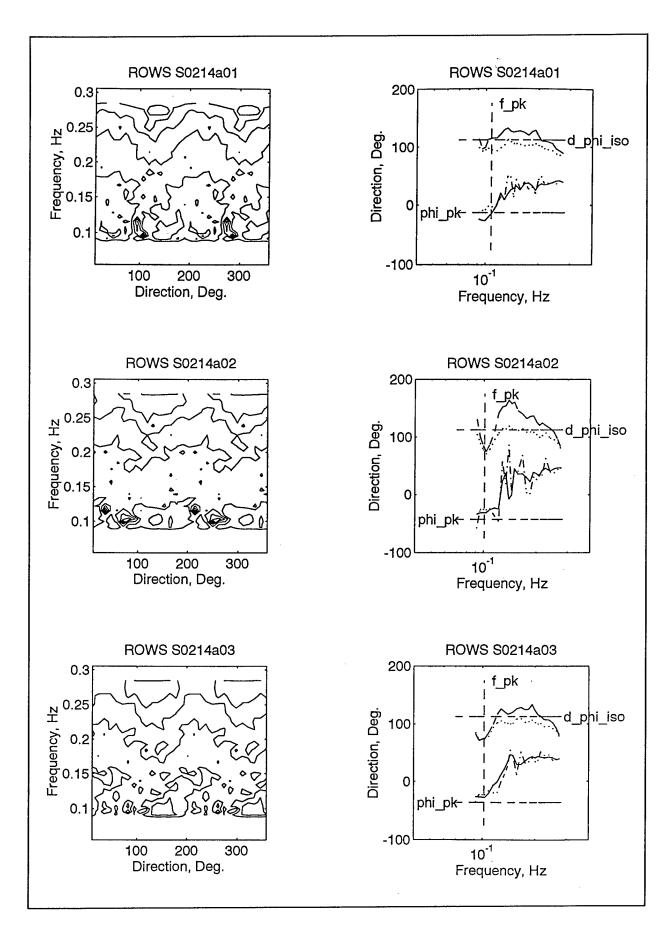


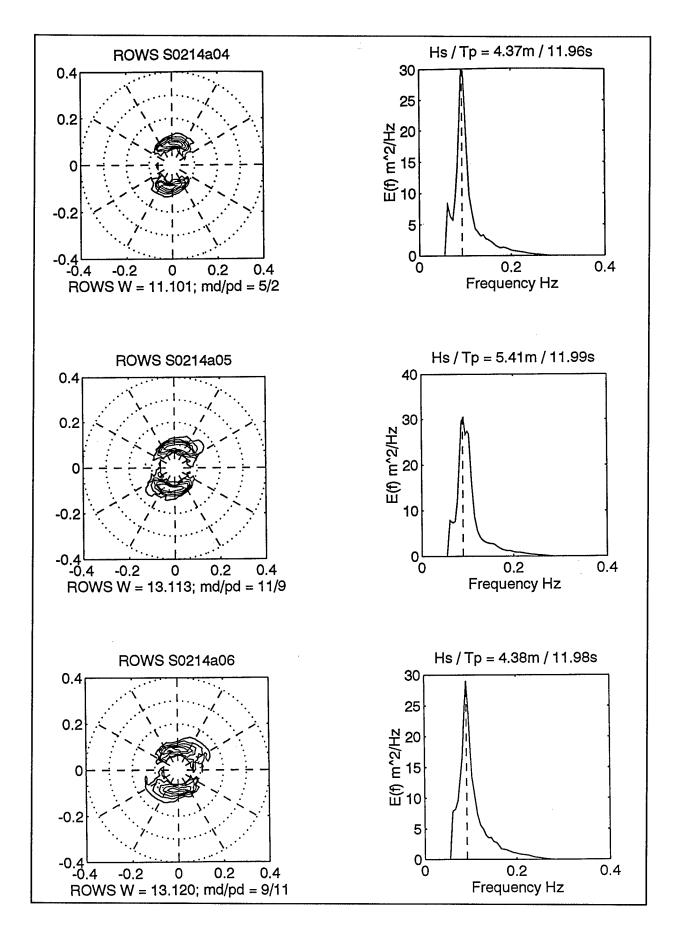
ROWS SWADE FLIGHT NAVIGATION AND FILE DATA FEB 14, 1991--FLIGHT #1

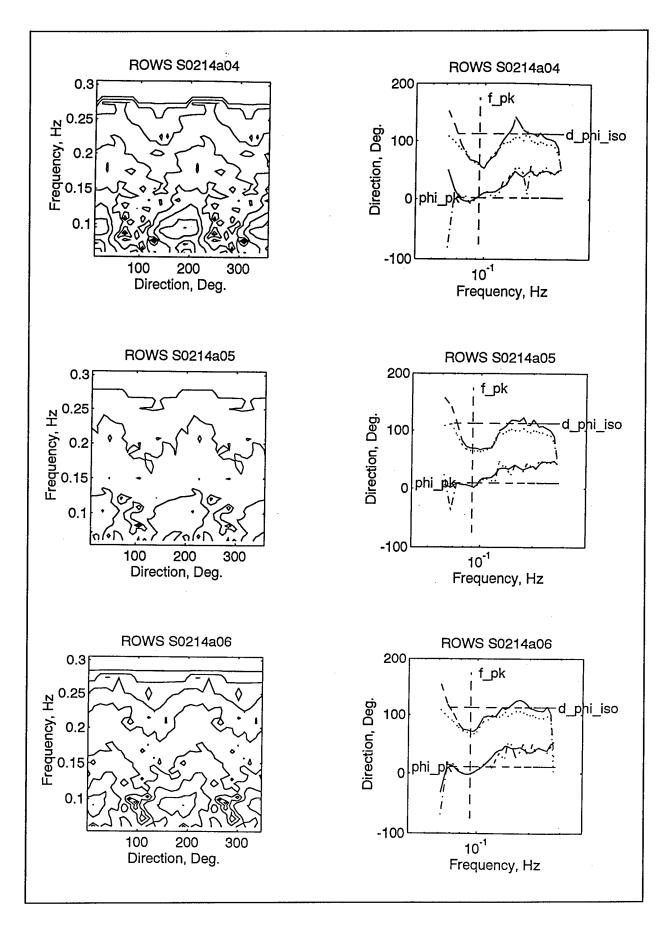
1 : 1 :
1 : 1 :
1 : 1 :
1 : 1 :
1 :
1
1 :
1 :
1 1
1
1 1
1
1 :
1
1 1
1
1. 1
1 1
1 1
1
1
1
1 1
1

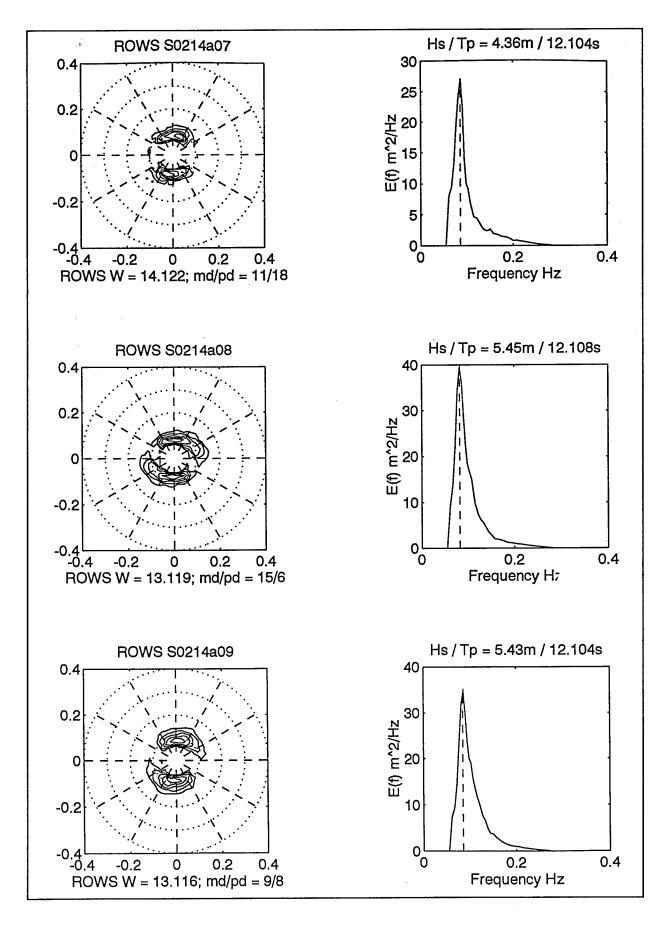
NOTES: (1) HEADINGS BETWEEN 140 AND 148 DEG ON OUTBOUND LEG ARE INTERPOLATED VALUES. ALTHOUGH HEADINGS IN LOG ARE LISTED AS IN DEG TRUE, 140 DEG IS THE MAGNETIC HEADING ACCORDING TO FLIGHT PLAN, AND SO JUST POSSIBLY THIS HEADING MAY BE MAGNETIC RATHER THAN TRUE!

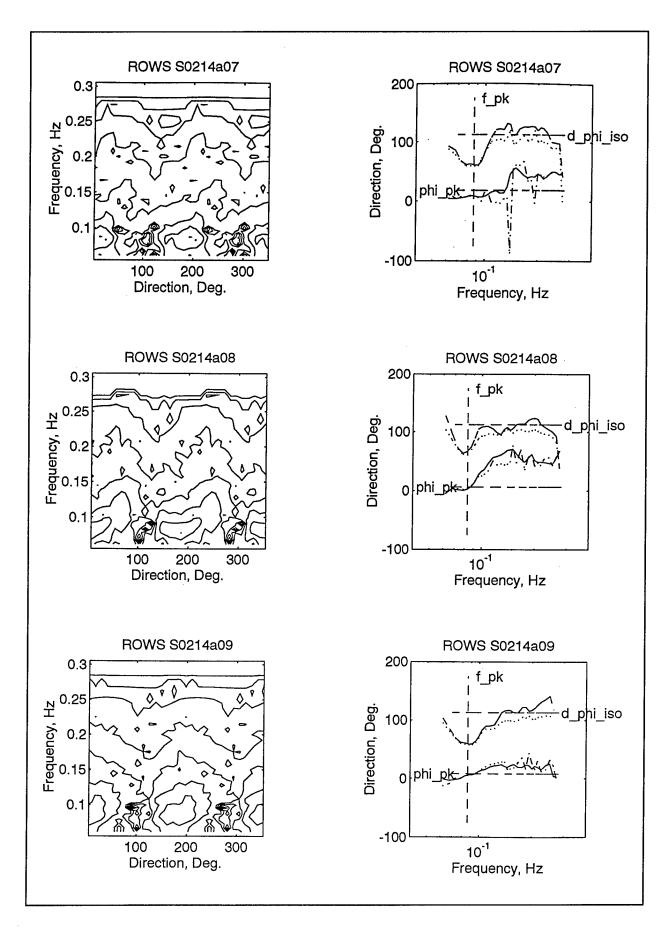


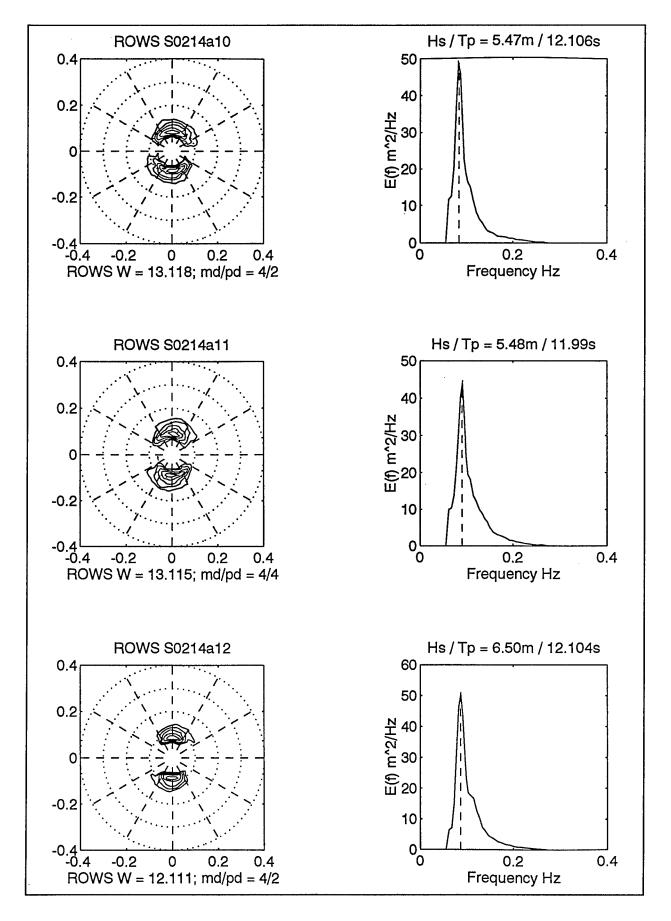


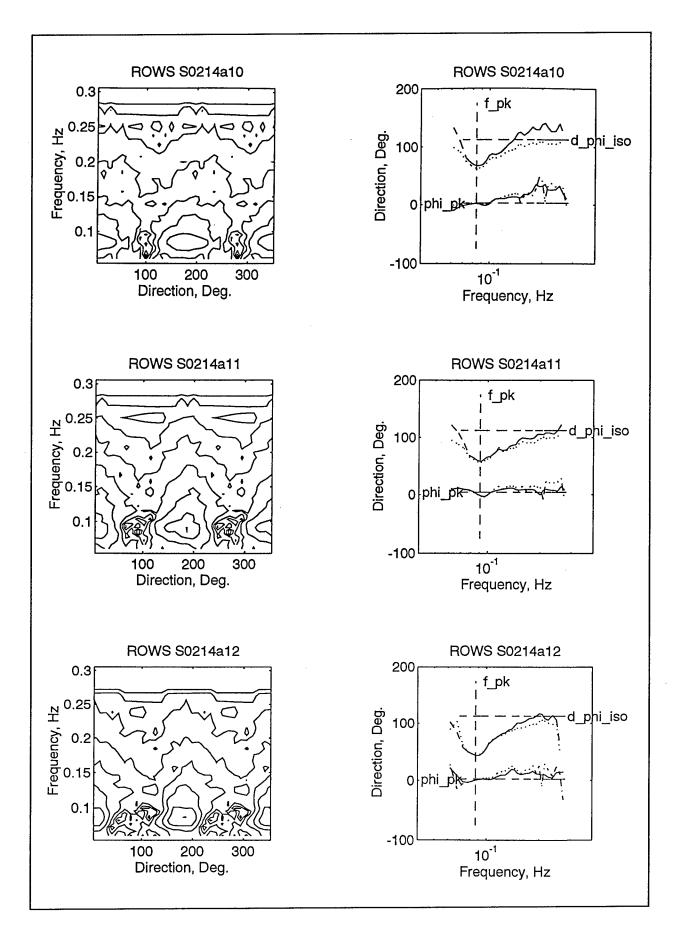


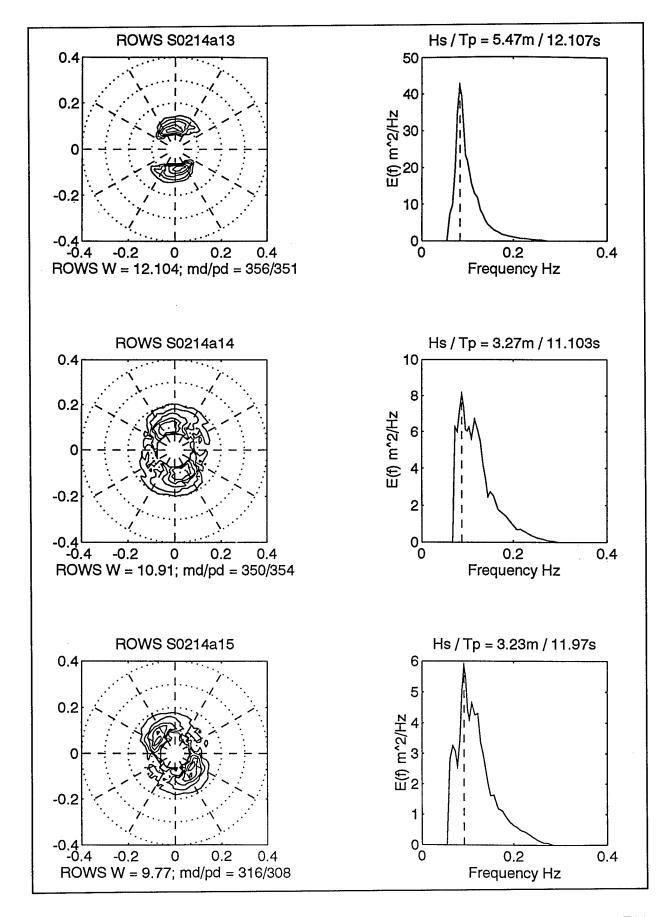


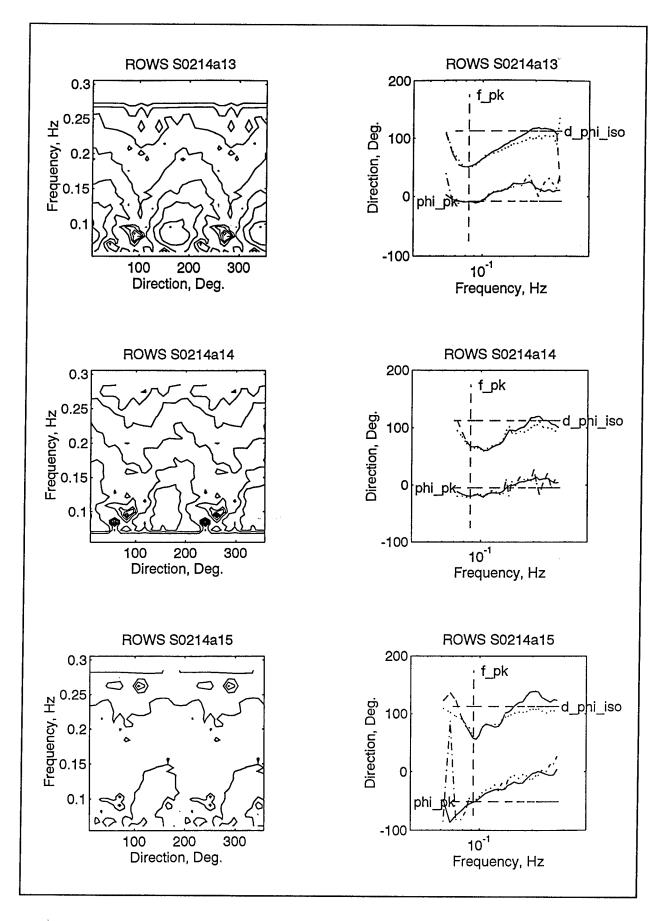


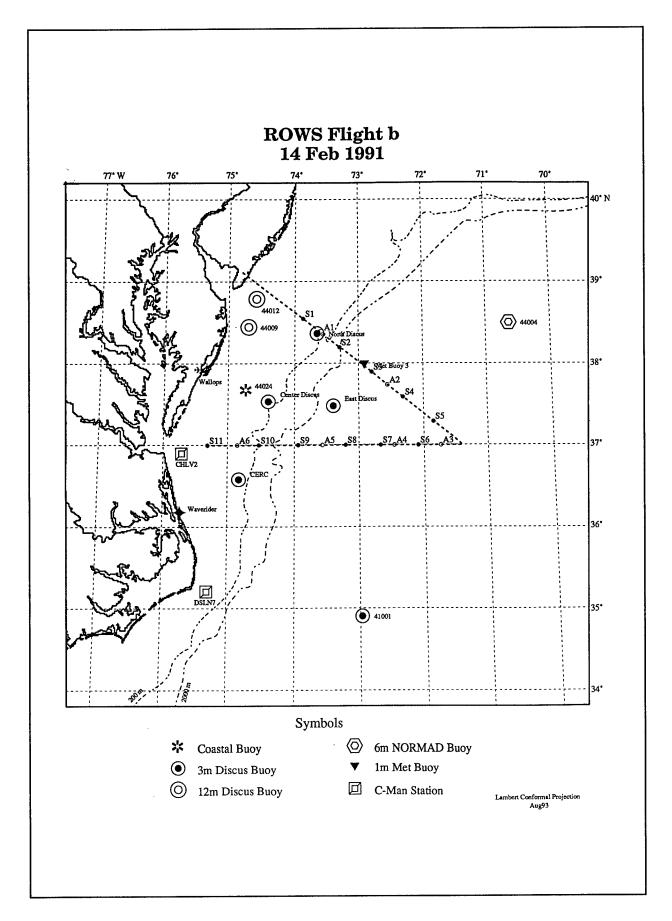








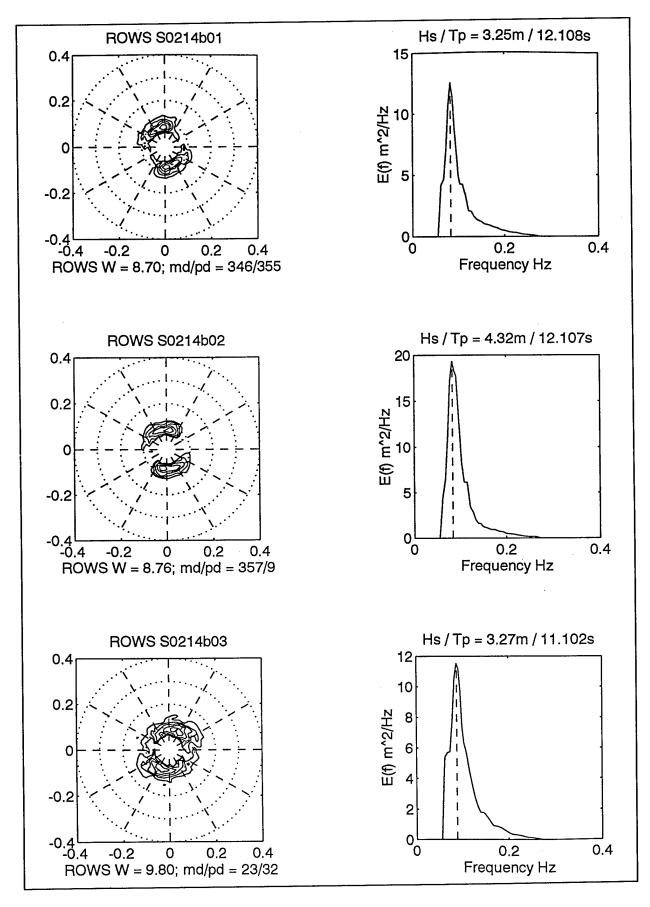


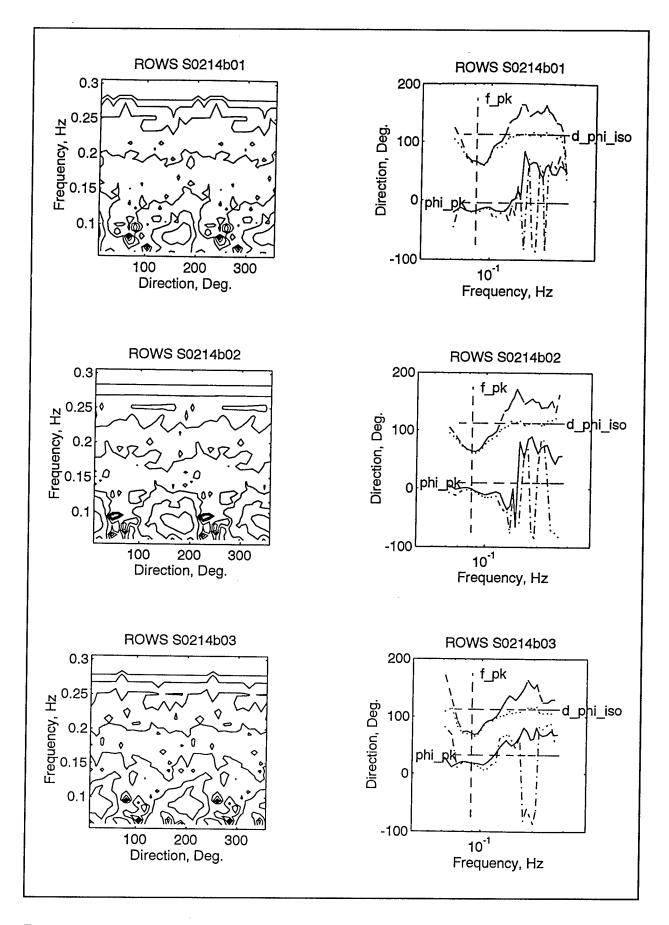


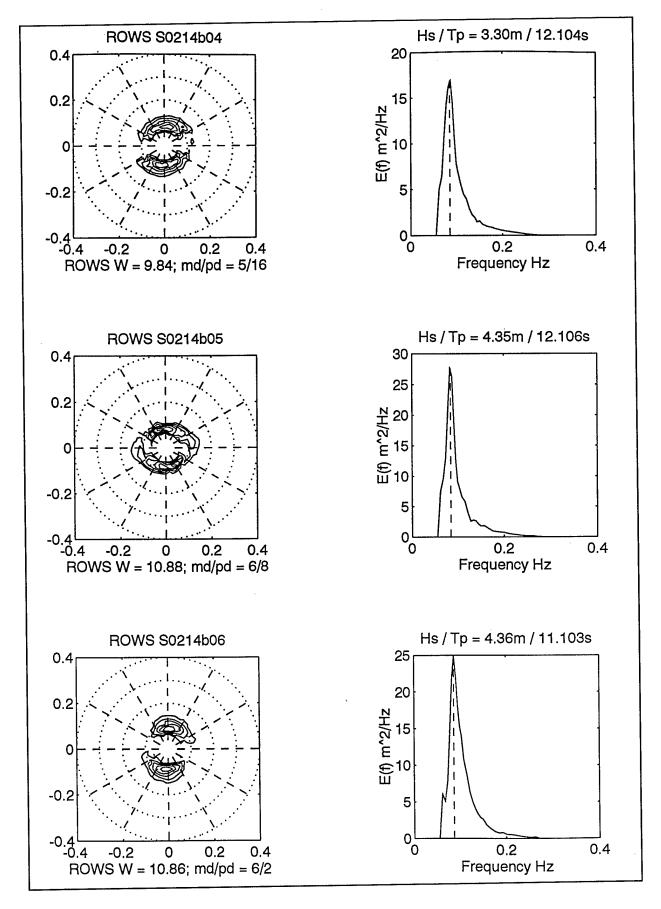
ROWS SWADE FLIGHT NAVIGATION AND FILE DATA FEB 14, 1991--FLIGHT #2

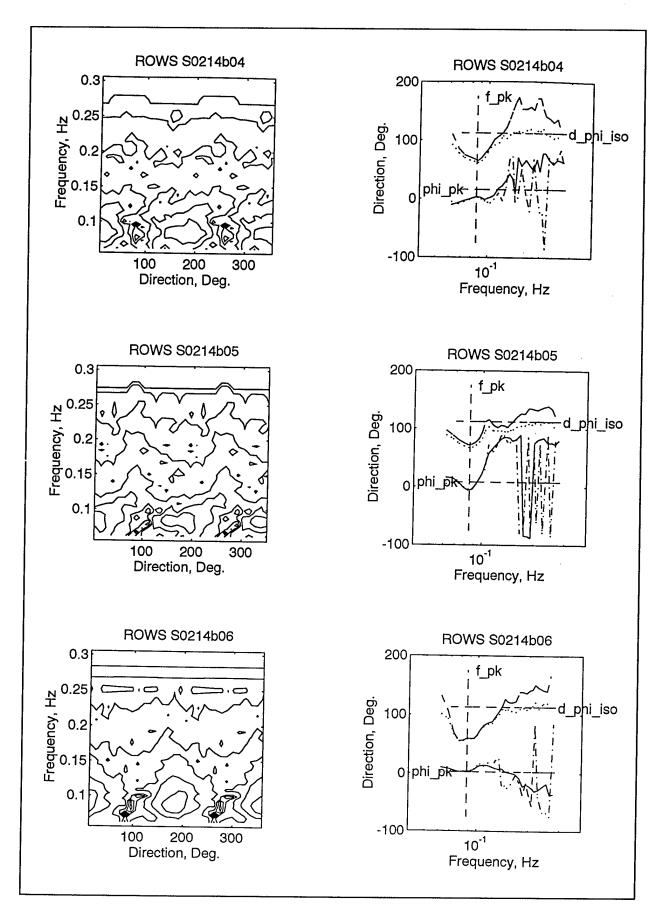
TAPE1/1	POS	ROWS	BUOY/		EST		LAT	LON	ALT	SPD	HDG	PC-TIC	REC #	0 DEG	LEN
FILE	FIX	MODE	WP	НН	MM	SS				M/S	TRU	START	START	DELTA	ME
	1		SIE/3	20	28	00	39.11	-74.80							
S01	1			20	37	50	38.55	-73.87	7625	192	138	203723	28401		12
A01	0							-73.56					23901		1
S02	0											204243	32101		12
	1	0						-73.24							
S03	0	1											69001		12
A02	0	2											79401		2
S04	0	1		20	54	22	37.59	-72.32	7625	174	150	205311	85501		12
S05	0	1										205819	116301		12
	1	0	_					-71.56		174	157				
	1	0	6					-71.40							
A03	0	2										210603	151801		2
	1	0						-72.01							
S06	0	1		21	10	22	37.00	-72.09	7625	126	250	210834	163801		18
A04	0	2		21	14	23	37.00	-72.46	7625	126	250	211356	193801		2
S07	1	1	7	21	16	35	37.00	-72.67	7625	126	250	211518	199901		12
S08	0	1		21	21	53	37.00	-73.21	7625	126	250	212030	231301		12
A05	0	2 1		21	25	22	37.00	-73.57	7015	156	249	212440	244401		2
S09	1			21	28	59	37.00	-73.94	7015	156	249	212733	253801		12
S10	0	1		21	34	10	37.00	-74.53	7015	156	249	213242	284701		12
A06	0	2		21	37	02	37.00	-74.86	7015	156	249	213625	301801		2
~	1	0						-75.25							
S11	0	1		21	41	03	37.00	-75.31	7015	165	254	213904	314101		18

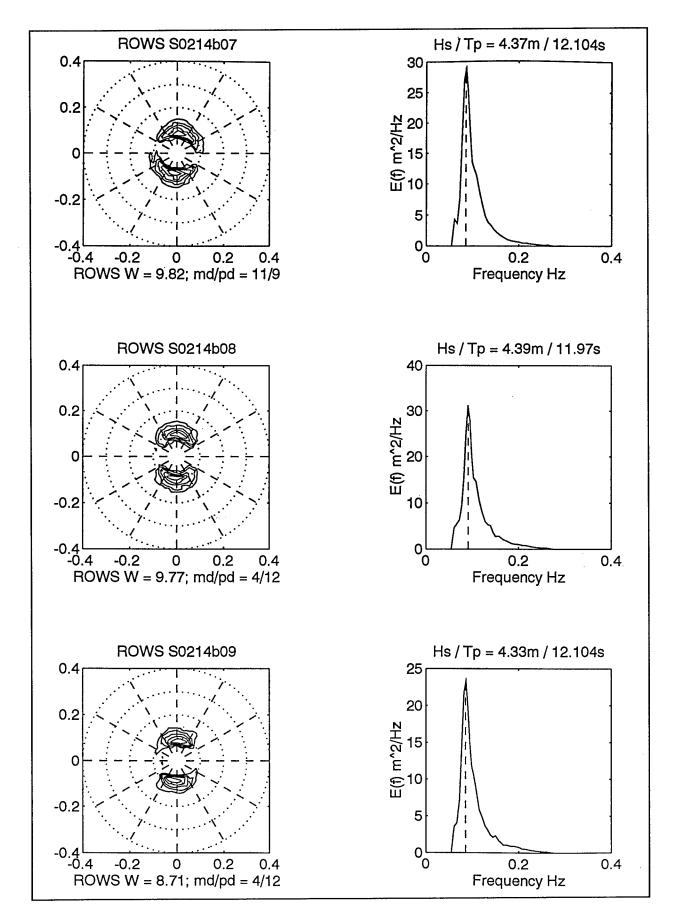
NOTES: (1) S05 HEADING MAY BE IN ERROR. (2) SOME POSITION DATA ON OUTBOUND LEG (OMITTED SINCE WE USE INTERPOLATION BETWEEN 20:44:16 AND 21:02:45 POSTION FIXES.

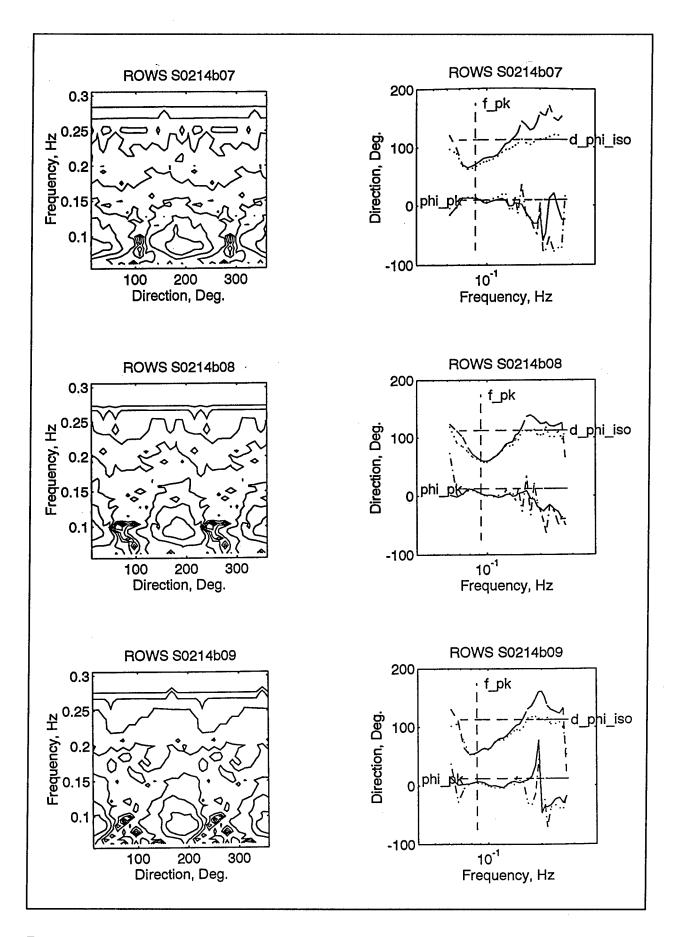


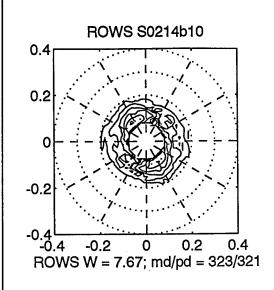


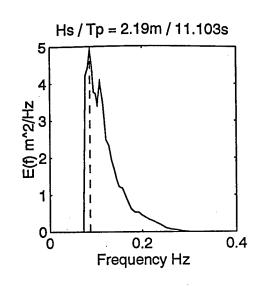


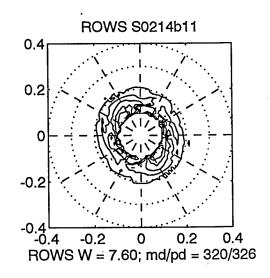


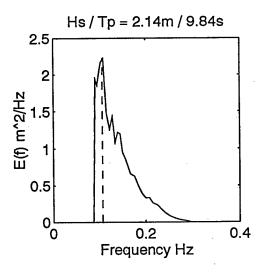


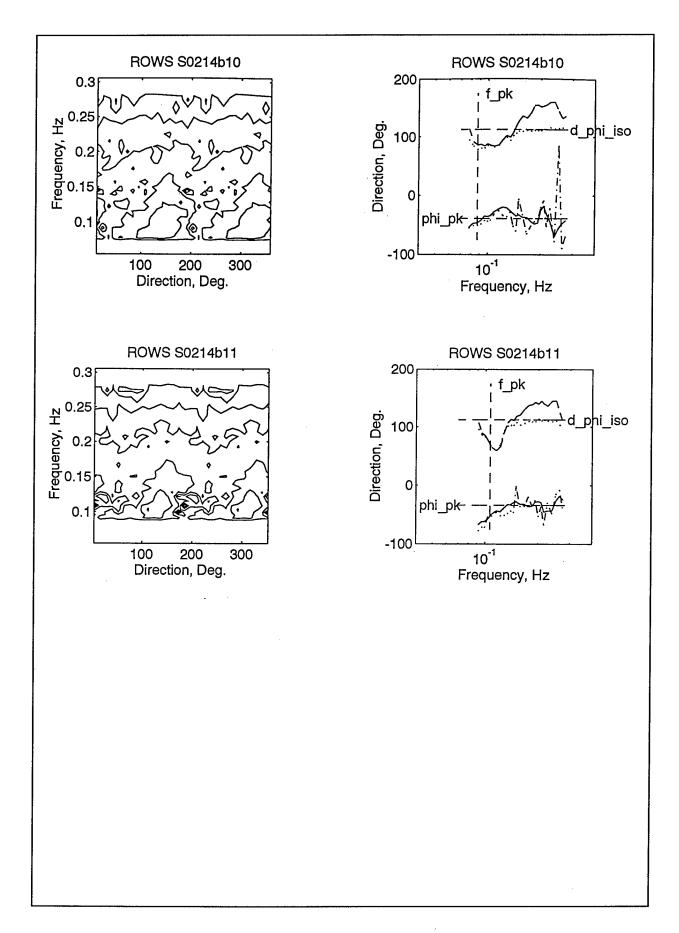


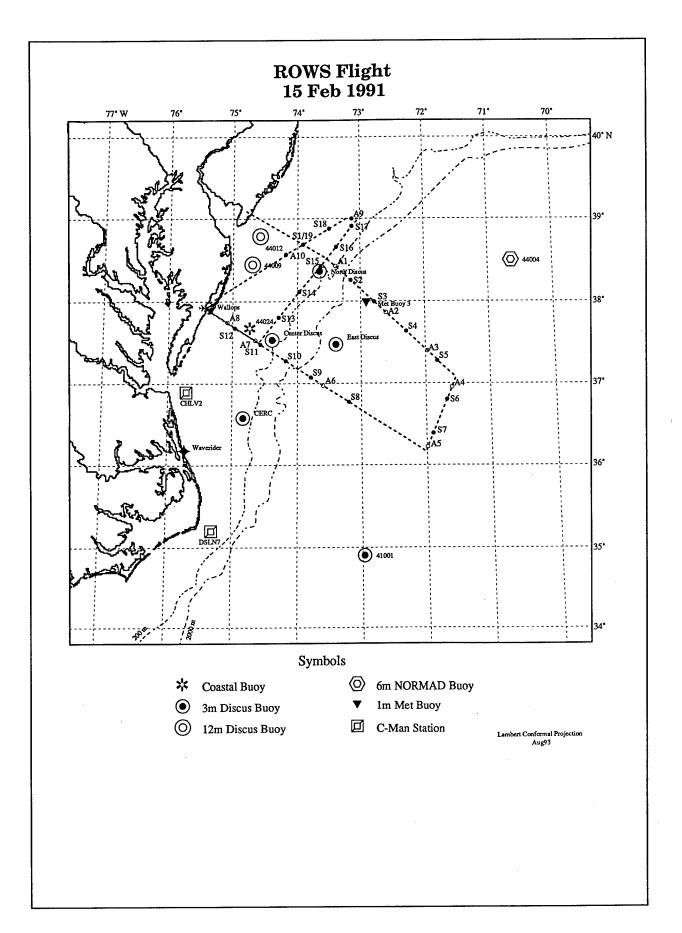








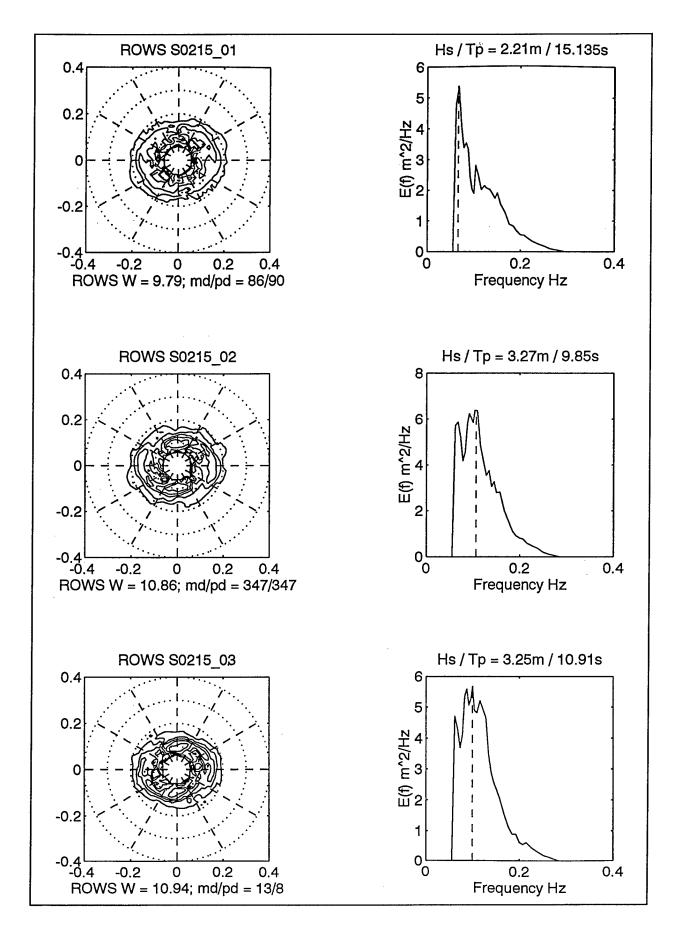


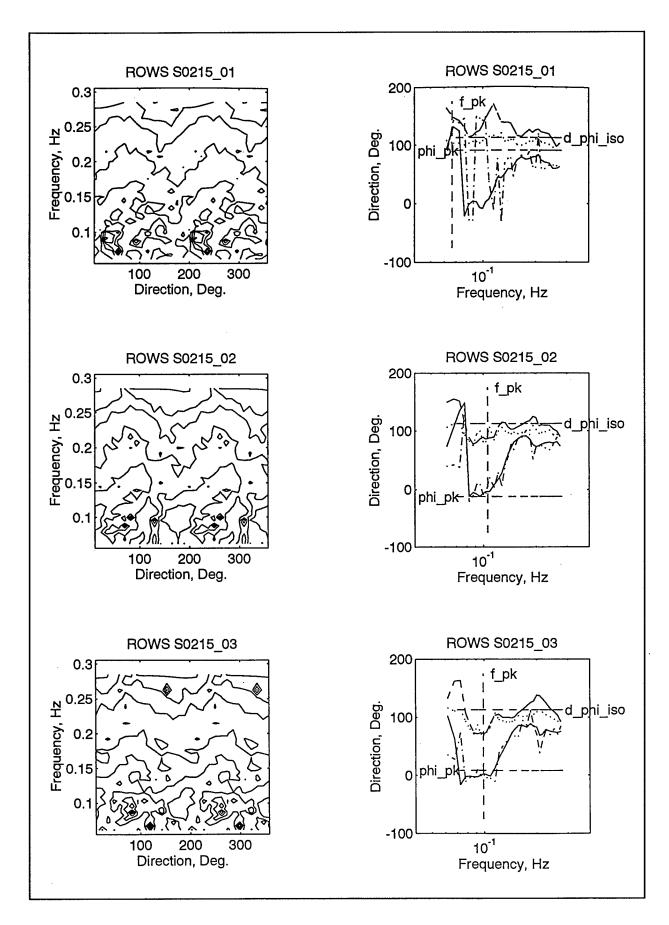


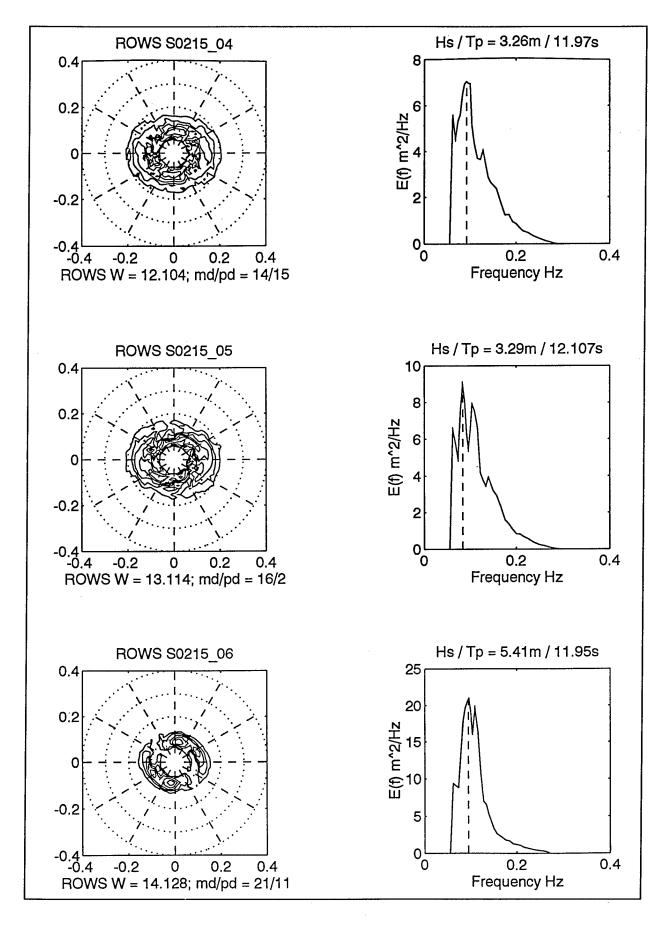
ROWS SWADE FLIGHT NAVIGATION AND FILE DATA FEB 15, 1991

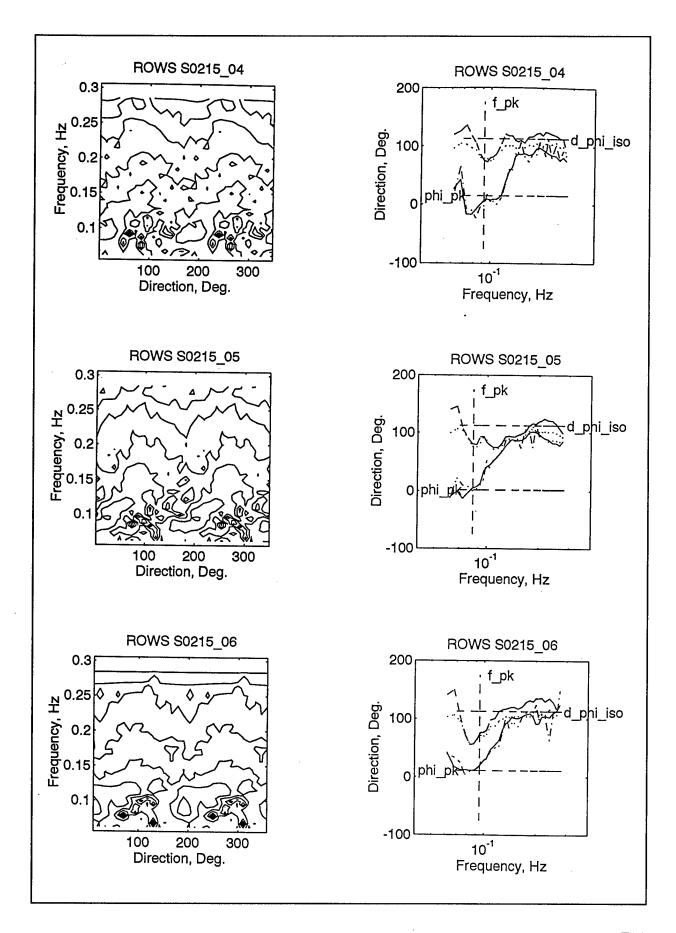
TAPE1/1	POS	ROW:	S BUO	¥/	ES	T CC	LAT	LON	ALT	SPI	HDG	PC-TIC	REC # START	0 DEG	LE
	1	1	SEI/	3 15	5 27	7 00	39.09	-74.80	7625						
	1	0	4	1 15	31	03	•								
S01	0	1		15	34	23	38.69	-73.91	7625	182	138	153300	14901		1
	1	0	5	15	38	80	38.53	-73.56	7625						_
A01	0	2		15	40	05	38.43	-73.40	7625	172	!	153939	47901		
S02	1	1		15	42	24	38.26	-73.16	7625	172	151	154107	53201		1
S03	0	1		15	47	10	38.00	-72.79	7625	167	152	154548	81301		-
A02	0	2		15	49	40	37.87	-72.61	7625			154907	98401		_
S04	0	1		15	53	24	37.64	-72.30	7625	161	154	155201	112401		1
A03	0	2		15	57	25	37.40	-71.97	7625			155650	132701		
	1	0		1.5	59	23	37.30	-71.83	7625	155	156	133030	138/01		
S05	0	1		15	59	38	37.28	-71.82	7625	155	156	155010	144501		-
	1	ō	6'	16	02	52	37.08	-71 54	7625	133	130	133612	144501		1
A04	0	2	•	16	0.6	40	36 96	-71.54 -71.60	7625	104	212	160604	171701		
	1	0		16	٥٥	70	36 03	-71.00	7625	104	212	100004	1/1/01		
S06	ñ	1		16	00	10	36.02	-71.67	7625	104	212	160045			
507	1	1		16	17	16	30.01	71.08	7025	104	212	160715	175201		1
305 305	ñ	2		10	7/	10	36.39	-/1.90	7625	108	209	161500	221401		1
	1	Õ	7	16	21	05	36.16	-71.99 -72.01	7625	108	209	161927	244901		
TAPE2/2													START 14901 53201 81301 112401 138701 144501 175201 221401 244901		
308	0	1		16	33	34	36.78	-73.20	7625	169	285	163341	6101		18
A06	0	2		16	38	03	36.98	-73.60	7625	169		163855	30801		
509	0	1		16	40	13	37.08	-73.79	7625	169	288	164013	35401		1:
S10	0	1		16	44	16	37.28	-74.18	7625	169	288	164416	59701		1:
511	0	1		16	48	20	37.48	-74.57	7625	169	288	164815	83601		1:
	1	0	8	16	48	40	37.50	-74.60	7625						
407	0	2		16	50	00	37.53	-74.65	7625	174	285	164018	96201		:
	1	0		16	52	23	37.68	-74.97	7625						-
512	0	1		16	52	38	37.68	-74.97	7625	174	285	165235	104301		1 1
	1	0	WFF				37.94	-75.47	7625				104501		
804	1	2		17	00	34	37.75	-75.09	7625	186	150	170113	138101		-
	1	0	8	17	05	08	37.50	-74.60	7625			1,0113	130101		-
313	0	1		17	09	32	37.81	-74.29	7625	226	042	170921	180501		1.5
:11	1	1		17	13	56	38.12	-73.97	7625	226	042	171345	206901		12
, _ ~	1	1	DIS-N	17	16	15	38.42	-73.64	7625	226	042	171604	214901		12
315		1		17	19	08	38.66	-73.39	7625	227	042	171851	231401		12
315 316	ō							70.03	7625	229	041	172140	531401		12
515 516 517	0 1	ī	14	17	22	01	38.91	-/3.14							14
315 316 317	0 1 1	1	14 TEMP	17	22	01	38.91 39.00	-73.14 -73.03	7625		·	1/2140	248401		
15 16 17	0 1 1 0	1 0 2	14 TEMP	17 17	22	01 00	38.91 39.00 39.00	-73.14 -73.03 -73.14	7625 7625 7625		• • •	1/2140	248401		
315 316 317	0 1 1 0	1 0 2 0	14 TEMP	17 17	22 26	01 00	38.91 39.00 39.00	-73.14 -73.03 -73.14 -73.23	7625 7625 7625		• • •	172140	248401		
115 116 117	0 1 1 0 1	1 0 2 0	14 TEMP TEMP	17 17 17	222627	01 00 50	38.91 39.00 39.00 39.00	-73.14 -73.03 -73.14 -73.23 -73.34	7625 7625 7625 7625	149	227	1/2140	248401		
315 316 317 309	0 1 1 0 1 1	1 0 2 0 0	14 TEMP	17 17 17 17	22 26 27 29	01 00 50 20	38.91 39.00 39.00 39.00 38.95	-73.14 -73.03 -73.14 -73.23 -73.34 -73.50	7625 7625 7625 7625 7625	149	227	172820	272201		10
115 116 117 109 118 119	0 1 1 0 1 1 0	1 0 2 0 0 1	14 TEMP	17 17 17 17 17	22 26 27 29 33	01 00 50 20 38	38.91 39.00 39.00 39.00 38.95 38.88 38.69	-73.14 -73.03 -73.14 -73.23 -73.34 -73.50 -73.91	7625 7625 7625 7625 7625 7625	149 149	227 227 227	172820	272201		18
TAPE2/2 S08 A06 S09 S10 S11 A07 S12 A08 S13 S14 S15 S16 S17 A09	0 1 1 0 1 0 0 0	1 0 2 0 0 1 1 2	14 TEMP	17 17 17 17 17 17	22 26 27 29 33 36	01 00 50 20 38 03	38.91 39.00 39.00 39.00 38.95 38.88 38.69	-73.14 -73.03 -73.14 -73.23 -73.34 -73.50 -73.91	7625 7625 7625 7625 7625 7625 7625	149 149 130	227 227 227 227	172820 173244	272201 297701		18 18
115 116 117 .09 18 19	0 0 1	1 2 0		17 17 17	33 36 36	38 03 15	38.69 38.57	-73.91 -74.18 -74.20	7625 7625 7625	149 149 130 121	227 227 227 227	172820 173244 173630	272201 297701 317001		18 18 2
15 16 17 09 18 19	0 0 1	1 2 0		17 17 17	33 36 36	38 03 15	38.69 38.57	-73.14 -73.03 -73.14 -73.23 -73.34 -73.50 -73.91 -74.18 -74.20 -75.47	7625 7625 7625	149 149 130 121	227 227 227 227	172820 173244 173630	272201 297701 317001		18 18 2

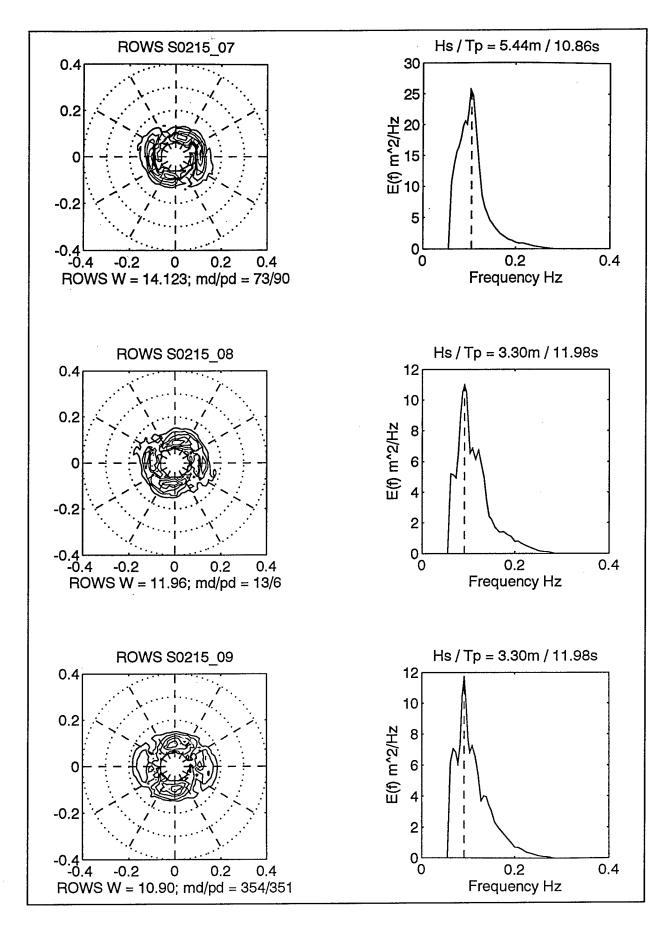
OTES: (1) 138 DEG E PECTRUM WITH CROSSI EADING ESTIMATED FF	EADING ON OUTBOUND I RACK OVERLAY SPECTRU OM TRACK = 304 DEG N	LEG SOMEWHAT UNC JM S19. (2) INBO IINUS DRIFT ANGL	ERTAINCHECK S UND SOUTHERN LI	301 3G
	e e			
•				

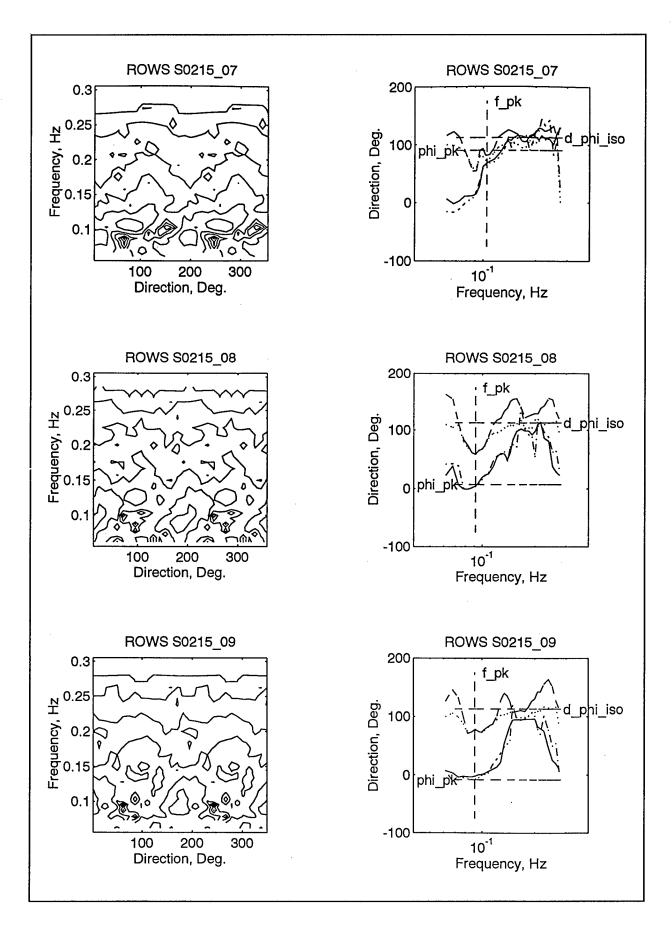


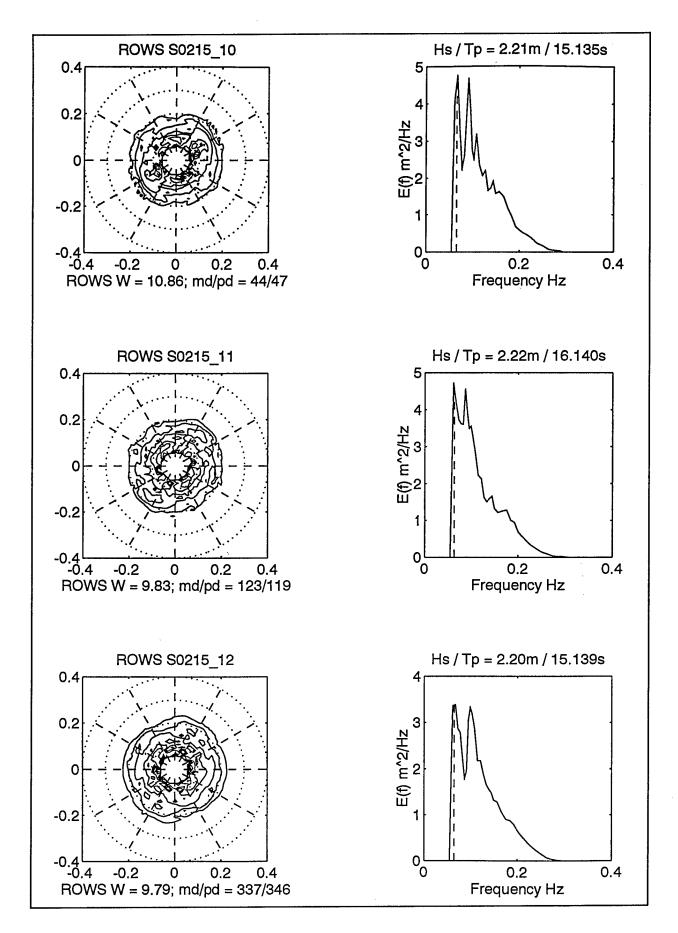


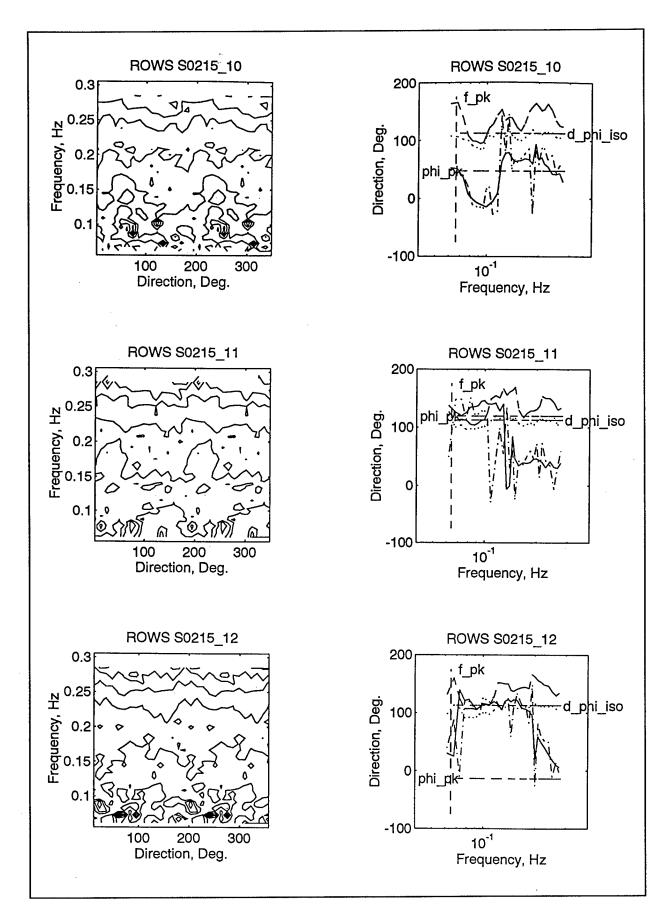


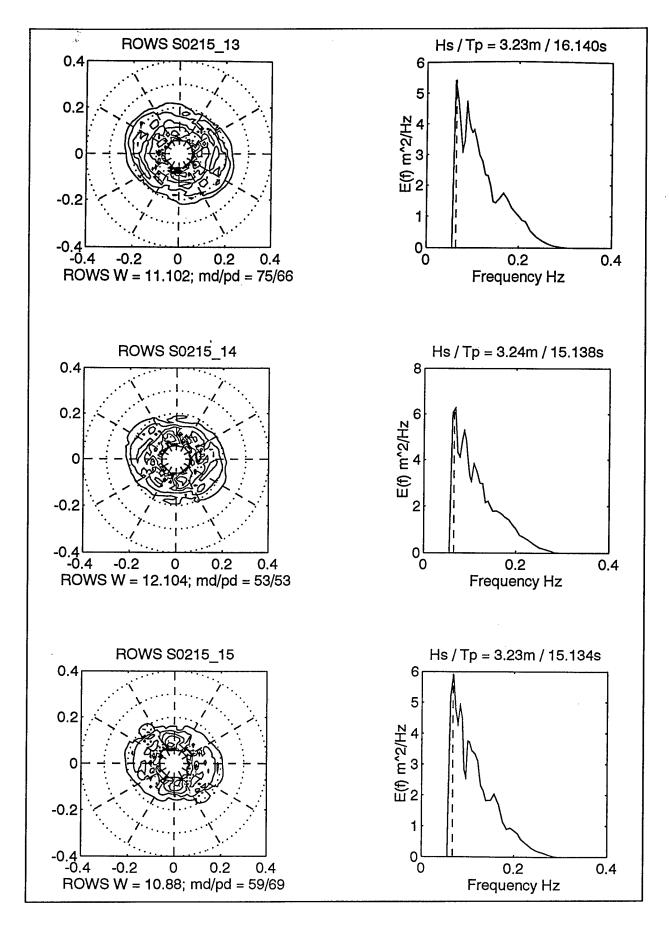


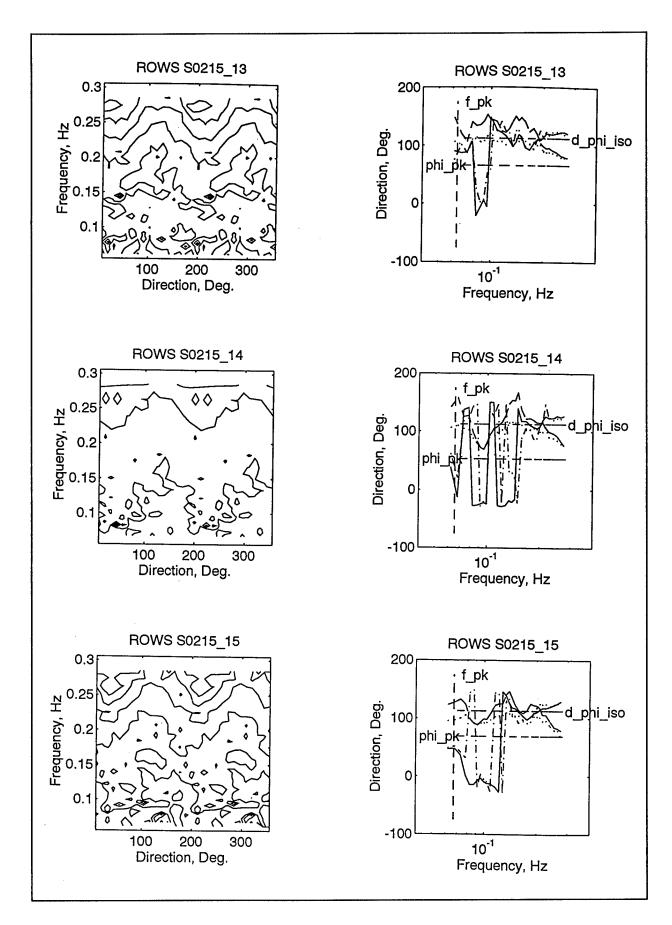


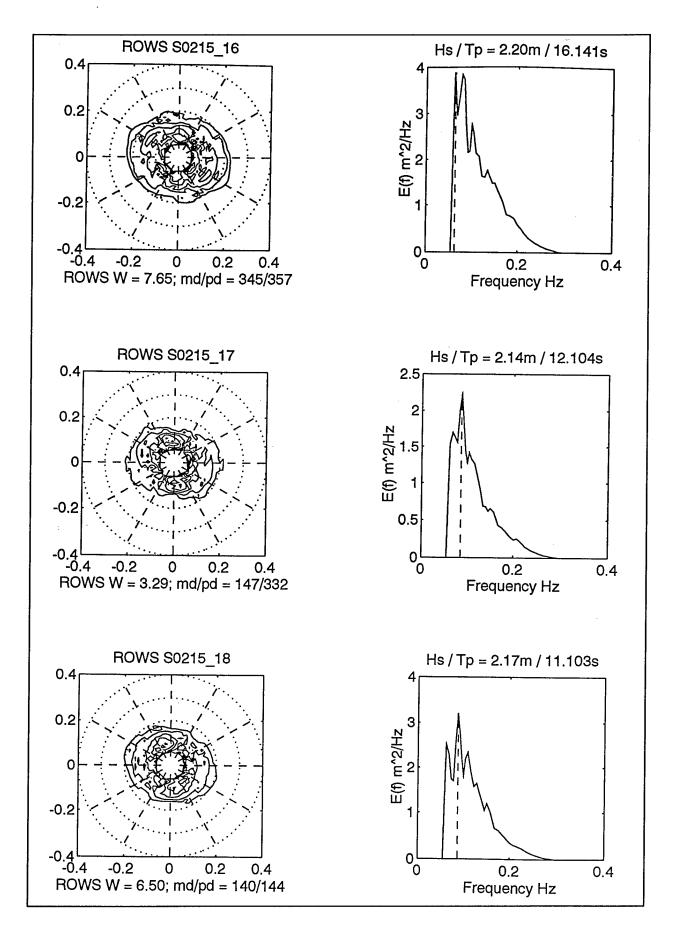


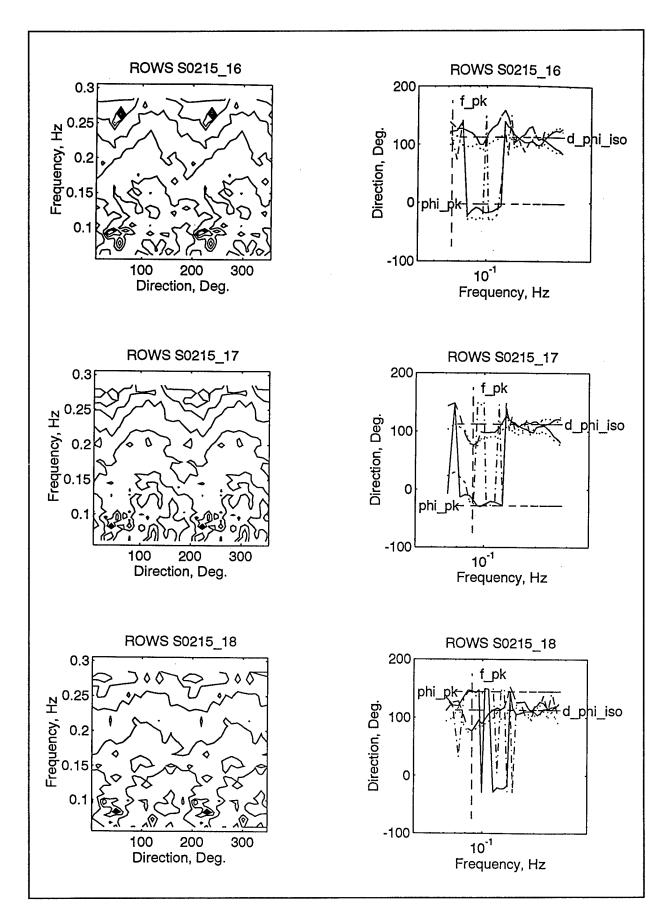


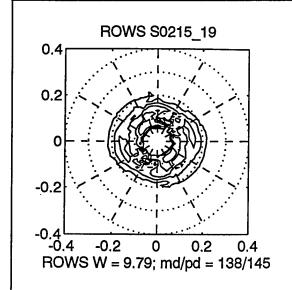


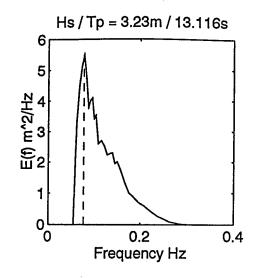


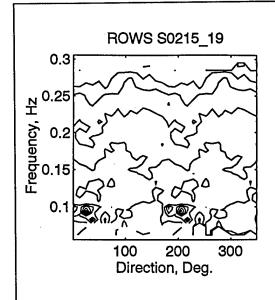


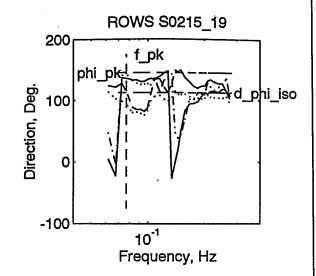


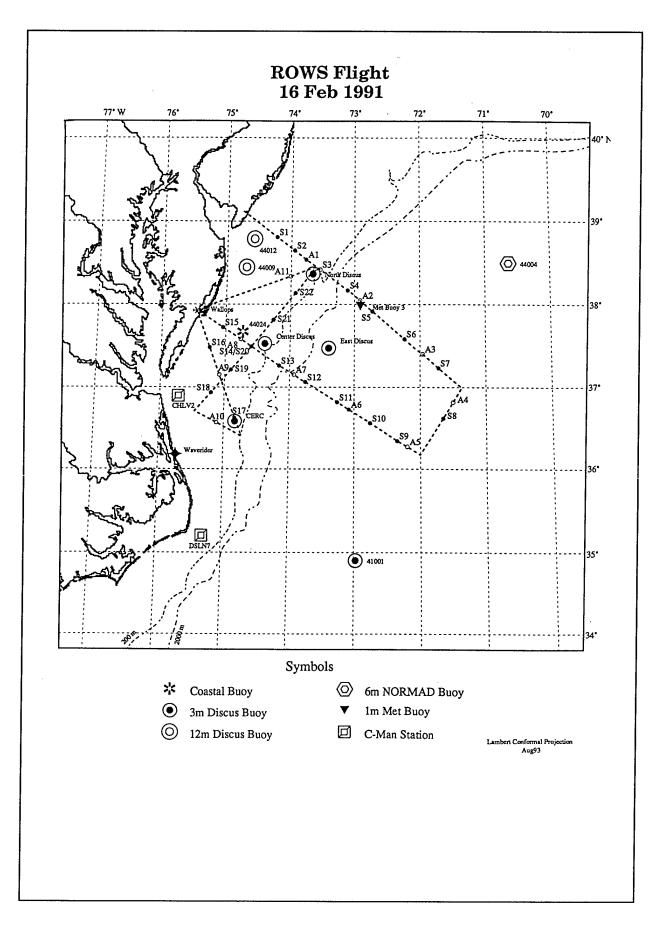










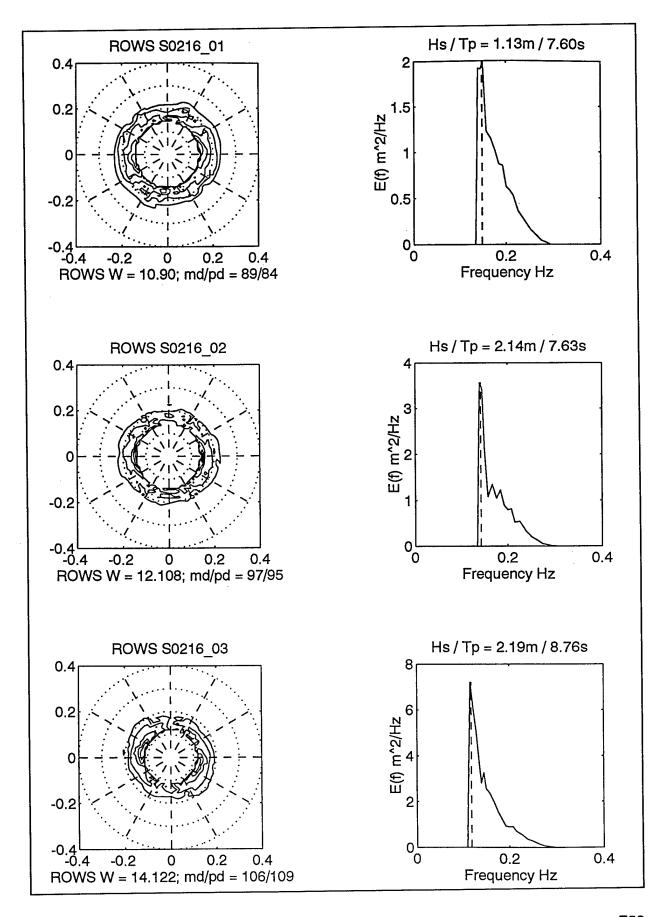


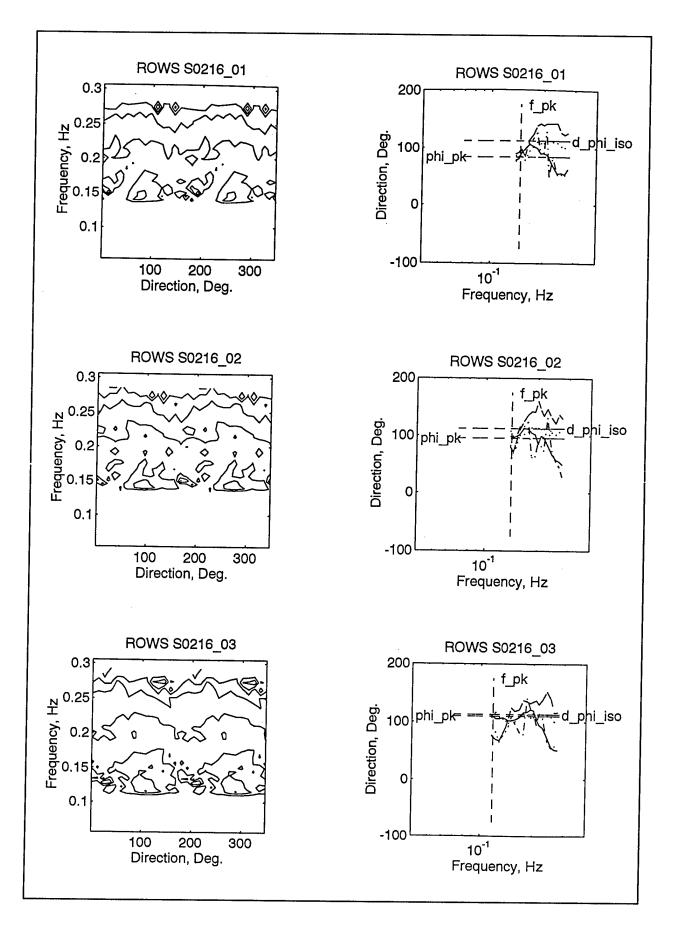
ROWS SWADE FLIGHT NAVIGATION AND FILE DATA FEB 16, 1991

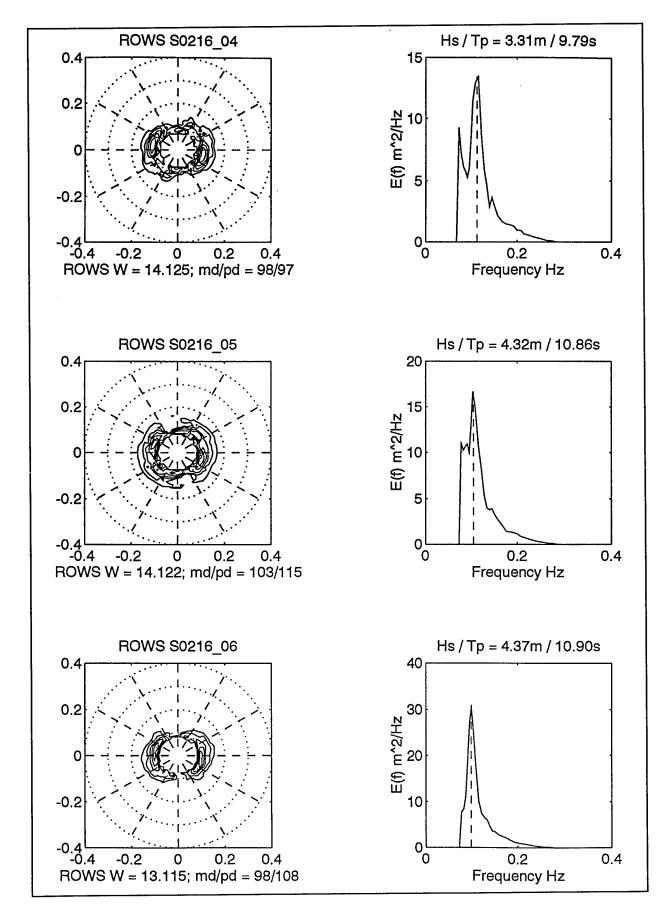
TAPE1/1 FILE	POS FIX	ROWS	BUOY,	/ HH	ES!	r ss	LAT DEG N	LON DEG E	ALT M	SPD M/S	HDG TRU	PC-TIC START	REC # START	O DEG DELTA	LEN
	[1							-74.76							
	1	0	3,	09	27	28	39.17	-74.76	7625						
	[1	1 1 2		09	32	42	38.84	-74.21	7625	187	130	}			
S01	1	1	,	09	32	42	38.81	-74.22	7625	187	130	093235	8401		12
S02	0	1		09	35	21	38.65	-73.94	7625	187	130	093513	24201		1:
A01	0	2		09	37	13	38.54	-73.76	7625	187	130	093513 093804 093909	39801		:
S03	. 0	1	DIS-N	09	39	21	38.42	-73.54	7625	187	130	093909	45201		1:
~ ~ 4	^	-		α	42	40	20 17	_72 11	フェント	197	130	ロロルマフR	71101		1:
	1	1 0		09	44	14	38.14	-73.05	7625	194	133				
A02	ō	2		09	45	36	38.05	-72.92	7625	194	133	094616	86301		:
505	ñ	1		09	47	38	37.92	-72.73	7625	196	133	094727	90701		1:
506 506	Ô	ī		09	52	48	37.59	-72.23	7625	196	133	095236	121701		1:
500	1	ñ		09	54	23	37.48	-72.08	7625	196	133				
3 03	ō	2		09	55	15	37.41	-71.96	7625	196	133	095549	139801		
AU3 207	ň	1		09	57	58	37 24	-71.72	7625	196	133	095742	149101		1
507	1	ń	6	10	01	17	37 00	-71 37	7625						_
304	<u> </u>	2	0	10	0.7	71	36 92	-71.57	7625	175	218	100305	179801		
A04	1	1		10	02	20	36.62	-71.50 -71.65	7625	175	218	100303	185701		1
500	1	7	7	10	10	15	26 17	-71.05	7625	1,5	210	100410	100/01		-
305	<u> </u>	0	,	10	10	7.0	26 27	-72.00	7625	173	299	101304	235701		
COO	0	- 2		10	14	12	26.21	-72.19	7625	173	299	101358	239801		1
509	. 0	1		10	14	22	26 56	-72.34	7625	173	299	101338	265201		1
210	0	7		10	10	2/	30.30	-72.70	7625	173	200	101011	203201		-
300	7	Ü		10	18	28	30.39	-72.01	7625	173	200	102215	289001		
AU6	Ü	2		10	21	45	30./3	-73.06	7625	171	201	102213	203001		1
217	Ü	1		10	23	40	30.82	73.20	7625	160	207	102322	293301		1
S12	0	Ţ		10	28	46	37.07	-/3./5	7625	169	302	102630	324101		_
		0		10	29	28	37.10	73.02	7625	170	202	102102	220201		
A07	0	2		TO	30	30	37.10	-/3.93	7025	170	202	103103	247201		1
S13	0	1	_	10	33	00	37.27	-/4.16	7625	174	302	103240	34/301		1
S14	1	1	8	10	37	10	37.50	-/4.60	7625	174	30T	103032	372000		
A08	0	2		10	38	52	37.59	-/4.//	7625	1/5	300	103925	386101		-
A02 S05 S06 A03 S07 A04 S08 A05 S09 S10 A06 S11 S12 A07 S13 S14 A08 S15	0	1		10	41	38	37.73	-75.05	7625	1/6	300	104106	391401		1
	[1	0		10	44	32	37.92	-75.27	7625	1/8	300	1			
	1	0	WFF												
S16	1	0 1 2 1 0		10	52	27	37.49	-75.25	7625	188	159	105205 105622 110013	455501		Т
A09	0	2		10	55	52	37.16	-75.09	7625	188	159	105622	479201		
S17	0	1		11	01	10	36.63	-74.84	7625	188	159	110013	540401		1
	1	0 (CERC/9					-74.82		188	159				
	1		TEMP	11	02	50	36.40	-74.73	7625						
A10	1	2								177	298	110806	539201		
		0	TEMP	11	80	50	36.71	-75.46	7625						_
S18	1	1		11	12	47	36.94	-75.21	7625	203	041	111220	561101		1
S19	0	1		11	16	07	37.22	-74.91	7625	203	041	111540	581101		1
S20	1	1	8	11	19	28	37.50	-74.60	7625	203	040	112001	607201		1
S21	0	1	11′	11	23	21	37.82	-74.26	7625	202	039	111220 111540 112001 112354 112747	630501		1
S22	0	1		11	27	15	38.14	-73.92	7625	202	038	112747	653801		1
	1	0		11	27	45	38.18	-73.87	7625	202	038				
	1	0	11'					-73.61							

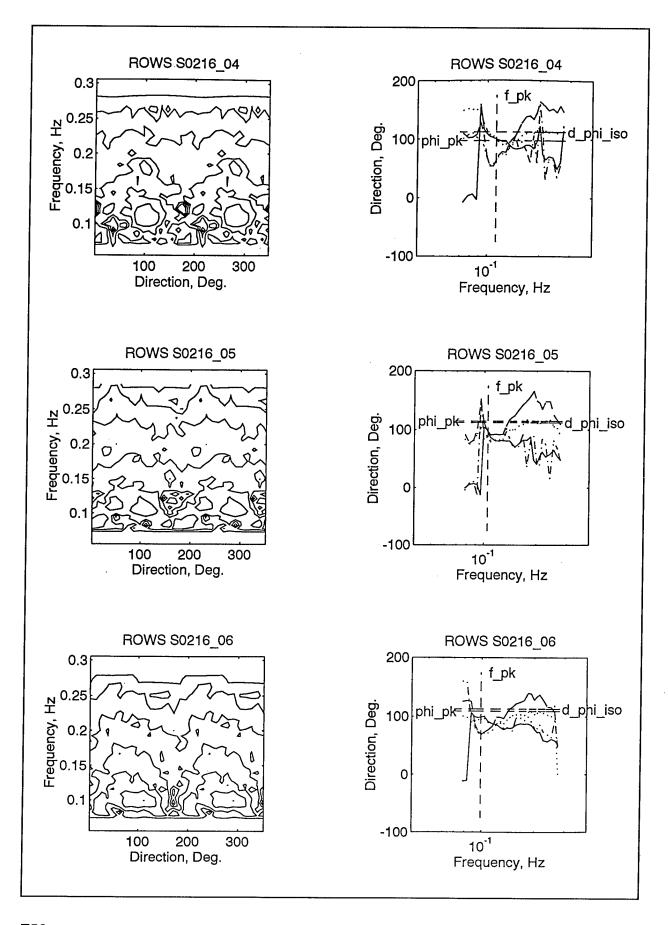
11 34 30 38.34 -74.00 7625 113500 692001 WFF 11 55 00 37.94 -75.47 0 0 2 1 0

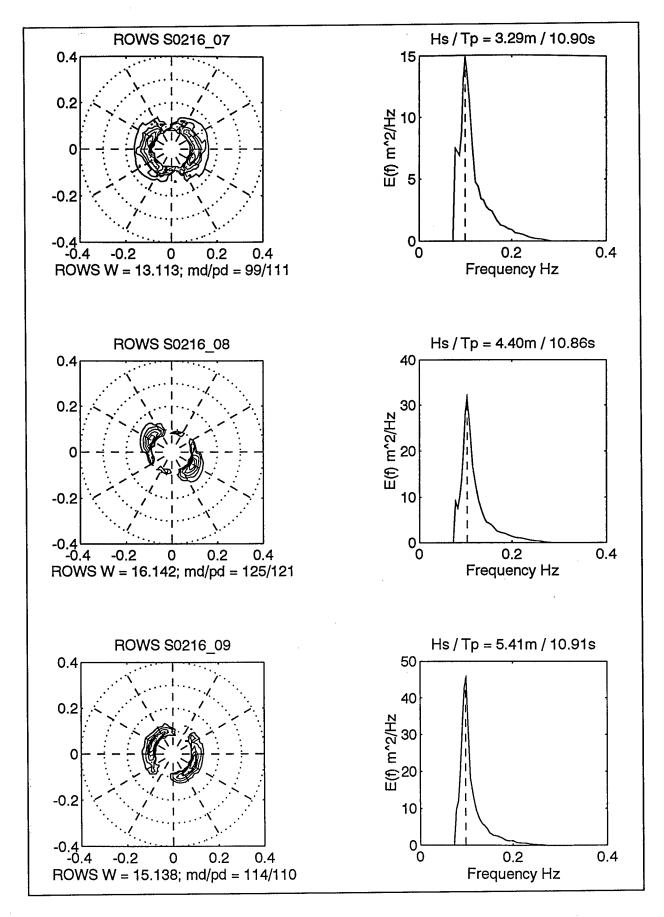
NOTES: (1) BREAK FOR TURN AT 6 AT 100000; EST ARRIVAL AT 6 ASSUMING CONSTANT COURSE. (2) ON INBOUND LEG ARRIVAL WFF ESTIMATED. (3) LAST ALT FILE POSITION ESTIMATED ONLY ROUGHLY.

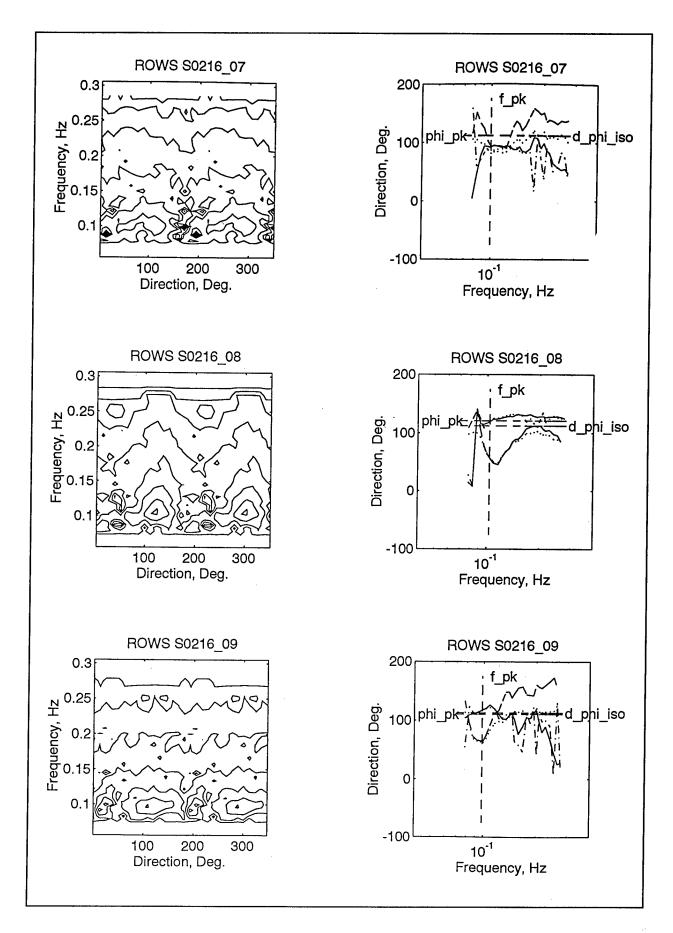


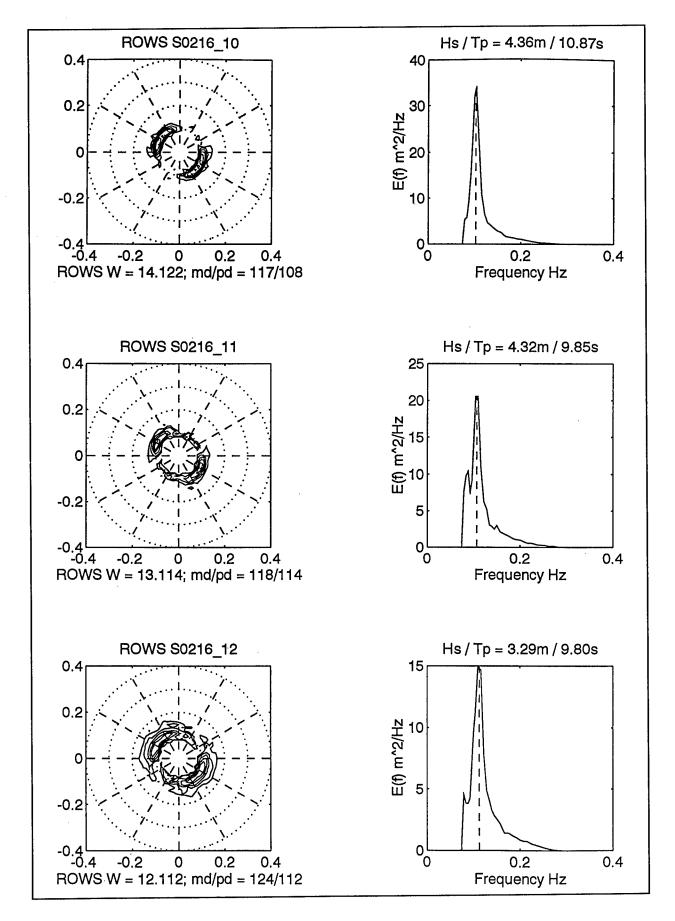


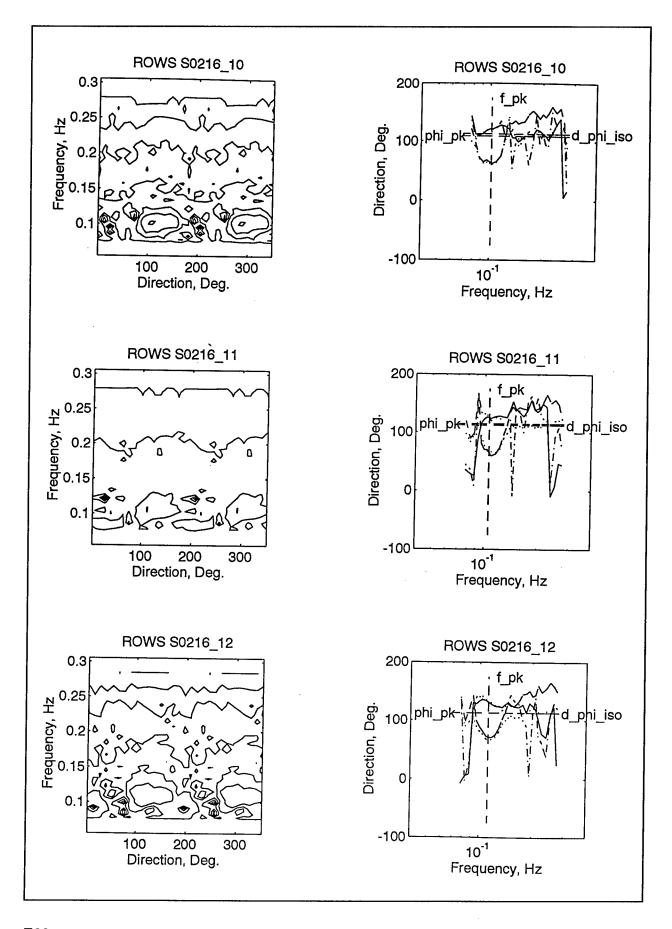


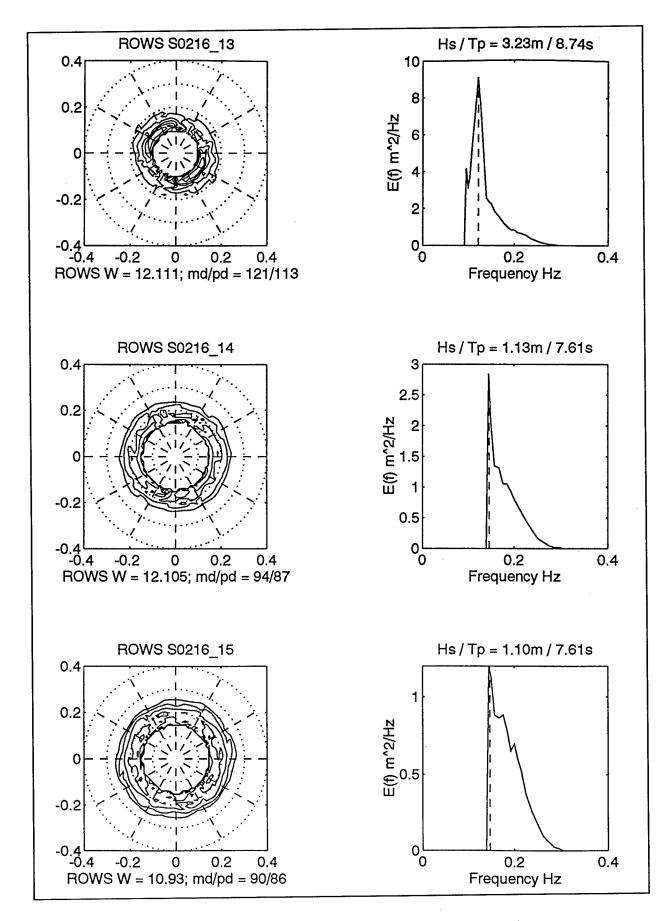


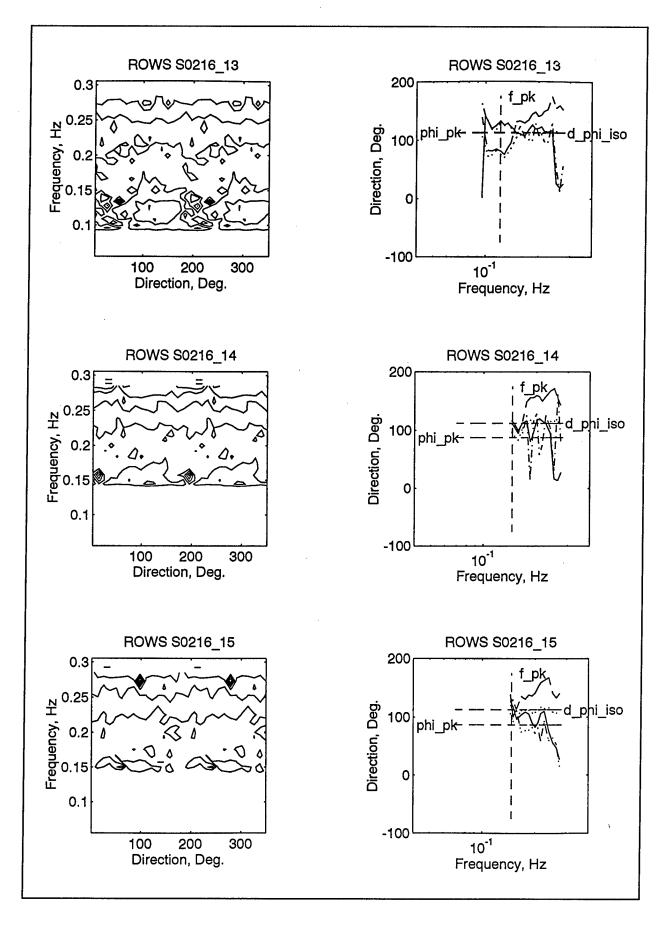


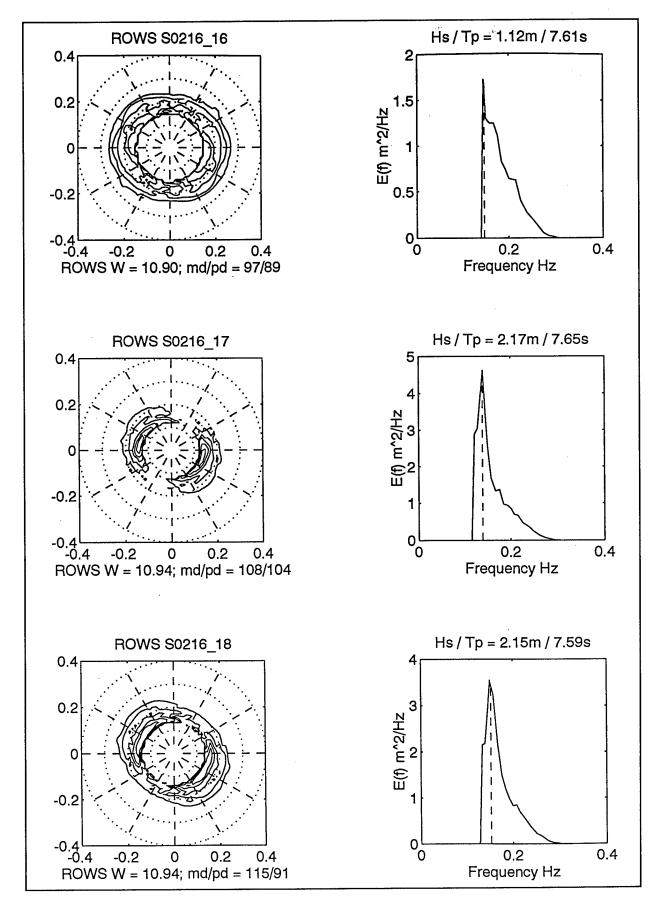


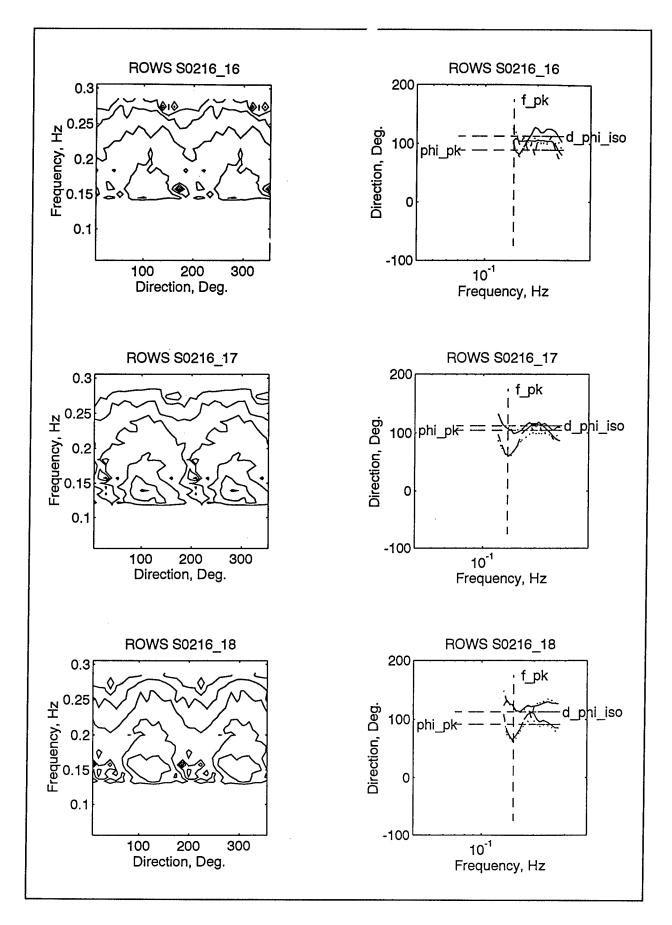


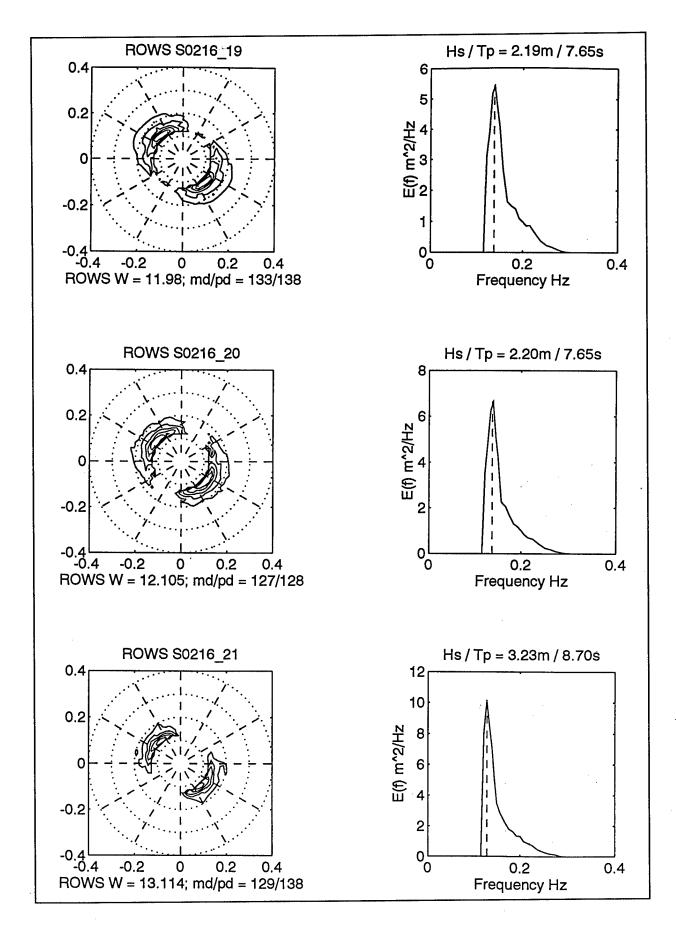


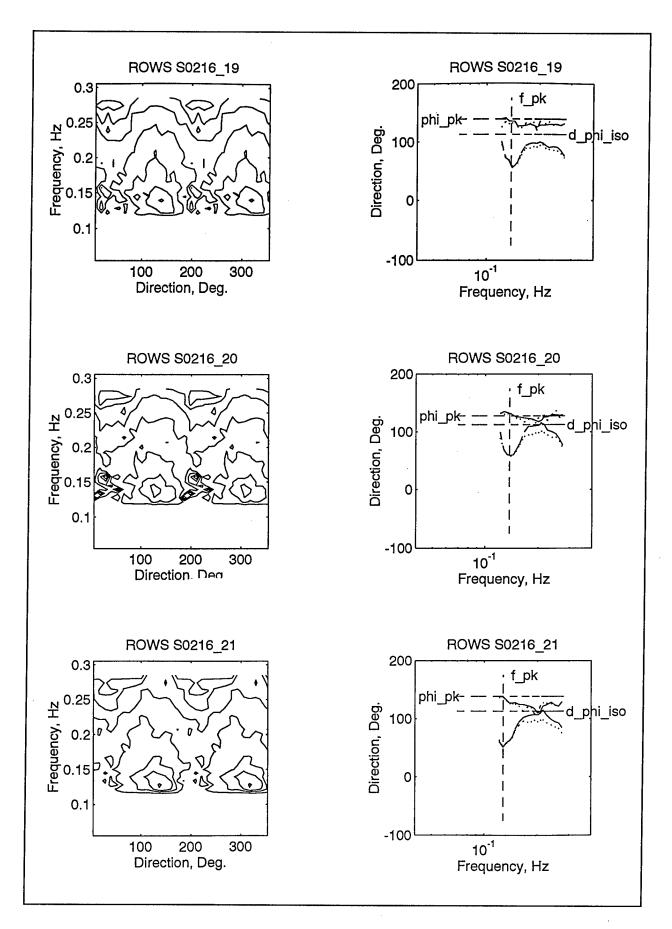


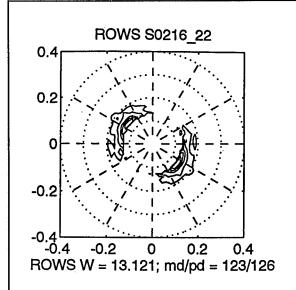


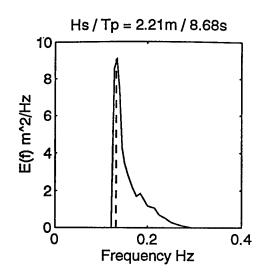


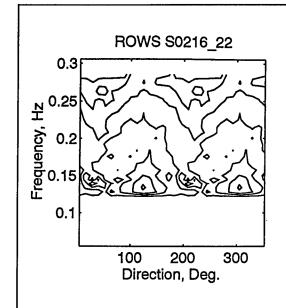


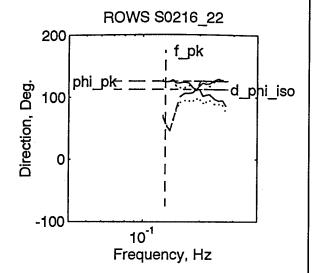






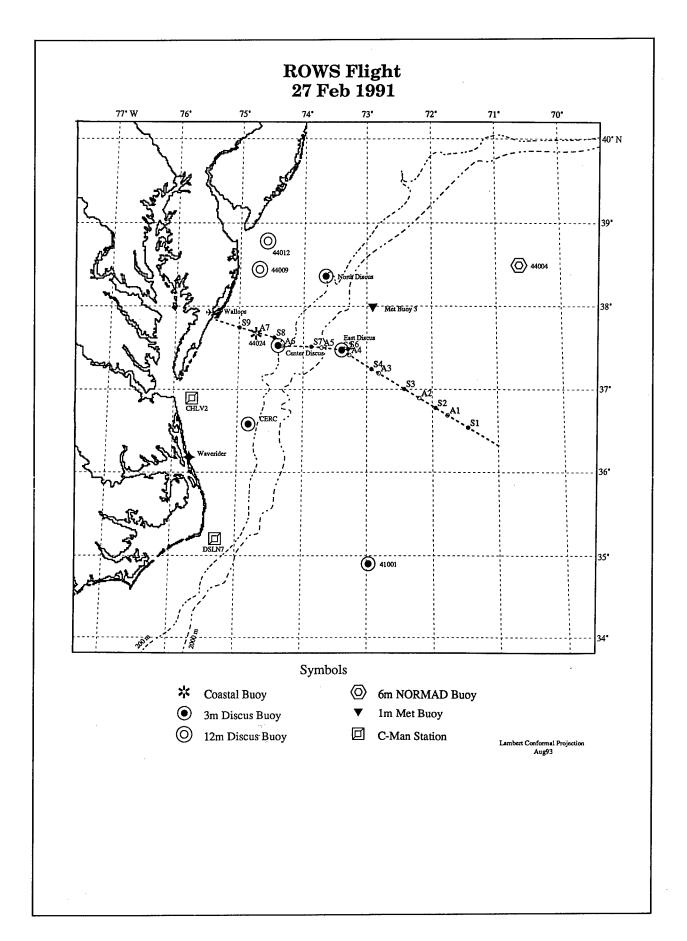






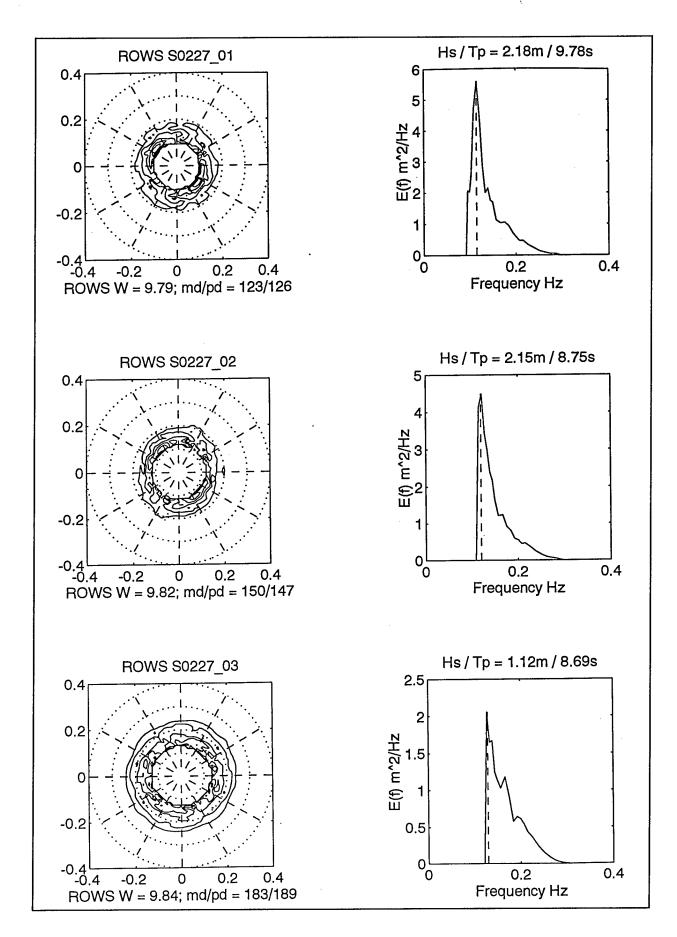
Appendix E3: ROWS Spectra for IOP-3, 27 February - 7 March 1991

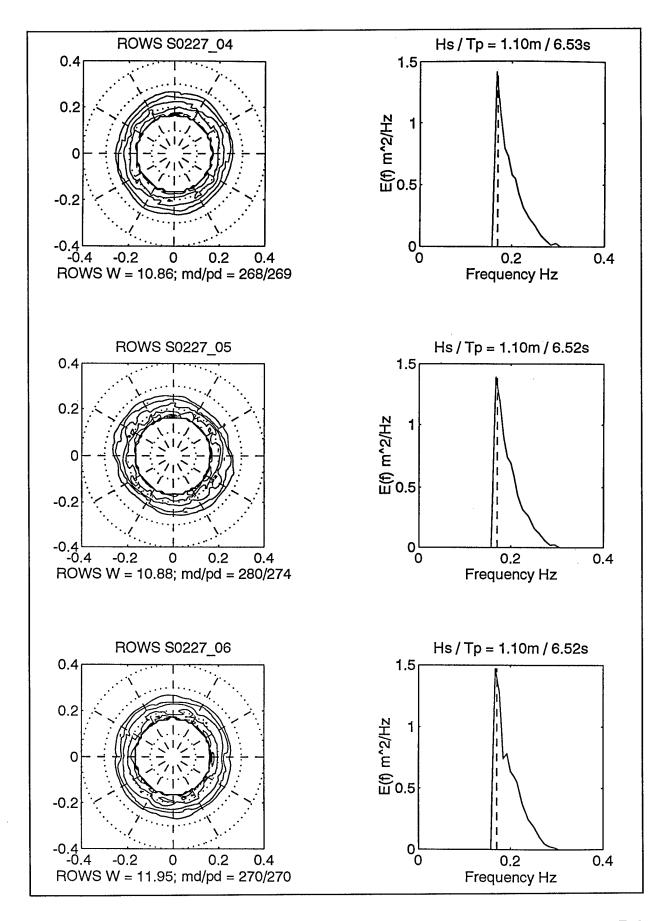
The ROWS directional spectra plots for the seven SWADE IOP-3 flights in this appendix are augmented with zoom plots for 5 March, the SWADE priority day. In the 5 March zoom plots, the maximum frequency is 0.2 Hz instead of 0.4 Hz. These plots help to better resolve the complex, trimodal structure of the swell on this day.

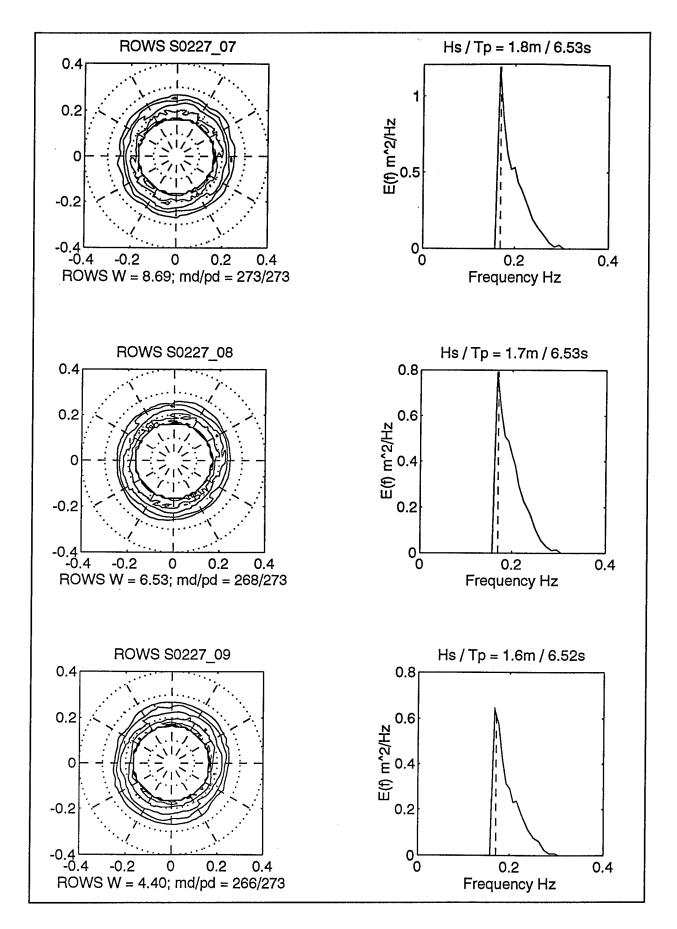


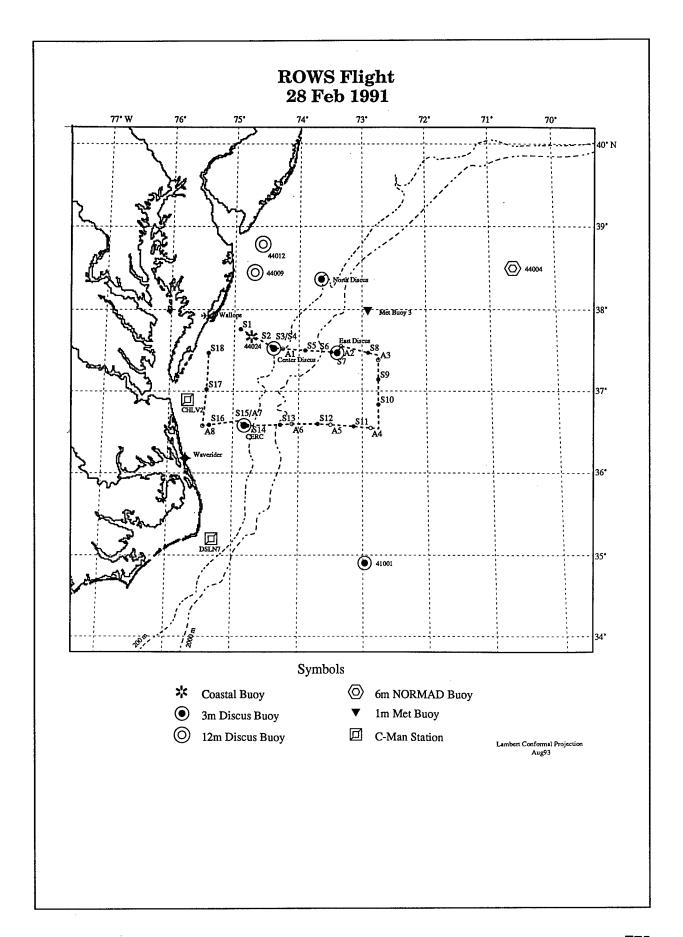
ROWS SWADE FLIGHT NAVIGATION AND FILE DATA FEB 27, 1991

TAPE2/2 FILE								LON	ALT			PC-TIC START		0 DEG DELTA	
	0	0	TP1'				36.32	-71.00	7625	135	291				
S01	0	1										002419	6401	418	12
	1	0		19	19	13	36.58	-71.54	7625	135	291				
A01	0	2		19	22	06	36.69	-71.77	7625	135	291	002924	34901		1
S02	0	1		19	24	21	36.78	-71.95	7625	135	291	003042	40401	902	12
A02	0	2		19	28	36	36.90	-72.20	7625	135	291	003553	70201		1
S03	0	1		19	30	36	37.01	-72.43	7625	135	291	003657	75201	356	12
A03	0	2		19	35	36	37.20	-72.82	7625	135	291	004251	107201		1
S04	0	1		19	37	02	37.25	-72.93	7625	135	291	004323	108801	438	12
A04	0	2		19	41	36	37.42	-73.28	7625	135	291	004850	140301		1
S05	1	3	DIS-E									004924	142801	381	6
	1	0		19	54	02	37.50	-73.19	7625	131	269				
S06	0	1										010121	212201	553	12
	1		DIS-E					-73.40							
A05	0	2						-73.71							1
S07	1	1											250101	968	12
A06	0	2						-74.32				011251	277301		1
	1			20	07	23		-74.39		130	272				
	0	0	TEMP					-74.33							
S08	1	1											347401		12
A07	1	2	EXP										366301		1
S09	0	1							7625	138	283	013234	388001	32	12
	0	0	COAST	20	29	03	37.84	-75.37							
NOTES:	ALL I	DATA	ON REV	ÆRS	SE C	COU	RSE ON	TAPE 2							





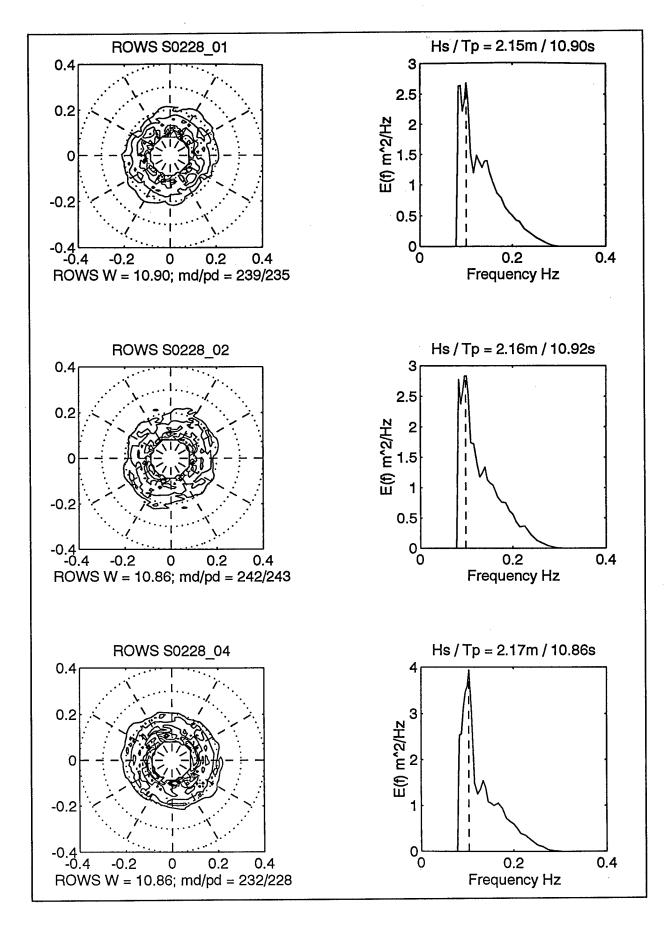


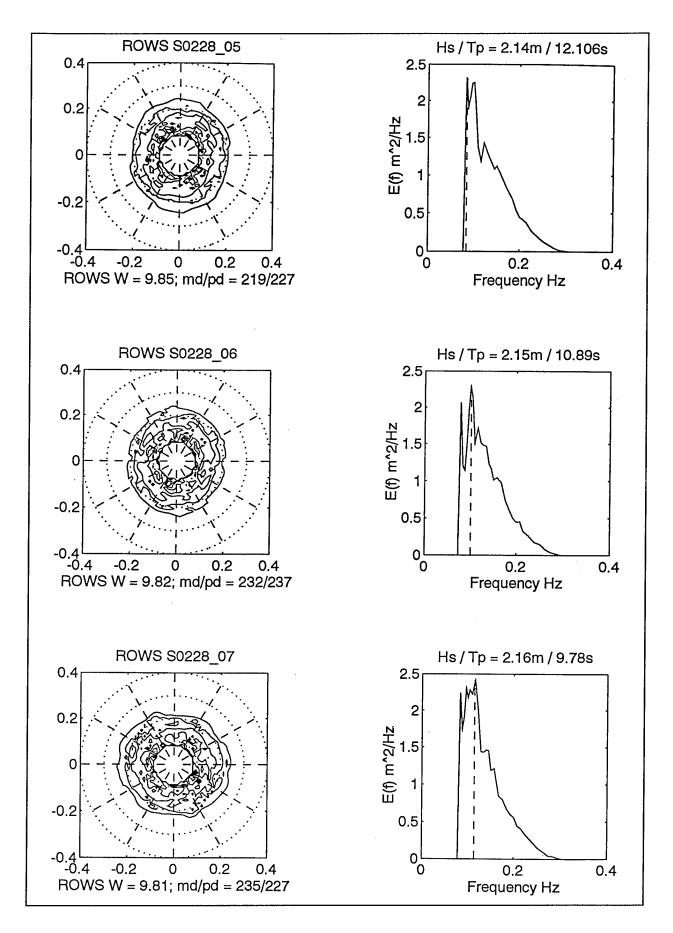


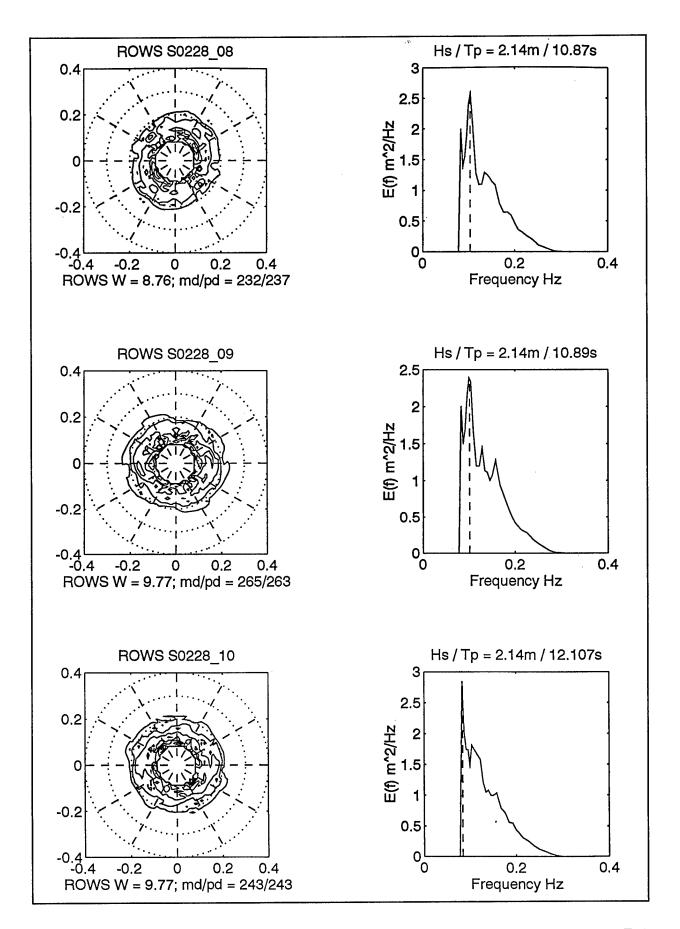
ROWS SWADE FLIGHT NAVIGATION AND FILE DATA FEB 28, 1991

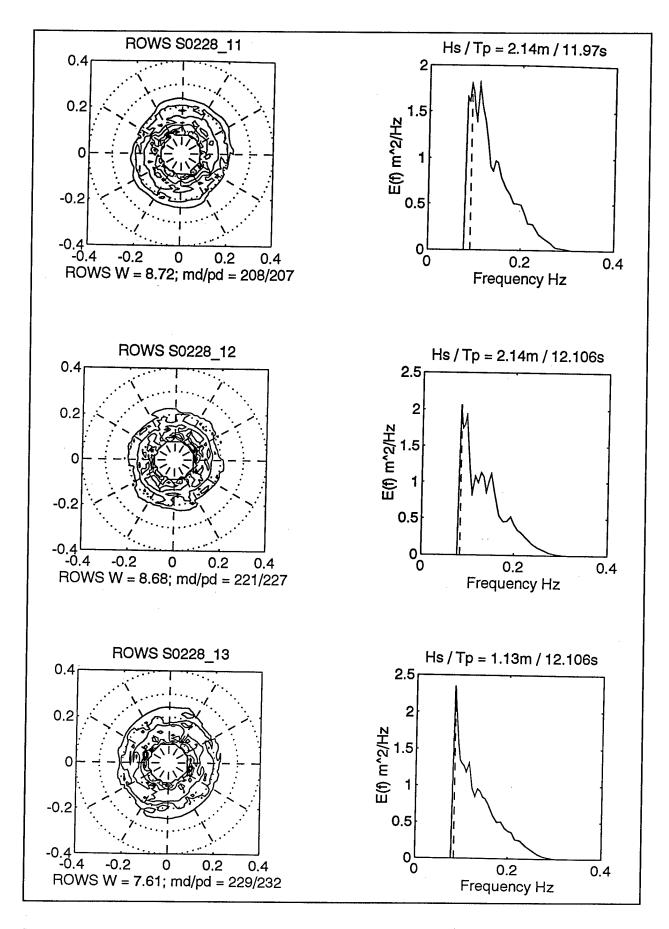
TAPE1/1	POS	ROWS	BUOY,	/	ES'	r	LAT	LON	ALT				REC #		
FILE	FIX	MODE	WP	НН	MM	SS				M/S	TRU		START		
	1	0	SWL				38.13	-75.47							
S01		1		16	29	05	37.77	-74.91	5338	199	125	042730	7201	877	:
	1	0	EXP	16	30	45	37.69	-74.72	5338	199	125				
S02	0											043134	31601	. 417	:
	1							-74.39							
S03	0												47801	176	
S04	0		DIS-C										63001	941	
A01	0	2		16	42	10	37.53	-74.25	5338	201	090	044130	90101		
505	0	1		16	44	45	37.51	-73.90	5338	201	090	044305	98901	163	
S06	0	1	DIS-E	16	47	50	37.49	-73.49	5338	201	090	044613	117701	318	
	1							-73.40							
507	0	3	DIS-E	16	52	20	37.48	-73.40	5338	160	193	045114	147701	241	
A02	0	2		16	56	00	37.56	-73.34	5338	201	107	045519	169301		
	1	0		16	57	20	37.53	-73.16	5338						
808	0	1		16	58	00	37.48	-72.91	5338	201	107	045624	175101	964	
	1	0	TPN	16	59	01	37.45	-72.75	5338						
703	0	2		17	0.0	30	37.39	-73.16 -72.91 -72.75 -72.75 -72.75	5338	165	191	045948	195501		
	1	ō		17	02	12	37.24	-72.75	5338						
309	ō	1		17	03	12	37.15	-72.75	5338			050133	204301	1035	
310	Ö	ī											219601		
310	1	ō	TTPS	17	ng.	40	36.58	-72.75	5338			000101	217001	001	
	ō	Õ	TEMP					-72.75							
A04	0-	2								145	275	050940	252101		
511	1							-73.03							
J	ō	1										051128	261901	541	
405	Ö	1 2											285401		
512	ō	ī		17	18	57	36.60	-73.70	5338	145	269	051714	295101	846	
	1	ō						-73.79						• • • • • • • • • • • • • • • • • • • •	
106	ō	2										052217	324501		
313	ŏ	ī											329601		
514	ō		CERC										359901	375	
	1	ō						-74.83							
515	ō	1										053301	389101	1082	
107	ŏ	2											408701		
	í	ō	OLINO					-74.91					100701		
316	ō.											054109	435601	1084	
	1		ਘਰਾ	17	43	46	36.58	-75.47	5338	100	20,	224103	-33001	1004	
804	ō									174	351	054419	452601		
317	0	1		17	4 Q	1.1	37 03	-75 42	5338	174	351	054705	452601 468601	383	
	1	Ŏ						-75.42				034703	40000T	303	
	1	1		Ι,	50	24	37.10	-75.41	2330	1/4	JUL				

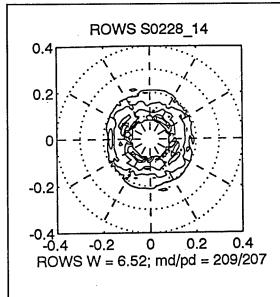
NOTES: (1) MODE '3' IS X-TRACK SPEC MODE DATA FOR CAL AND AVG POWER COMP; PC-TIC TIME HERE IS LST-12 HOURS. (2) S09 MAY HAVE HIGH 'INTERFERENCE' TYPE NOISE LEVEL (3) S10 IS OVER THE FRENCH MERLIN AT 11 KFT. (4) FILES S01-03 AND S06 RERUN WITH NEW PC-TIC TIMES ON 1/28/93 (TIMES HERE LISTED) TO AGREE WITH FILE START TIMES ('ACCURATE TIMES'). (5) RUNS FOR S03 AND S15 BOMBED W/ 'alloc br failure.'

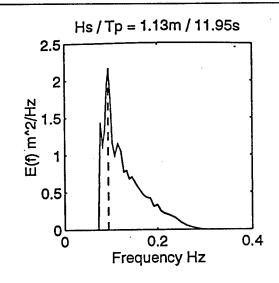


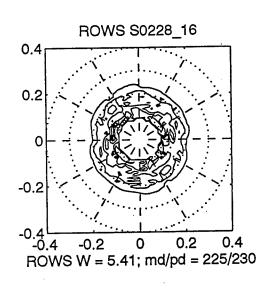


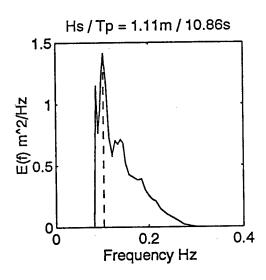


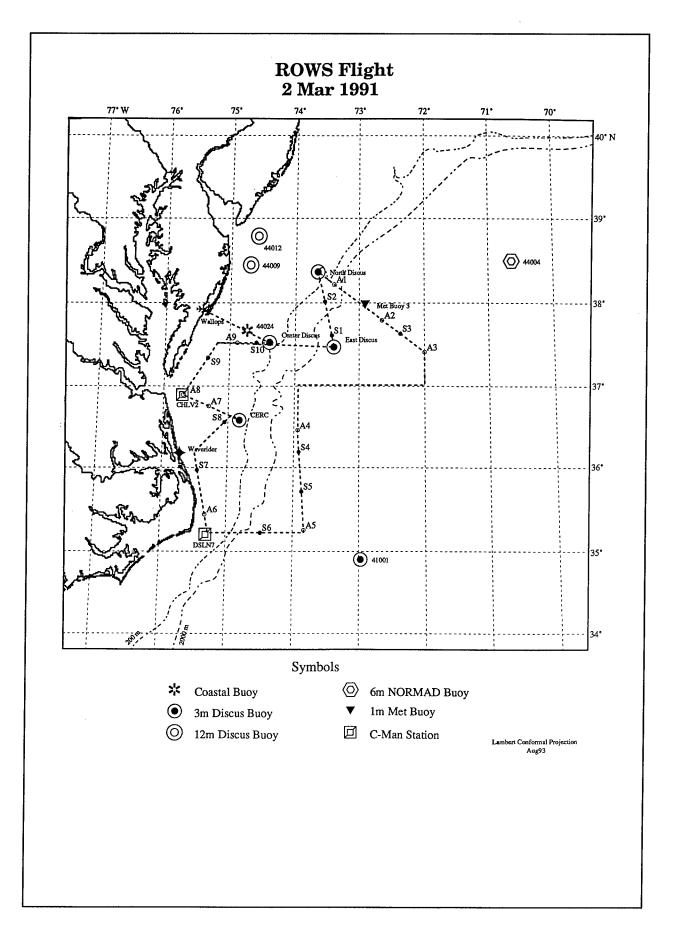








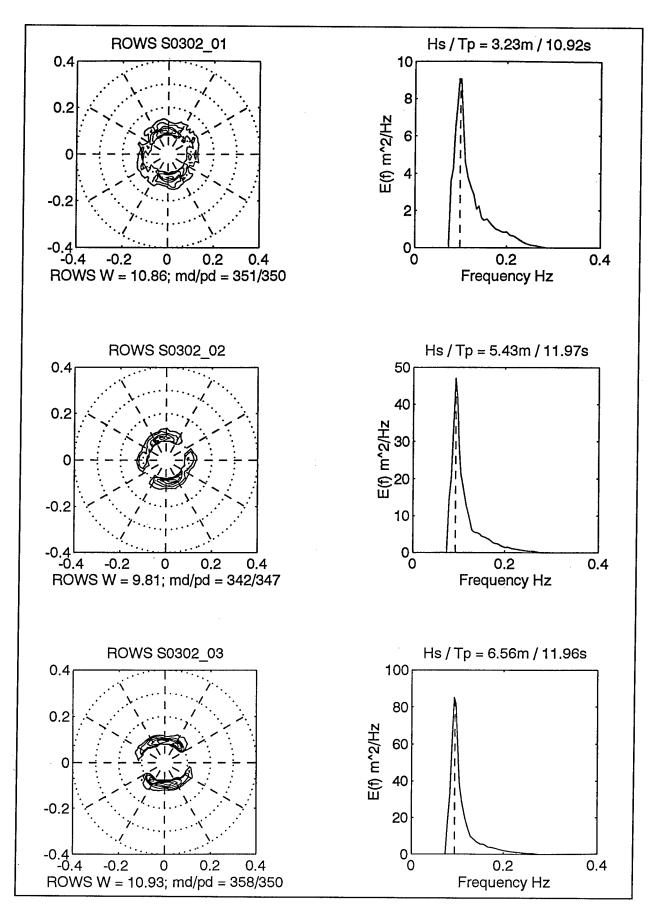


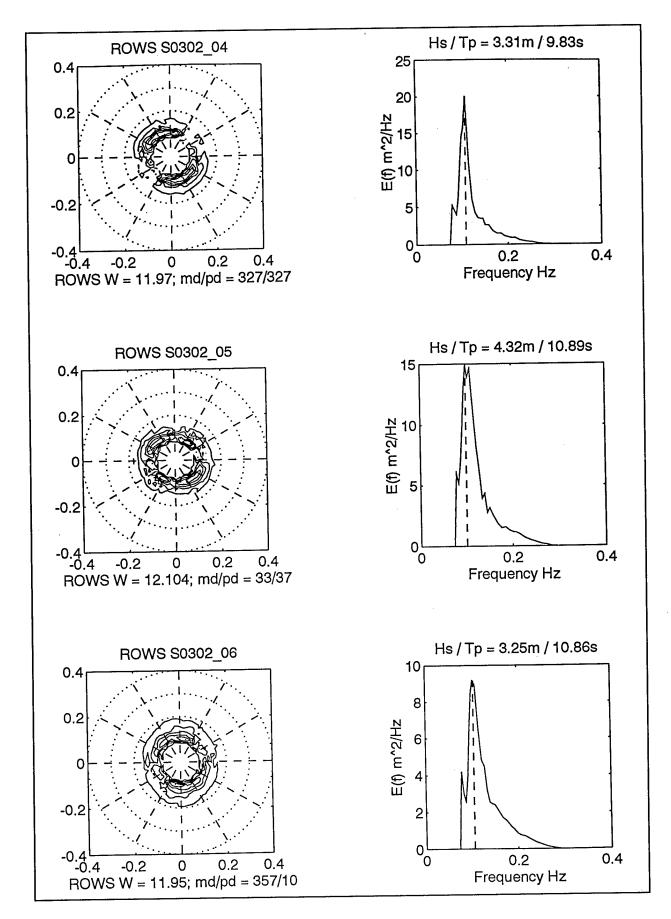


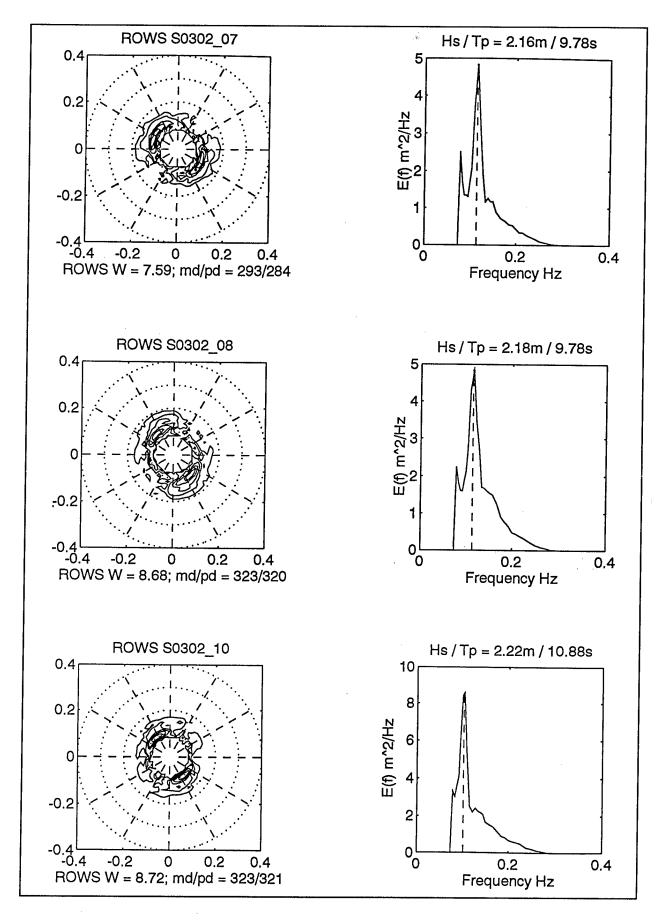
ROWS SWADE FLIGHT NAVIGATION AND FILE DATA MAR 02, 1991

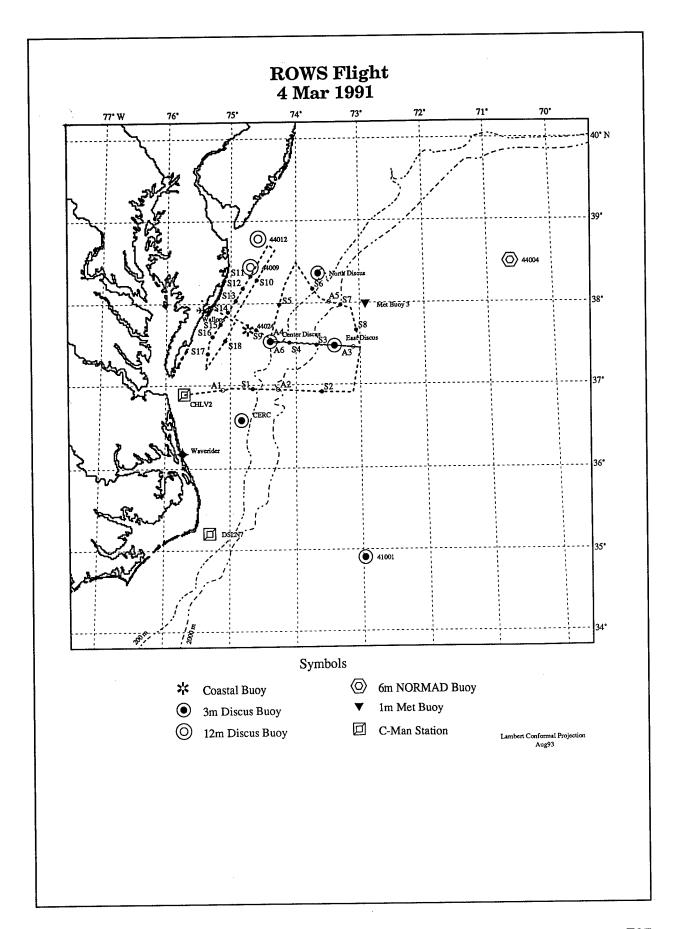
TAPE1/1 FILE	POS FTX	ROWS	BUOY,	/ НН	EST	r ss	LAT	LON				PC-TIC START			
	1		WFF					-75.47	0						
	1	_		15	48	25		-74.39							
	0	_	TEMP1					-75.19							
	1		DIS-E					-73.40							_
S01	1	1		16	03	03	37.62	-73.43	8235	206	336	155811	45601		
S02	0	1							8235	206	336	160122	64701	822	1
	1		DIS-N					-73.66							
A01	0	2										160900	10000	L	
	1	0		16	19	14	37.86	-72.74	7930	165	143				
A02	0	2		16	20	05	37.80	-72.65	7930	165	143	161715	146003	L	
S03	0	1		16	22	57	37.64	-72.37	7930	165	143	161837	15250		
A03	1	2	TPN	16	26	40	37.42	-72.00	7930	165	143	162336	18040	L	
	0	0	TEMP2				37.02	-72.00							
	1	0		16	37	09	37.02	-72.59							
	0	0	TEMP3					-73.94							
A04	0	2		16	56	26	36.46	-73.94	10553	3 17	5 18	1 165319	22970	L	
	1	0		16	57	80	36.40	-73.94	10553	3 17	5 18	1			
S04	0	1		17	00	00	36.19	-73.92	10553	3 17	5 18	1 165609	24510	1 404	1
S05	0	1		17	04	30	35.71	-73.87	10553	3 17	5 18	1 170039	26900	1 444	1
A05	0	2		17	07	08	35.25	-73.83	10553	3 17	5 18	1 170357	28970	1	
	1	0	TPS	17	07	30	35.22	-73.83	10553	3					
S06	1	1		17	16	30	35.22	-74.48	10553	3 18	9 26	7 171147	33530	1 304	1
	1	0	TPW				35.22	-75.27							
A06	10	2		17	26	36	35.44	-75.32	701	5 18	5 35	0 172322	35640	1	
	1	0		17	28	20	35.64	-75.37							
S07	0	1		17	32	40	35.97	-75.45	701	5 18	5 35	0 172714	37780	752	1
	1	0	TPW'	17	33	50	36.19	-75.50	701	5					
S08	1	1		17	38	15	36.56	-75.06	701	5 20	5 07	0 173353	41760	1 857	1
	0	0	TEMP4				36.66	-74.96							
	1	0	CERC	17	45	10	36.58	-74.83	9608	В					
A07	0	2						-75.30		В		174618	43310	1	
A08	1		CLT					-75.70				174944	45060	1	
S09	ī	1		17	59	34	37.35	-75.33	1067	5 22	1 05	5 175506	45750	1 500	1
	1		TEMP1					-75.19							
A09	ō								1006	5 19	5 10	1 175940	47300	1	
S10	Ö			18	05	23	37.53	-74.59	1006	5 19	5 10	1 180013	47500	1 237	1
	1							-74.39							

NOTES: (1) S09 BOMBED, 'nadir return < 25 bins'. (2) S07 RERUN W/ NEW PC TIC TIME. (3) LAT/LON CORRECTION FOR TIMING PROBLEMS (PC TIC VS LOG TIME) WITH FILES S01 (SECTOR 1 START TIME 160058) AND S02 (SECTOR 1 START TIME 160407).





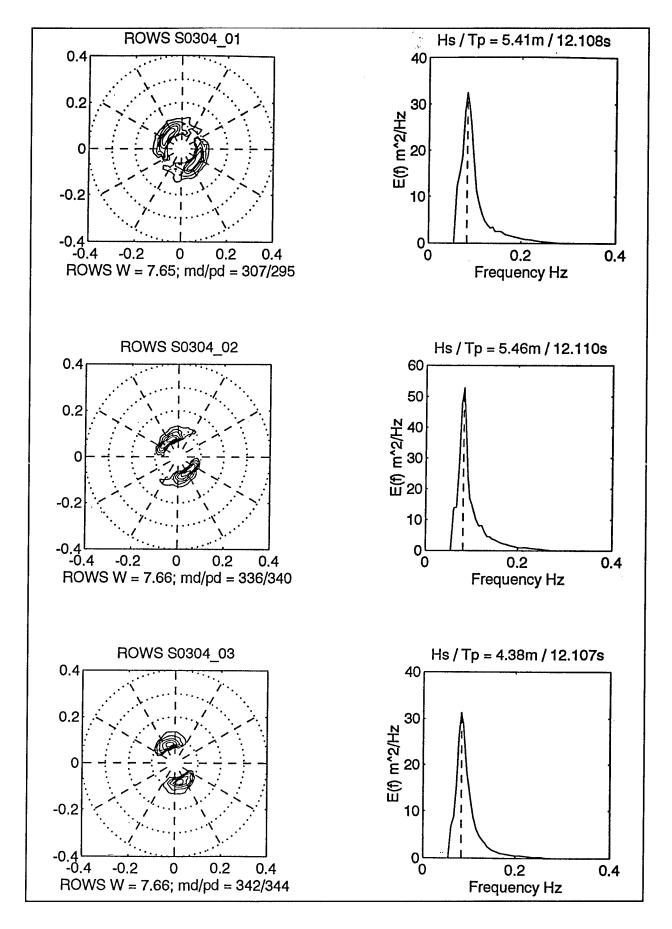


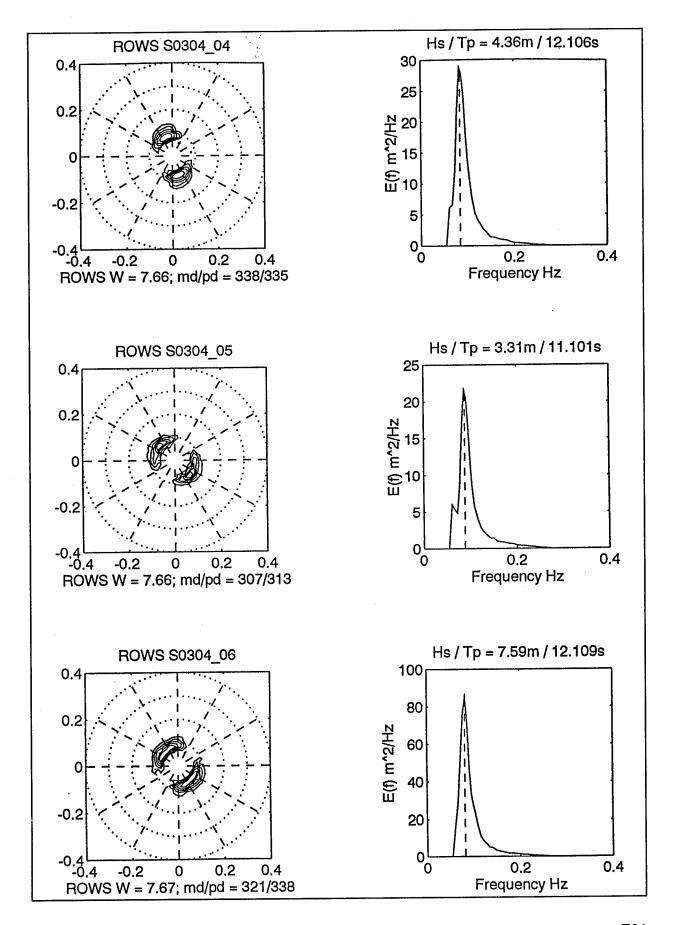


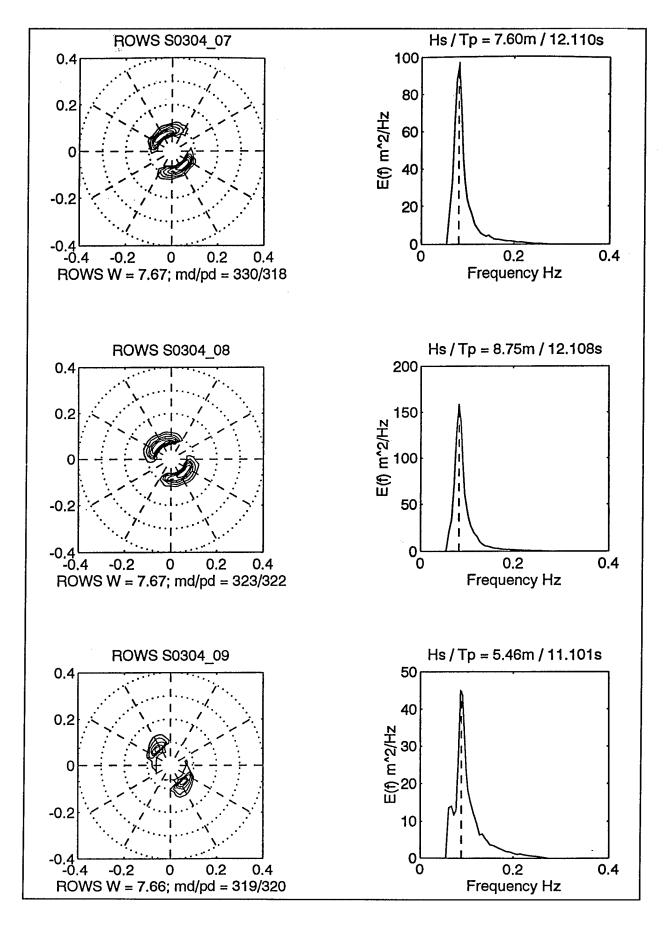
ROWS SWADE FLIGHT NAVIGATION AND FILE DATA MAR 04, 1991

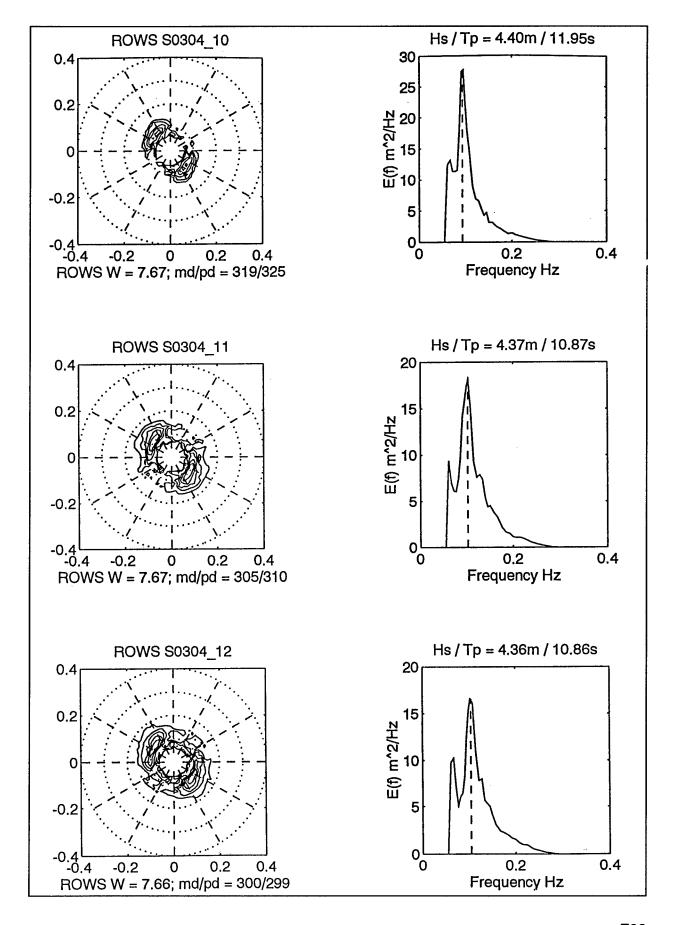
TAPE1/1 FILE	POS FIX	ROW!	S BUOY E WP	/ HH	ES MM	T SS	LAT	LON	ALT	SPD M/S	HDG TRU	PC-TIC START	REC #	0 DEG DELTA	LE
A01	0	2		16	34	26	36.95	-75.12	7625			163312	16901 26201 54301 66601 128201		
S01	1 0	1		16	35	26	36.97	-74.99	7625	205	103				
	0	7		16	38	22	36.96	-74.66	7625	205	103	163506	26201	638	
AUZ	1	0		16	41	11	36.95	-74.27	7625	205	103	163959	54301		
S02	ō	1		16	46	40	36.92	-73.00 -73.60	7625	205	103	164225	66601	426	
	1	ō	TPS	16	49	35	36.91	-73.12	7625	205	103	104333	999AT	426	1
	1	ō	TP1			-	37.45	-73.00	8235						
A03	0	2		17	04	05	37.46	-73.11	8235			170235	128201		
	1	0	DIS-E	17	06	45	37.48	-73.40	8235	161	256	1,0200	ILULUI		
S03	0	1		17	07	55	37.49	-73.68	8235	161	256	170529	133001	260	1
S04	0	ī		17	11	05	37.52	-74.10	8235	161	256	170829	150901	330	_
	1	0	DIS-C	17	13	05	37.54	-74.39	8235						_
A04	0					21	37.56	-74.39	8235	262	000	171441	172501		
	1	0		17	18	30	37.92	-74.27	8235	262	000				
S05	0	1	TPN	17	19	00	37.99	-74.25	8235	262	000	171607	180101	879	1
	1	0		17	20	30	38.23	-74.17	8235	262	000				
	1	0	\mathtt{TPN}					-74.00							
306	0	1		17	24	00	38.18		8235	163		172110	195101	1009	1
,	1	0		17	25	02	38.13	-73.69	8235	163	157				
. 0.5	0	0	TEMP	17	25	26	38.06	- 73.62	8540						
A05	0	~		Τ,	21	ΤO	30.02	-/3.48	8540	1//	128	172529	211701		
307	0	1		17	29	00	37.98	-73.30	8540	177	128	172602	213401	1106	1
	1 0	0	ments.					-73.24		177	128				
,	1	0	TEMP	17	30	20	37.94	-73.14	8540	100					
808	0	1		17	33	06	37.74	-73.08	8540	136	177	170004			_
,00	1	Ō	TP1	1/	34			-73.00		136	1//-	1/3034	231801	259	1
	ī			17	40			-73.40							
106	ō	2	DIS-C	17	40	00	37.40	-74 31	Q540	171	251	17/552	289501		
509		1	D10 C	17	52	50	37.68	-74.51	8540	201	278	174993	318001	815	1:
	ĭ	ō	TP3	17	54	03	37.83	-74.96	8540	201	2/0	1/4033	310001	913	Ι,
310	1	1		17	59	03	38.29	-74.60	8540	263	กรล	175603	337701	811	10
	1	ō	TP4					-74.32		203	030	175005	337701	OTT	Τ,
	0	0	TEMP					-74.42							
311	1	1		18	05					132	207	180224	355901	153	1:
12	0	1		18	80	13	38.19	-74.82	8540	132	207	180450	370461	571	12
313	0	1		18	10	39	38.04	-74.93	8540	132	208	180716	385021	985	12
14		. 1		18	13	05	37.90	-75.05	8540	132	209	180942	399581	403	12
15	0	1		18	15	31	37.75	-75.16	8540	132	210	181208	414141	788	12
16	1	1		18	17					123	210	181434	428701	188	12
	0	0	TEMP				37.53	-75.33	8540						
17	1	1		18	21	10	37.39	-75.35	8540	143	179	181752	448501	358	10
1.0	0	0					37.20	-75.38	8540						
18	1	1	mmer	18	25	45	37.55	-75.09	8540	258	017	182226	463501	248	10
	0	0	TEMP				37.78	-74.94 -75.45							
	U	U	SNOW				38.U5	-/5.45							

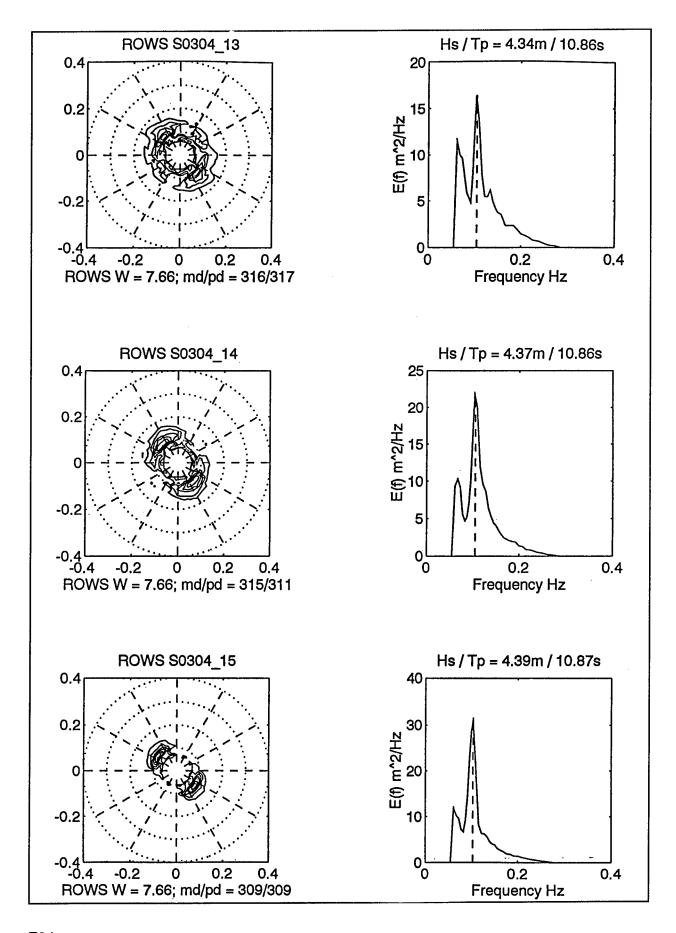
NOTES: (1) S17 BOMBED FOR 'alloc br failure'. (2) S09 TIMINGLAT/LON CORRE (3) A04 BOMBED, 'nadir fell into noise calc window'. (4) A06 BAD, FILE STAR TIME ERROR.	CTED.

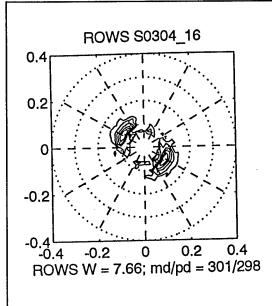


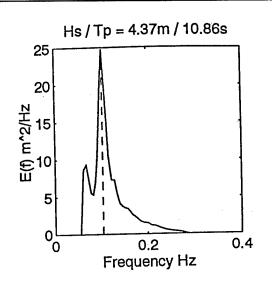


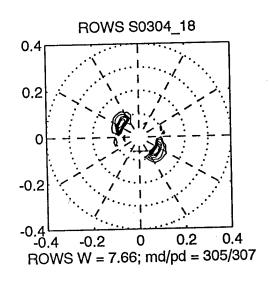


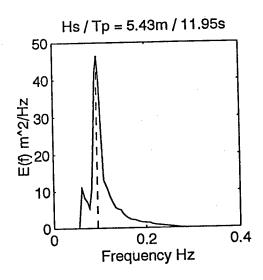


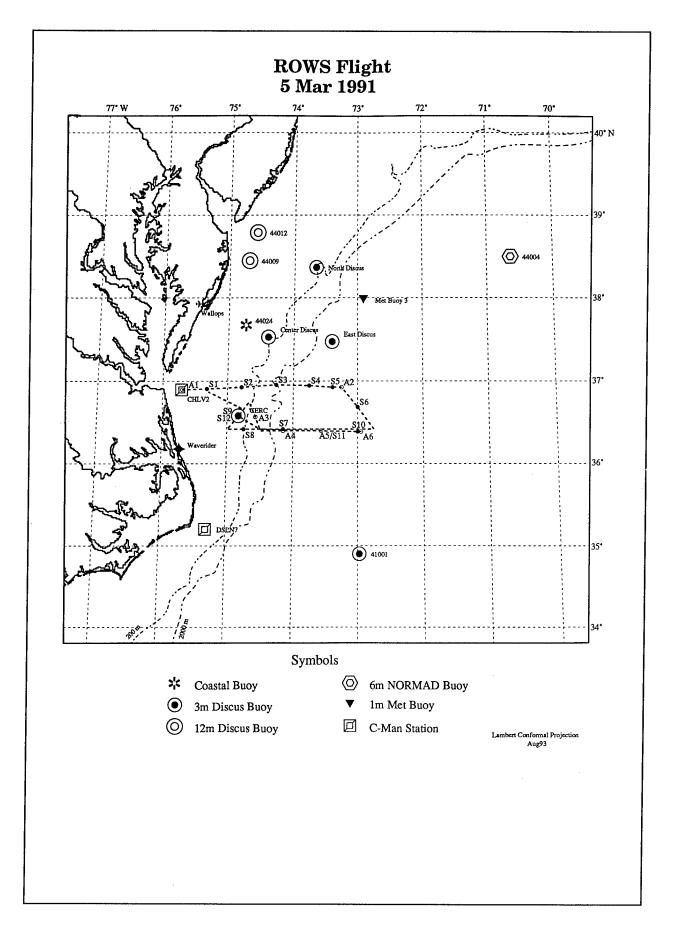








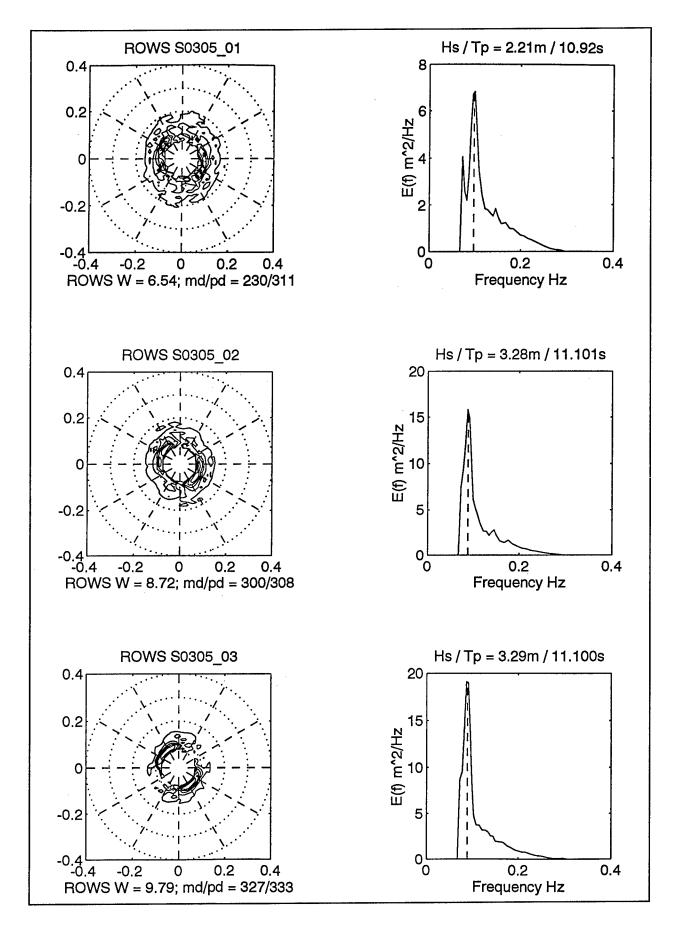


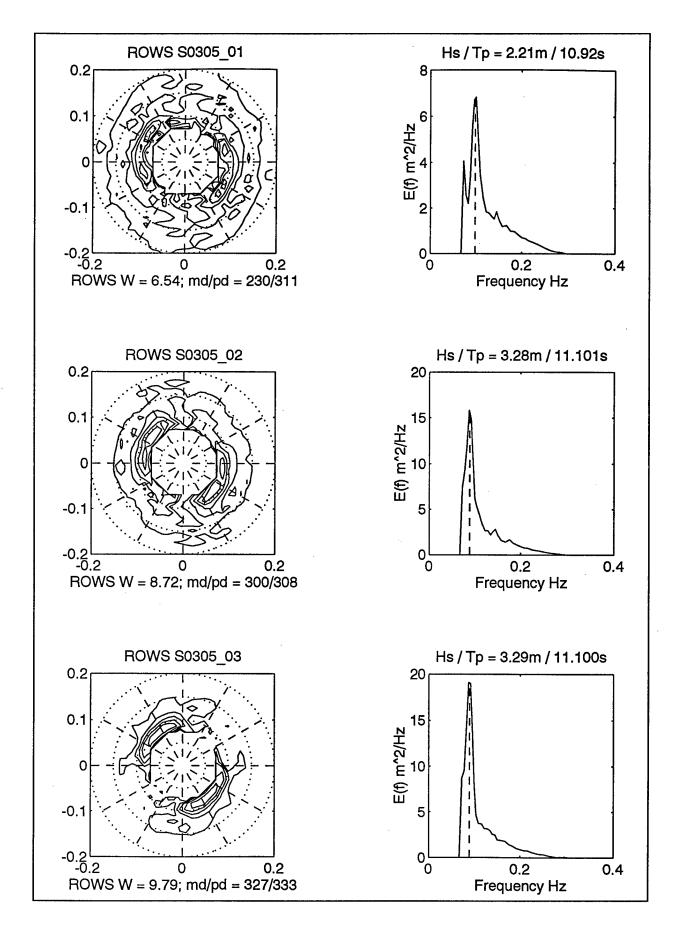


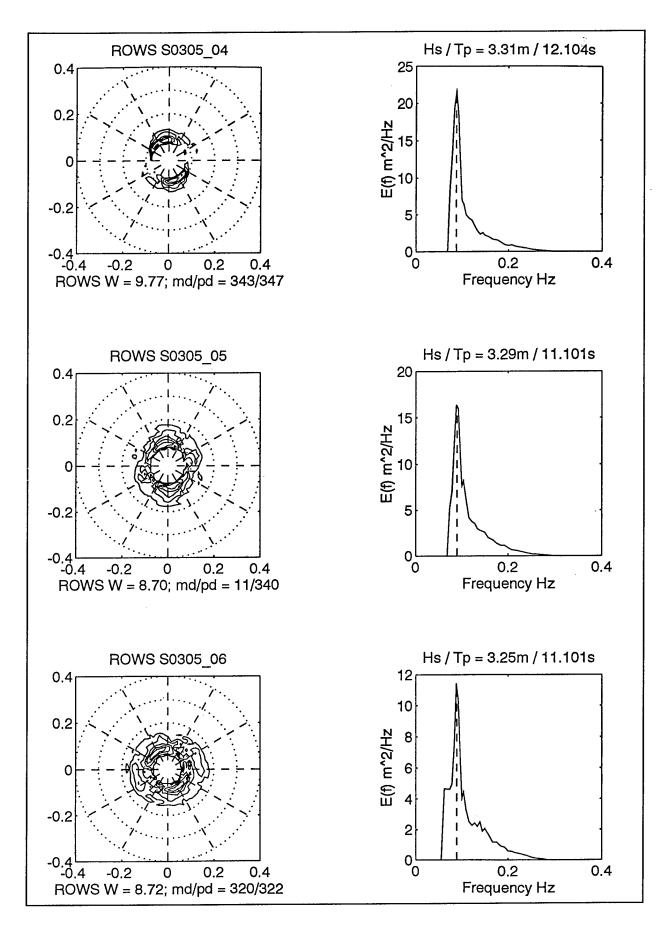
ROWS SWADE FLIGHT NAVIGATION AND FILE DATA MAR 05, 1991

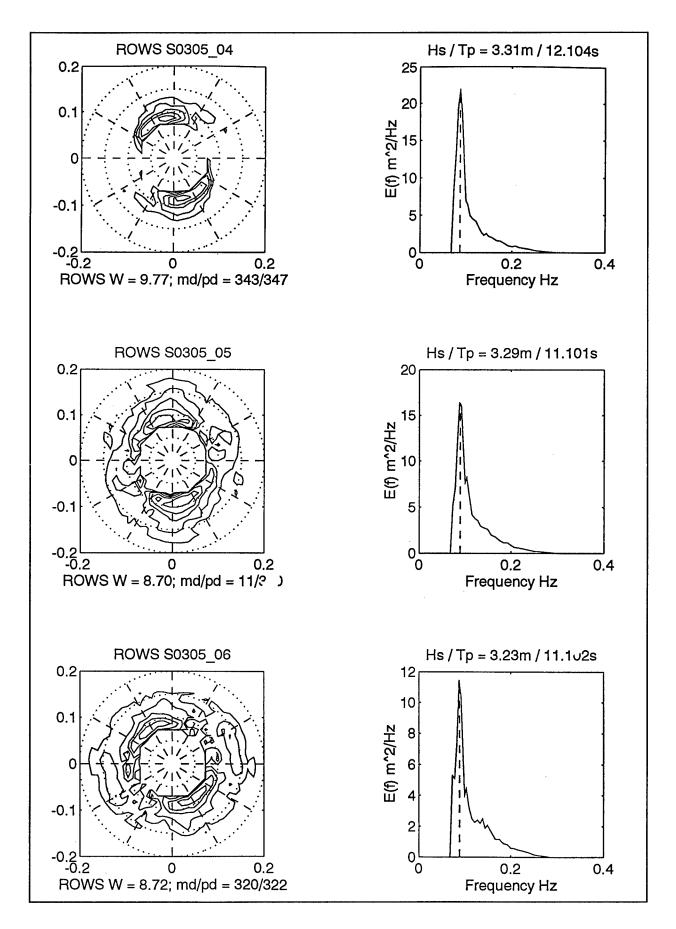
TAPE1/1 FILE	POS FIX	ROWS MODE	BUOY, WP	и НН	EST MM	ss	LAT	LON	ALT M	SPD M/S	HDG TRU	PC-TIC START		O DEG DELTA	
A01	 ·	2	CLT	12	02	33	36.90	-75.70	7000	183	086	120040	9400		1
S01	1	1		12	05	45	36.91	-75.32	7000	183	086	120220	18900	698	
S02	0	1		12	10	04	36.93	-74.79	7000	183	086	120639	44800	755	
S03	1	1		12	14	12	36.96	-74.26	7000	183	092	121047	69600		
S04	0	1		12	17	52	36.95	-73.75	7000	183	092	121427	91500	851	12
S05	0	1		12	20	28	36.93	-73.39	7000	183	092	121803	113000	421	12
	1	0	TPN	12	21	33	36.93	-73.25	9608						
A02	0	2		12	40	18	36.93	-73.25	9608	169	163	123754	123400		1
S06	1	1		12	44	08	36.69	-73.00	9608	169	163	124041	139300	846	12
	1	0	TPS	12	47	23	36.42	-72.75	9608					1010	
S07	0	1		12	59	26	36.42	-74.15	9608	165	255	125554	222100	1042	12
	1	0	TPW	13	02	36	36.42	-74.50	9608	165	255			4005	
S08	0	1		13	04	56	36.42	-74.75	9608	165	255	130103	253000	1095	16
	1	0	TPW'	13	07	15	36.42	-75.00	9608					251	
S09	1	1	CERC	13	11	42	36.58	-74.83	9608	232	018	130726	275100	351	10
	0	0	TEMP	13	14	00	36.75	-74.67	9608				004000		1
A03	1	2						-74.57		187	146	131446	304900		1
	1		TPW	13	19	02	36.40	-74.50	9608		400	101746	222700		1
A04	0	2		13	20	23	36.40	-74.15	9608	226	102	131/46	322700		1
A05	1	2		13	25	25	36.40	-73.56	9608	226	102	132228	350900		1
A06	0	2	•		29	28	36.39	-72.95	9608	226	102	132631	3/5200		1
	1	0		1.3	34	33	36.39	-72.95	9608	170	259	100100	201400	634	12
S10	0	1		13	35	03	36.39	-73.00	9608	1/0	259	133123	421500	588	
S11	1	1		13	40	04	36.40	-73.56	9608	1//	262	133625	421500	500	12
	1	0	TPW	13	47	22	36.42	-74.50	9608		_	104010	466500		12
S12	1	2	CERC	13	50	31	36.58	-74.83	9608	177	200	134310	400000		12
	1	0		13	54	25	36.69	-74.82	9608	232	020				
	1.	0		14	02	52	36.67	-74.78	9608	187	290				
	1	0		14	11	28	36.87	-75.29	6700	183	285		_ ·		

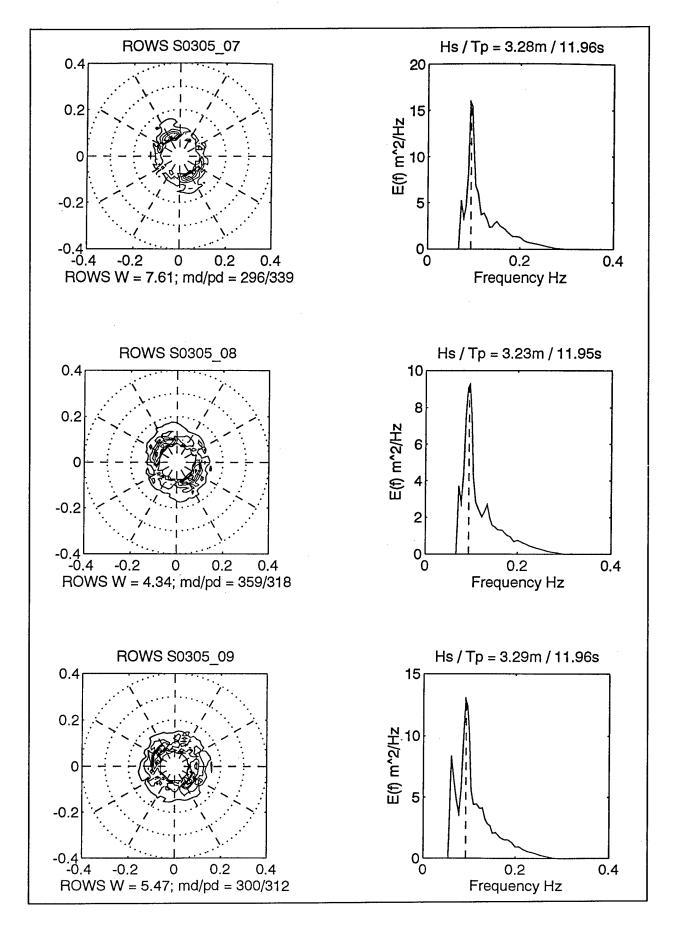
NOTES: (1) SO2 HDG MAY BE 92 DEG OR BETWEEN 86 AND 92 DEG. (2) TIME AT TPS MAY ONLY BE APPROXIMATE AS WAS INSIDE TURN. (3) WP TEMP ESTIMATED FOR PLOTTING. (4) SO9 ORIGINALLY BOMBED AT 16 MB; RERUN AS RESSCOM.RWS (ressac-compared-torows) AT 10 MB. (5) S12 NOT RUN BECAUSE OF UNCERTAIN HEADING. (6) SO6 ORIGINALLY BOMBED--RERUN OK.

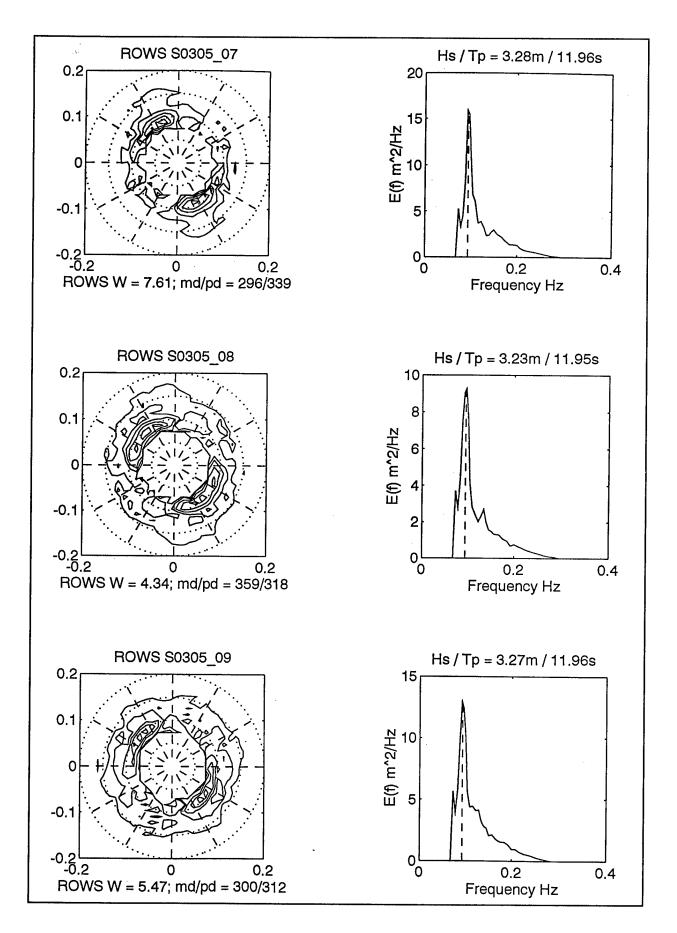


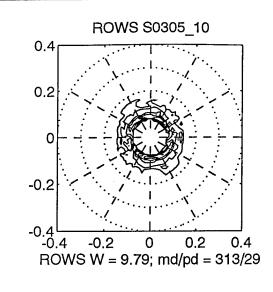


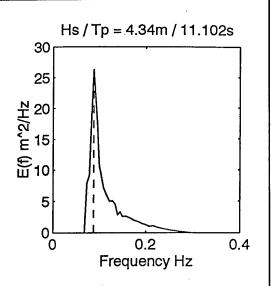


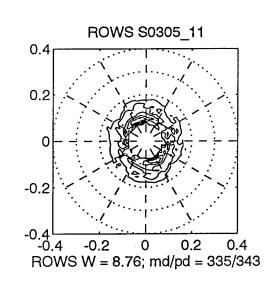


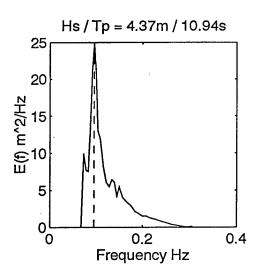


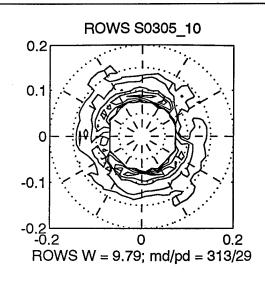


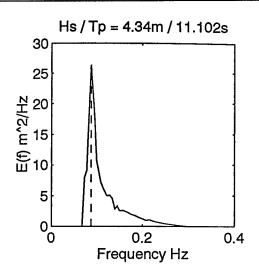


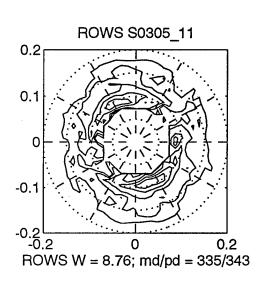


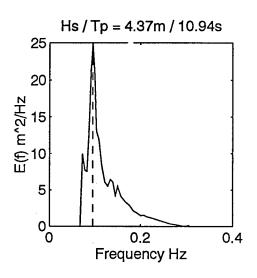


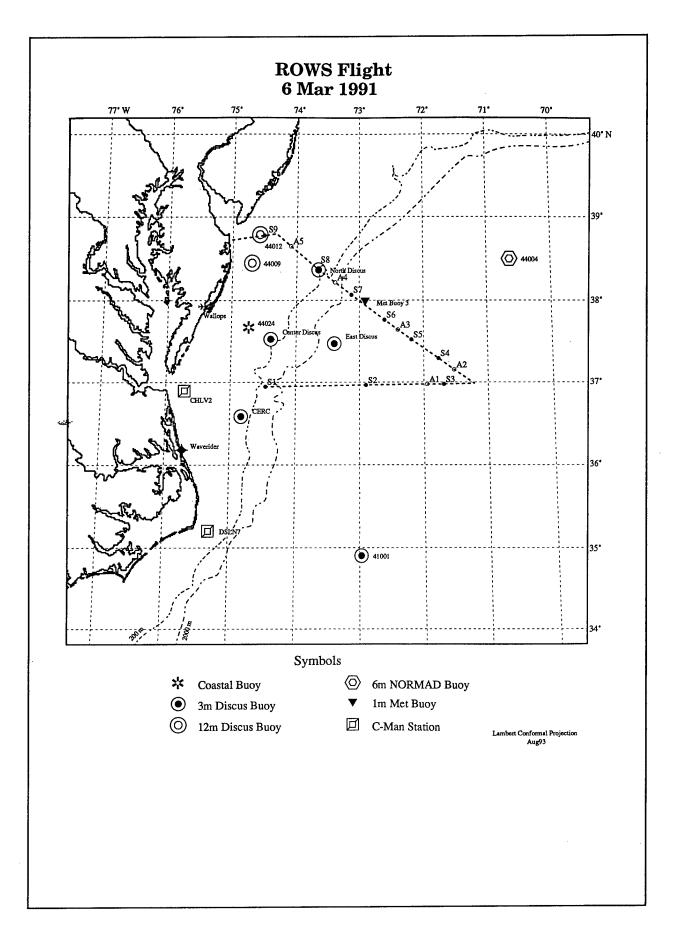








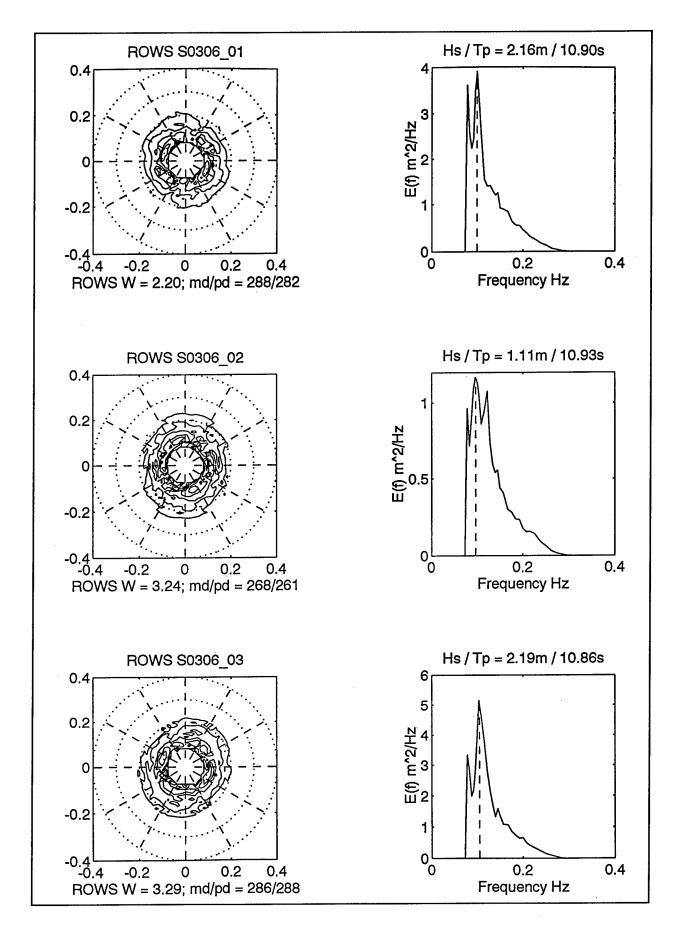


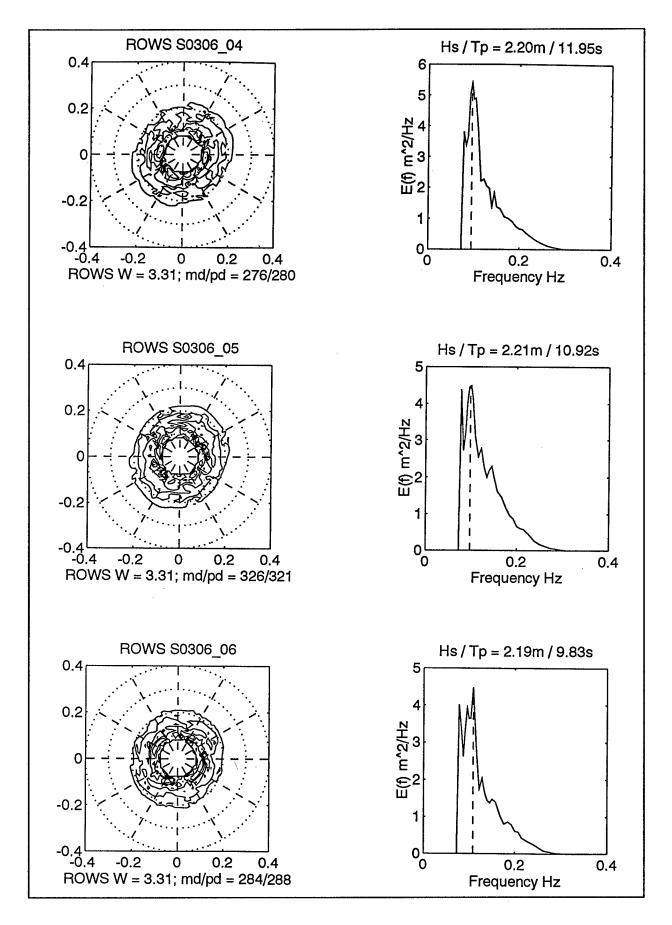


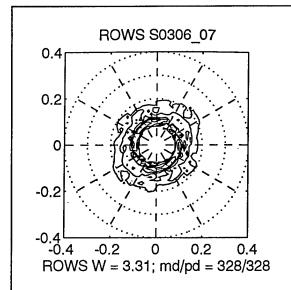
ROWS SWADE FLIGHT NAVIGATION AND FILE DATA MAR 06, 1991

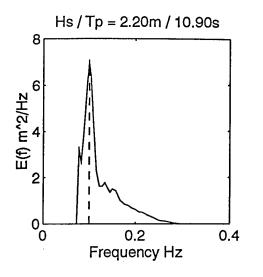
TAPE1/2 FILE		ROWS MODE			EST MM		LAT	LON	ALT			PC-TIC START		O DEG DELTA	
S01	1	1		14	32	10	36.95	-74.46	7075	209	083	142854	9301		12
TAPE2/2															
S02	 1	1		14	43	08	36.97	-72.90	7075	209	088	144118	3801	1035	12
A01	0	2		14	.50	10	36.98	-71.95	7075	209	880	144846	46901		1
S03	1	1		14	52	00	36.98	-71.69	7075	212	105	144933	50401	427	12
	1	0	TPE	14	54	00	36.99	-71.22	7075						
A02	0	2		14	58	27	37.17	-71.53	7075	166	308	145656	75601		1
S04	1	1		15	01	06	37.30	-71.77	7075	166	308	145826	83801	277	12
S05	0	1		15	05	56	37.53	-72.19	7075	162	308	150320	112901	119	12
A03	0	2		15	08	23	37.65	-72.40	7075	160	307	150649	132701		1
S06	1	1		15	10	49	37.77	-72.61	7075	157	307	150803	139801	536	12
S07	0	1		15	16	43	38.07	-73.13	7075	157	307	151407	175101	357	12
A04	0	2		15	19	33	38.22	-73.39	7075	157	307	151750	195101		1
S08	1	1	DIS-N	15				-73.65					203301	498	12
A05	0	2		15				-74.09				152536	231601		1
	1	0	A	15				-74.32							
	1	0		15				-74.48							
S09	1	1		15	32					158	265	152947	253301	312	12
	1	0	COAST	15	37	14	38.72	-75.07	6710						

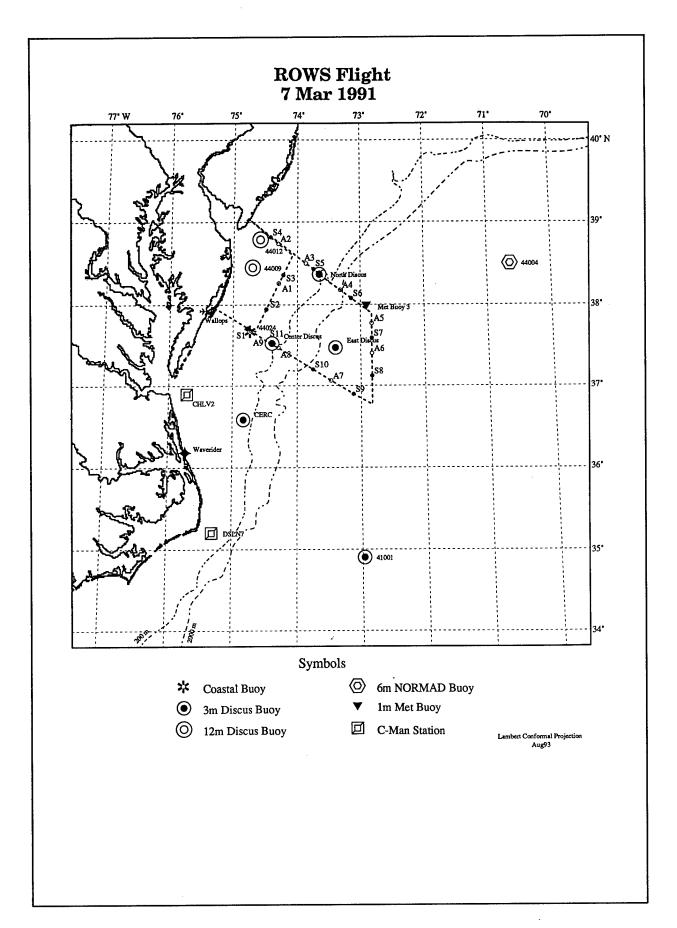
NOTES: (1) SO8 AND SO9 SKIPPED BECAUSE OF STRANGE TIME TAGS AND BAD A/C ROLLS.







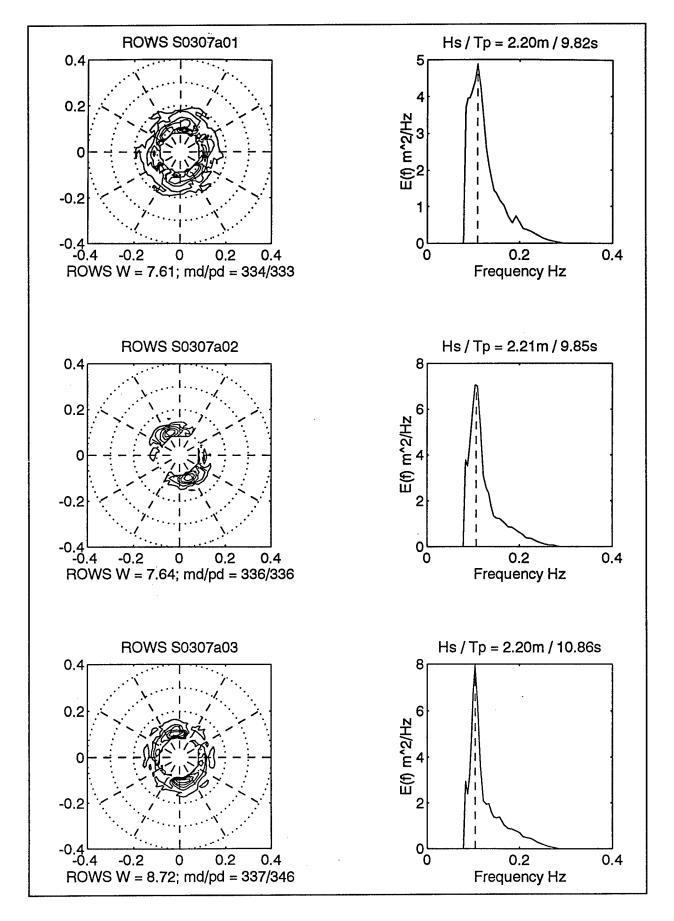


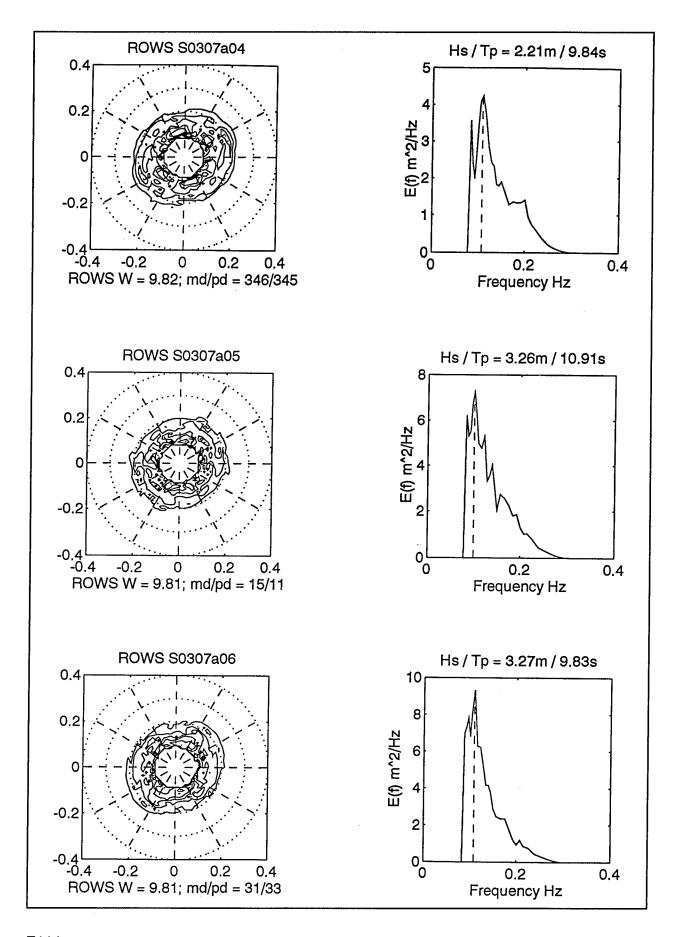


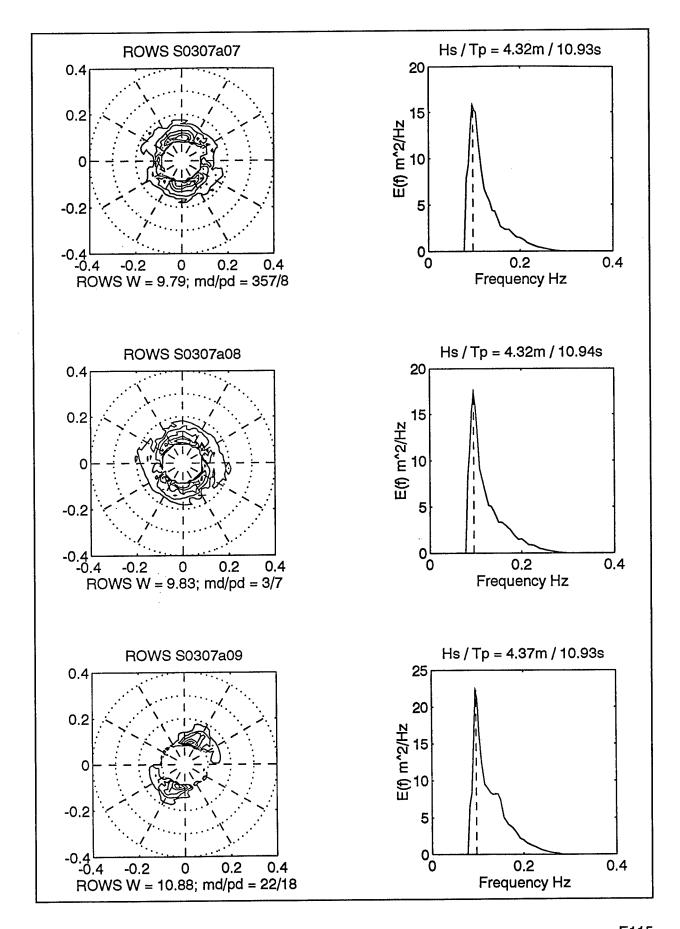
ROWS SWADE FLIGHT NAVIGATION AND FILE DATA MAR 07, 1991--FLIGHT #1

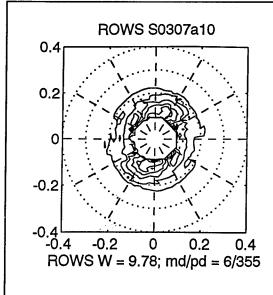
TAPE1/2 FILE	FIX	MODE	WP	HH	MM	SS			M	M/S	TRU	START	REC # START	DELTA	M
													101		
S01	0	1		17	04	26	37.72	-74.77	4575	200	130	170129	101	939	9
	1	0	EXP	17	05	09	37.69	-74.72 -74.65							
	ō	ō	TEMP				37.68	-74.65							
	1								4575	148	015				
S02	Λ	1		17	12	29	37.95	-74.48	4575	148	015	170857	28601	565	1:
A01	ñ	2		17	16	50	38.26	-74.29	4575	148	015	171414	59701		:
S03	ñ	1		17	18	24	38.36	-74.22	4575	148	015	171459	63801	334	1:
202	1	Ō		17	19	24	38.44	-74.17					59701 63801		
	1	0	mp 1	17	20	50	30 60	-74 07							
3.00	7	2	TLI	17	24	56	20.00	-74.30	4575	132	309	172213	106701		•
A02 S04	1	2		17	24	33	20.74	-74.30	1575	132	300	172253	110401	891	12
S04 	 T				<u> </u>		30.02	-/4.42							
TAPE2/2															
								-74.77	7625	227	133				
A03	ñ	2		17	47	30	38.50	-73.86	7625	227	133	174612	30901		:
S05	ŏ	1		17	48	40	38.43	-73.74	7625	227	133	174636	30901 32801	377	9
505	1		DTC_N	17	40	20	30.43	-73.65	7625	227	133				
	_		DT2-N	1,	42	~~	JU.J/	-73.47	, 020						
	1	U		1/	2T	1/	30.20	-/3.4/	7625	227	122	175110	57301		:
A04	0	2		1/	52	30	38.18	-73.32 -73.15 -72.83 -72.83	7625	227	133	175115	60301		Ġ
S 06	0	1		1/	53	50	38.08	-/3.15	7625	221	133	1/5145	00301	203	•
	1	0	TPZ	17	55	08	37.90	-/2.83	7625	100	100	175540	92001		1
AUD .	0	2		17	57	04	37.78	-/2.83	7625	109	190	175540	83001	836	12
s07	0	1		17	58	59	37.60	-72.83	7625	189	190	1/2039	99901	630	14
	1	0		17	59	39	37.50	-72.83	7625	189	190	175027	100001		
A06	0	2		18	01	04	37.41	-72.84	7625	189	190	175937	100001	007	
S08	1	1		18	03	50	37.13	-72.83	7625	189	190	180128	T1000T	927	12
	1	0	TP3	18	05	54	36.78	-72.83	7625				83001 88601 106001 116601 155701	- 4-	
S09	0	1		18	10	12	36.90	-73.12	7625	119	293	180800	155701	747	
A07	0	2		ı×	ı n		1/.0/	-/3.4/	/023	117	293	TOT44/	エシンシしエ		
S10	1	1		18	20	06	37.21	-73.75	7625	119	293	181750	213701	637	
80A	0	2		18	27	49	37.48	-74.29	7625	119	293	182623	263901		:
	1	0	DIS-C	18	29	05	37.52	-74.39	7625	124	296				
S11	0	1		18	29	40	37.54	-74.42	7625	124	296	182648	266101	818	18
	1	ō		12	31	25	37.59	-74.53	7625	124	296				
A09	ō	2	EXP	18	34	12	37.69	-74.72	7625	124	296	183246	301501		:
	ŏ		-TURN							-				•	
	1						37.54	-74.39	7625	242	132				
	1		DI3-C	10	47	17	37.02	-73.33	7625	242	132				
	0		-TURN				37.02	,,,,,	. 023						
	-	0 0	-IOKN	10	43	25	37 1/	-73.56	7625	124	295				
	1			10	12	70	27 64	-74.39	, 523		درے				
	1	0	DTCC				37.34	- /4.33							
	1	U	DIS-C	19	14	09									

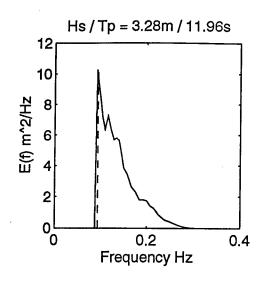
NOTES: (1) REVERSE COURSE DATA AFTER 183500 OMITTED AND TRACK NOT PLOTTED.

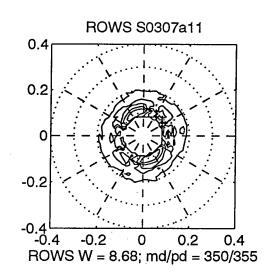


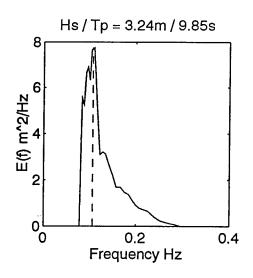












Appendix F Daily Weather Maps

The figures found in thix appendix are derived from weekly publications by the National Oceanic and Atmospheric Administration, National Weather Service, and the National Meteorological Center Climate Analysis Center. They are based on operational surface weather analyses. Each figure represents the fronts, pressure centers, and observations at 7:00 a.m. E.S.T. for each day displayed in the figure caption. Precipitation is indicated by the shaded area. Movement of large low pressure centers is indicated by lines designated with arrowheads. Origin of movement is identified by a small box.

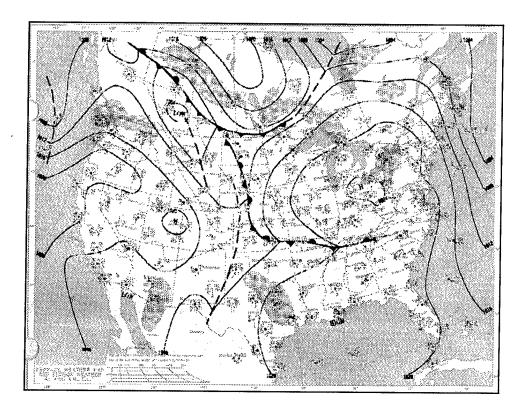


Figure F1. 12 February 1991

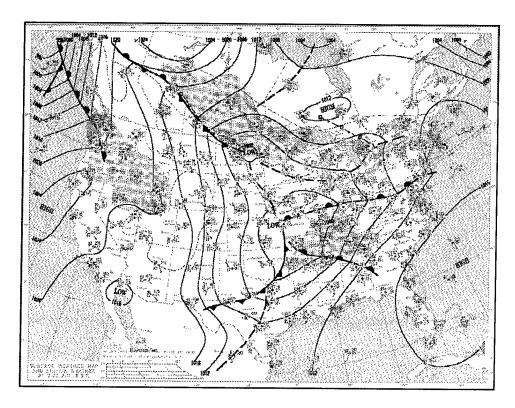


Figure F2. 13 February 1991

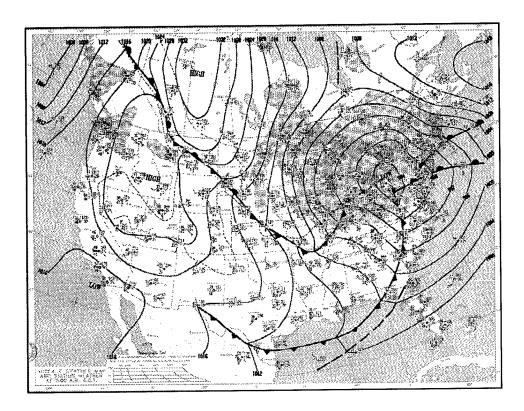


Figure F3. 14 February 1991

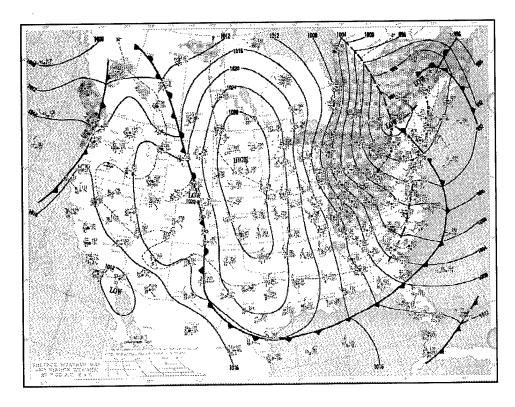


Figure F4. 15 February 1991

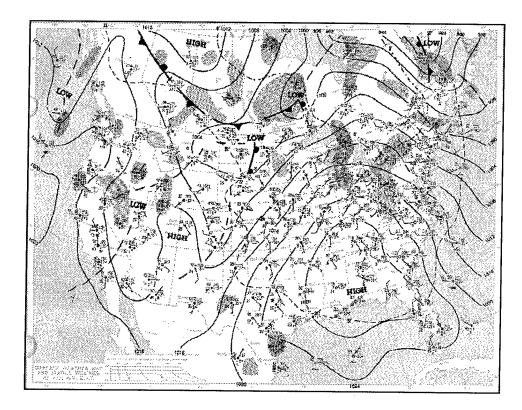


Figure F5. 16 February 1991

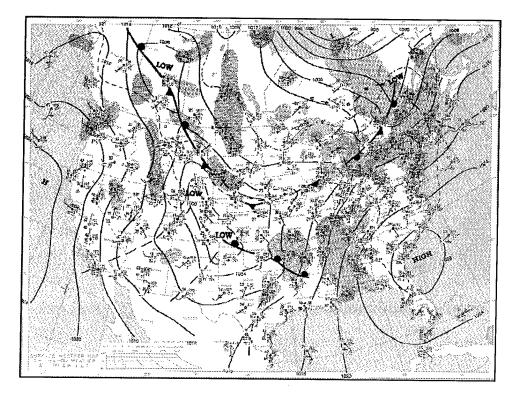


Figure F6. 17 February 1991

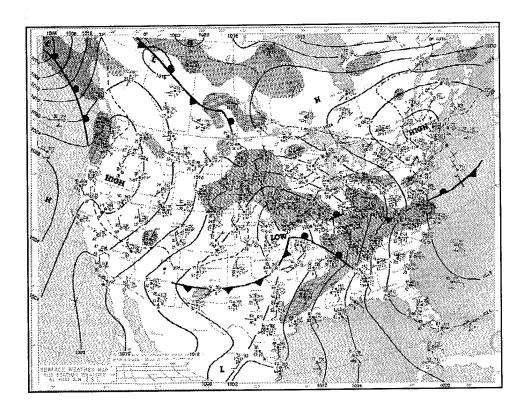


Figure F7. 18 February 1991

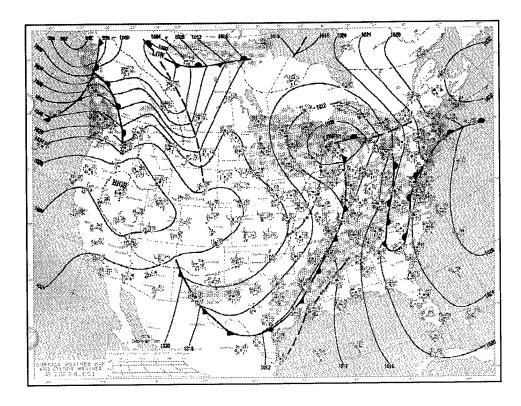


Figure F8. 19 February 1991

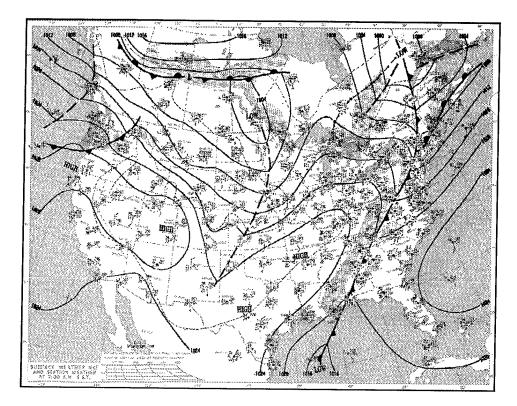


Figure F9. 20 February 1991

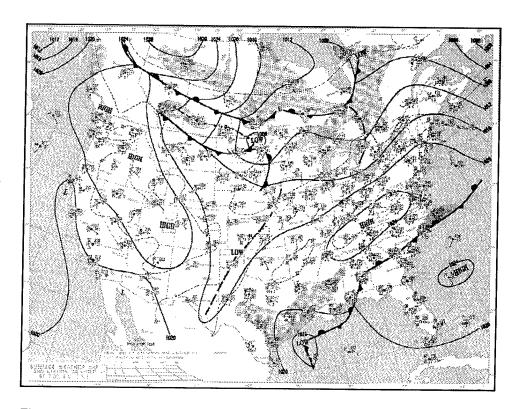


Figure F10. 21 February 1991

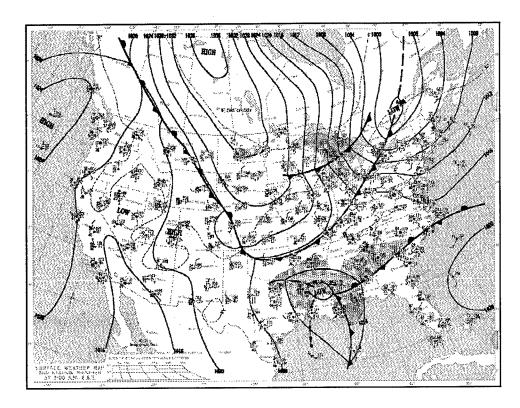


Figure F11. 22 February 1991

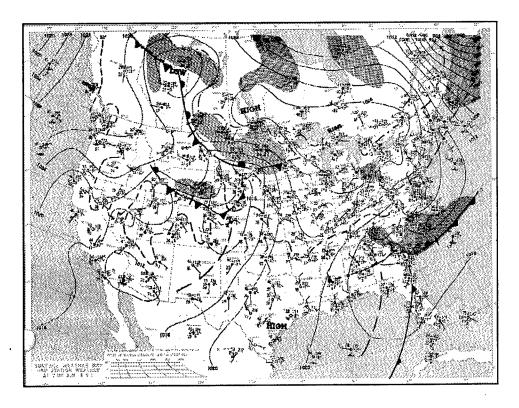


Figure F12. 23 February 1991

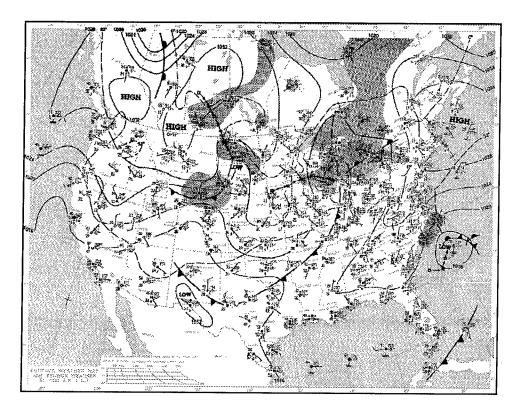


Figure F13. 24 February 1991

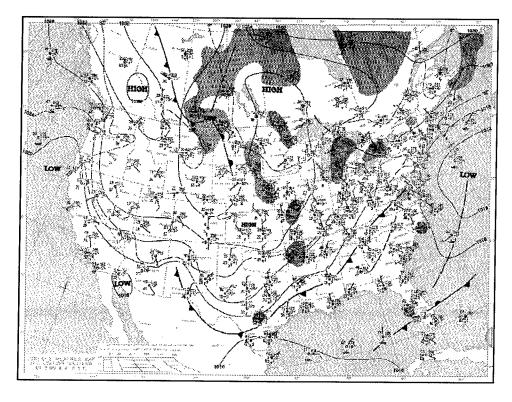


Figure F14. 25 February 1991

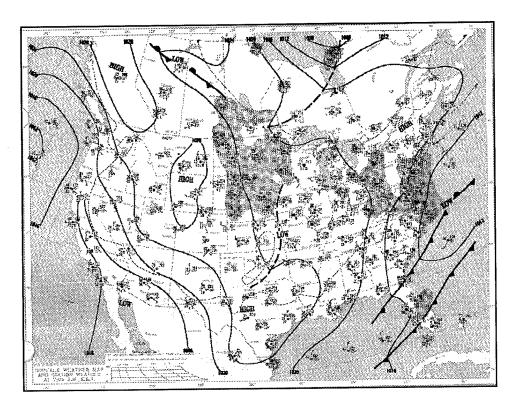


Figure F15. 26 February 1991

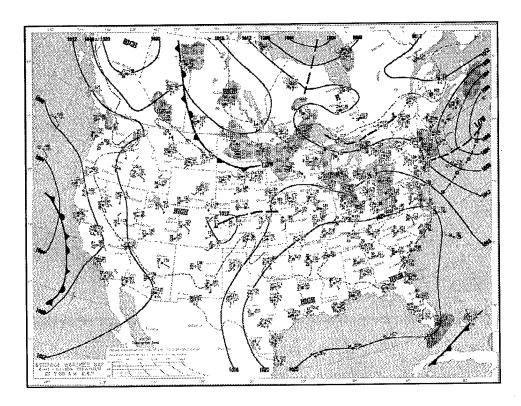


Figure F16. 27 February 1991

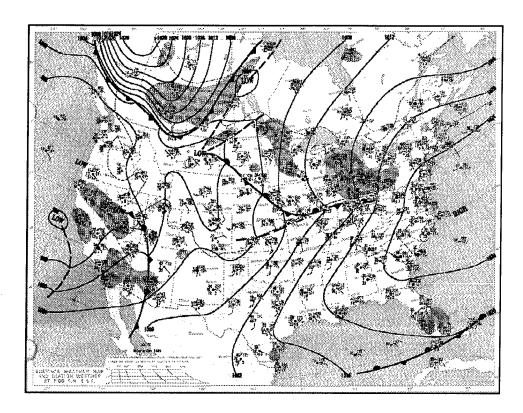


Figure F17. 28 February 1991

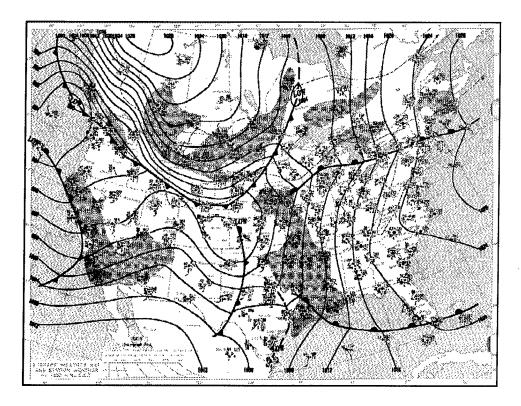


Figure F18. 1 March 1991

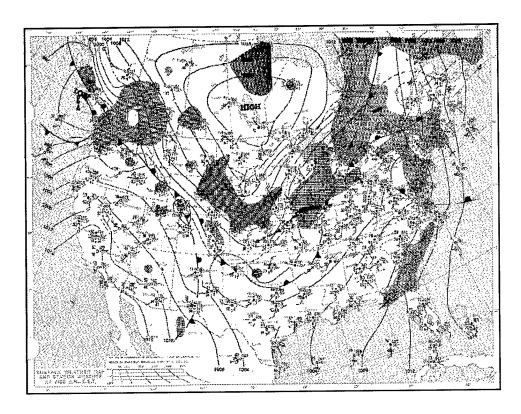


Figure F19. 2 March 1991

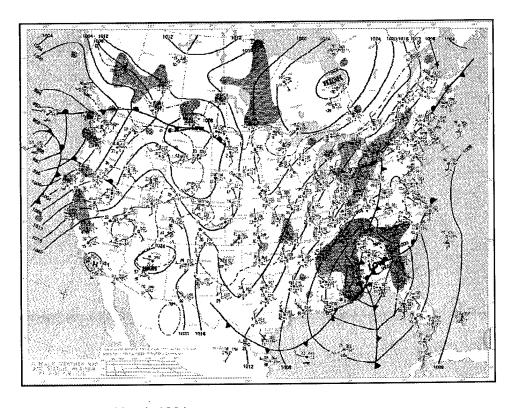


Figure F20. 3 March 1991

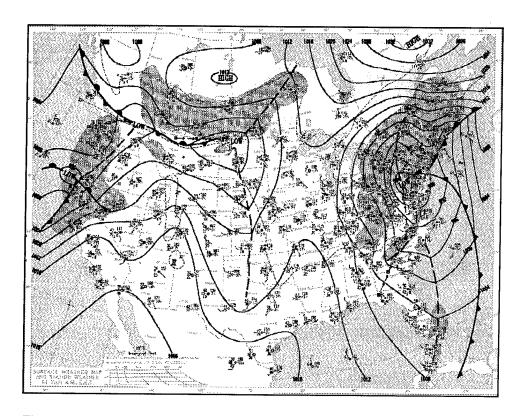


Figure F21. 4 March 1991

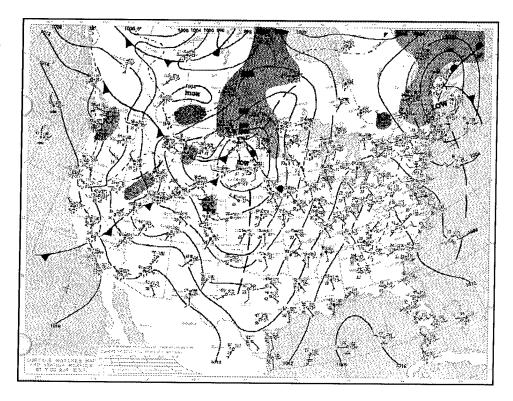


Figure F22. 5 March 1991

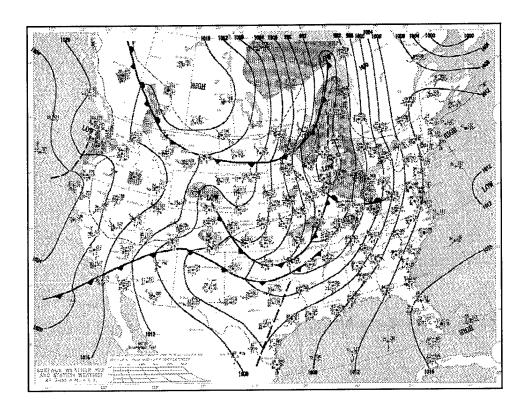


Figure F23. 6 March 1991

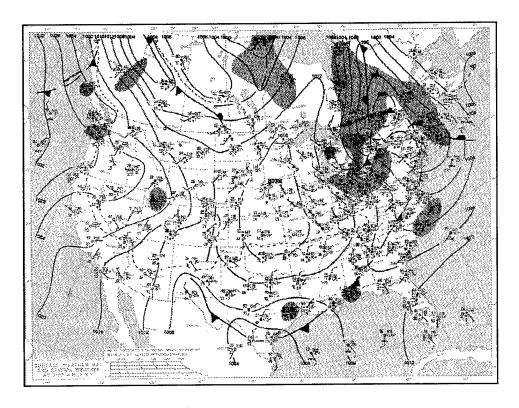


Figure F24. 7 March 1991

Appendix G Notation

- A Wave form amplitude
- c Speed of light
- Do Normalization constant
- E Energy spectrum
- Eo Wave height variance
- E* Nondimensional energy
 - f Frequency, hertz
- f* Nondimensional frequency
- F Directional wave-height variance, or energy, spectrum
- g Acceleration of gravity
- H Mean altitude, aircraft altitude
- Hs Wave height
 - k (Radian) wave number
- K Wave number, cycles per meter
- Ly Lateral, l-sigma, antenna footprint dimension
- md Mean direction
- MSS Mean square slope
- MSS₁, MSS₂ Principal mean square slope components

Appendix G Notation G1

- pd Peak direction
- R Slope anisotropy aspect ratio (MSS2/MSS1)
- s Spread parameter
- SWH Significant wave height
 - to Time of return from the mean sea surface (epoch)
 - Tp Peak period
- U_{10n} Equivalent neutral wind speed at 10-m-level
 - W Wind speed
- W(t) Average altimeter power return wave form
- X* Nondimensional fetch
 - α Measurement sensitivity coefficient
- Δφ Half-power directional spread
- $\Delta \phi_{iso}$ Isotropic limit for first harmonic half-power spread
 - θ_c Effective incidence angle
 - σ Leading edge wave form parameter
 - σ_b Antenna beam width parameter
 - σ_p l-sigma radar pulse width
 - τ Trailing edge wave form parameter
 - φ Azimuth of the antenna
 - ϕ_1 Major axis direction
 - φ₀ Mean direction

REPORT DOCUMENTATION PAGE

Form Approved OMB No. 0704-0188

Public reporting burden for this collection of information is estimated to average 1 hour per response, including the time for reviewing instructions, searching existing data sources, gathering and maintaining the data needed, and completing and reviewing the collection of information. Send comments regarding this burden estimate or any other aspect of this collection of information, including suggestions for reducing this burden, to Washington Headquarters Services, Directorate for Information Operations and Reports, 1215 Jefferson Davis Highway, Suite 1204, Adjoint on VA 2202-4302 and to the Office of Management and Budget, Paperwork Reduction Project (0704-0188), Washington, DC 20503.

1. /	AGENCY USE ONLY (Leave blank)	2. REPORT DATE August 1996		Report 4 of a seri			
. (TITLE AND SUBTITLE Observations and Modelling of Winds a Experiment; Report 4, ROWS Wind and	and Waves During the Sur	rface Wave February-7	Dynamics	5. FUNDING NUMBERS		
	AUTHOR(S) Frederick C. Jackson						
	PERFORMING ORGANIZATION NAME(S) A 218 North Pitt Street Alexandria, VA 22314	ND ADDRESS(ES)			8. PERFORMING ORGANIZATION REPORT NUMBER		
	U.S. Army Engineer Waterways Eng	10. SPONSORING/MONITORING AGENCY REPORT NUMBER Technical Report CERC-93-6					
12a	. DISTRIBUTION/AVAILABILITY STATEME Approved for public release; distr	ENT		- ' -	12b. DISTRIBUTION CODE		
13.	ABSTRACT (Maximum 200 words) The Surface Wave Dynamics Ex	periment (SWADE) w	as a large-	scale, multi-platfo	orm surface wave experiment		

The Surface Wave Dynamics Experiment (SWADE) was a large-scale, multi-platform surface wave experiment that was conducted in the southern mid-Atlantic Bight (MAB) off the U.S. east coast during the fall and winter of 1990-1991. The purpose of the experiment was to study the dynamics and evolution of the directional wave field in response to meteorological forcing making use of recent advances in analysis and in situ data collection, numerical wave modelling, and airborne remote sensing. Of the remote sensing instruments participating in the SWADE, the National Aeronautics and Space Administration's Radar Ocean Wave Spectrometer (ROWS) instrument was the most heavily exercised. ROWS collected approximately 45 hr of high-resolution, directional wave spectra and wind speed data on more than a dozen aircraft flights before, during, and after the last intensive observation period (IOP-3). Processed data include 158 spectra files and 88 wind speed files for 12 flights conducted over the period 12 February-7 March, 1991. This report presents all ROWS data that have been processed to date for the SWADE mission. Buoy and model data collected during the "St. Valentine's Day" frontal episode (14-16 February, 1991) are also presented.

14.	SUBJECT TERMS Airborne remote sensing Directional wave field Numerical wave modelling	Radar Ocean Wave Spect SWADE	rometer (ROWS)		245 PRICE CODE	
17.	SECURITY CLASSIFICATION OF REPORT UNCLASSIFIED	18. SECURITY CLASSIFICATION OF THIS PAGE UNCLASSIFIED	19. SECURITY CLASSIFICATION OF ABSTRACT	20.	LIMITATION OF ABSTRACT	